

University of Alberta

**Static and Dynamic Response of Sandstone Masonry Units Bound with
Fibre Reinforced Mortars**

by

Md Tohidul Islam

A thesis submitted to the Faculty of Graduate Studies and Research
in partial fulfillment of the requirements for the degree of

Master of Science

in

Structural Engineering

Department of Civil and Environmental Engineering

©Md Tohidul Islam

Fall 2010

Edmonton, Alberta

Permission is hereby granted to the University of Alberta Libraries to reproduce single copies of this thesis and to lend or sell such copies for private, scholarly or scientific research purposes only. Where the thesis is converted to, or otherwise made available in digital form, the University of Alberta will advise potential users of the thesis of these terms.

The author reserves all other publication and other rights in association with the copyright in the thesis and, except as herein before provided, neither the thesis nor any substantial portion thereof may be printed or otherwise reproduced in any material form whatsoever without the author's prior written permission.

Examining Committee

Dr. Vivek Bindiganavile, Department of Civil and Environmental Engineering
(Supervisor)

Dr. Roger Cheng, Department of Civil and Environmental Engineering

Dr. P-Y Ben Jar, Department of Mechanical Engineering

DEDICATION

To my Parents

ABSTRACT

This research project describes the impact resistance of masonry units bound with fibre-reinforced Type S mortars and hydraulic lime mortar. The dynamic impact factor and stress rate sensitivity were evaluated for the flexural strength of the mortar and the bond strength, and further, the pattern of failure was noted for each mix and loading rate. Results show that the impact resistance of the masonry units increased in the presence of fibres. However, the stress rate sensitivity of the bond strength decreased with an increase in fibre content. Also, whereas the mode of failure in those masonry units bound with plain Type S mortars was through fracture at the mortar-block interface, the addition of fibres transferred the failure plane to within the masonry block. For hydraulic lime mortar, fibre reinforcement retained the sacrificial nature of mortar and also increased the flexural toughness factor of the joint even under dynamic loading.

ACKNOWLEDGEMENTS

First of all, I am grateful to Almighty Allah, the most Gracious, most Merciful; nothing comes to reality without His wish.

This study was funded in part by the Network of Centres of Excellence on Intelligent Sensing for Innovative Structures (ISIS-Canada) and the Natural Sciences and Engineering Research Council (NSERC), Canada. The author also thanks the Masonry Contractors Association of Alberta (Northern Region) and Scorpio Masonry Inc., Edmonton for the supply of materials and technician time.

I would like to express my deepest gratitude to my supervisor Dr. Vivek Bindiganavile for his continuous support and persistent guidance during this time period. Working with him has been an amazing experience for me.

My thanks go to the following civil engineering laboratory technicians, Mr. Rizadly Mariano, Mr. Sean Watt, and Mr. Greg Miller, for their continuous support from time to time during this research program.

I am also thankful to my family, friends and colleagues, especially Mr. Muhammad Mamun, for their continuous support and cooperation throughout this study period.

Md Tohidul Islam

TABLE OF CONTENTS

Examining Committee	i
Dedication	ii
Abstract	iii
Acknowledgement	iv
Table of Contents	v
List of Tables	ix
List of Figures	xi
List of Symbols	xvi
CHAPTER 1 INTRODUCTION	1
1.1 General	1
1.2 Objective and Scope	4
1.3 Organization	5
CHAPTER 2 LITERATURE REVIEW	7
2.1 General	7
2.2 Type S Mortar	11
2.3 Hydraulic Lime Mortar (HLM)	12
2.4 Carbon Textile-Reinforced Mortar (CTRM)	17
2.5 Paskapoo Sandstone	20
2.6 Quasi-Static Response of Masonry Units	21
2.7 Impact Response of Masonry Units	22

2.8	Role of Fibre in Cement/Hydraulic Lime Mortar Composites	25
	CHAPTER 3 EXPERIMENTAL DETAILS	29
3.1	Introduction	29
3.2	Materials and Composition	29
3.2.1	Type S Mortar	29
3.2.2	Hydraulic Lime Mortar (HLM)	30
3.2.3	Paskapoo Sandstone	31
3.3	Specimen Preparation	33
3.4	Test Setup	37
3.4.1	Quasi-Static Testing	37
3.4.1.1	<i>Compression Test</i>	37
3.4.1.2	<i>Flexural Test</i>	38
3.4.2	Impact Testing	39
	CHAPTER 4 QUASI-STATIC AND IMPACT RESPONSE OF SANDSTONE BLOCKS	44
4.1	Introduction	44
4.2	Compressive Response	44
4.3	Flexural Response	47
4.4	Flexural Toughness Factor	50
4.5	Rate Effects	50
4.6	Conclusions	52
	CHAPTER 5 QUASI-STATIC AND IMPACT RESPONSE OF SANDSTONE MASONRY UNITS BOUND WITH TYPE S MORTAR	53
5.1	Introduction	53

5.2	Compressive Response	53
5.3	Flexural Response	57
5.3.1	Mortar	57
5.3.2	Masonry Units	58
5.4	Flexural Toughness Factor	63
5.5	Rate Effects	65
5.6	Conclusions	68
CHAPTER 6 QUASI-STATIC AND IMPACT RESPONSE OF SANDSTONE MASONRY UNITS BOUND WITH HYDRAULIC LIME MORTAR (HLM)		69
6.1	Introduction	69
6.2	Compressive Response	69
6.3	Flexural Response	72
6.3.1	Mortar	72
6.3.2	Masonry Units	73
6.4	Flexural Toughness Factor	78
6.5	Rate Effects	79
6.6	Conclusions	81
CHAPTER 7 EXTERNAL STRENGTHENING OF SANDSTONE MASONRY UNITS WITH CARBON TEXTILE-REINFORCED MORTAR (CTRM)		82
7.1	Introduction	82
7.2	Materials and mix design	83
7.3	Specimen preparation	85
7.4	Compressive Response of Binder used in preparing the CTRM	87

7.5	Quasi-Static Flexural Testing of Sandstone Masonry Unit Externally Strengthened with CTRM	89
7.5.1	Introduction	89
7.5.2	Quasi-static Test Results: Unit-R-0	89
7.5.3	Quasi-static Test Results: Unit-R-2	91
7.6	Impact Testing of Composite Sandstone/CTRM Specimen	93
7.6.1	Introduction	93
7.6.2	Impact Test Results	93
7.6.3	Discussion of Results	97
7.7	Quasi-Static Testing of Mortar Beam Specimens	97
7.8	Impact Testing of Mortar Beam Specimens	98
7.9	Conclusions	99
CHAPTER 8	CONCLUSIONS AND RECOMMENDATIONS	101
REFERENCES		104
APPENDIX		114

LIST OF TABLES

Table 2.1	Canadian Inventory of Historic Buildings (Cameron, 1986)	7
Table 2.2	Proportion Specification for Type S Mortar (CSA A179-04)	11
Table 2.3	Proportion Specification: Compressive Strength of Mortar Cubes (CSA A 179-04)	12
Table 2.4	Composition and Strengths of Masonry Lime Mortars	15
Table 2.5	Compressive Strength of Hydraulic Limes	15
Table 2.6	Physical Properties of Hydraulic Limes	16
Table 2.7	Chemical Composition of NHL2 (percentages related to original dry lime) (Lanas, 2004)	16
Table 2.8	Physical Characteristics of Sandstone from the Paskapoo Formation (Parks, 1916).	20
Table 3.1	Chemical Composition of Type S Binder (% mass)	31
Table 3.2	Properties of Polypropylene Microfibres	32
Table 3.3	Mix Design of Type S Mortar	34
Table 3.4	Mix Design of Hydraulic Lime Mortar	35
Table 3.5	List of Specimens	35
Table 4.1	Mechanical Properties of Paskapoo Sandstone	45
Table 5.1	Compressive Response of Plain and Fibre-reinforced Type S Mortar	57
Table 5.2	Flexural Response of Mortar Beams and Masonry Units for Type S Mortar	63
Table 6.1	Compressive Response of Plain and Fibre-reinforced Hydraulic Lime Mortar	72
Table 6.2	Flexural Response of Mortar Beams and Masonry Units for Hydraulic Lime Mortar	78
Table 7.1	Physical Properties of Carbon Textile used in the CTRM	85
Table 7.2	Compressive Results of the Binder used in preparing the CTRM	89

Table 7.3	Impact Test Results for Composite Sandstone/CTRM Specimens	94
Table 7.4	Quasi-Static Test Results : Mortar Beam Specimen	97
Table 7.5	Impact Test Results: Mortar Beam Specimen	98

LIST OF FIGURES

Figure 2.1	Parliament Buildings (West Block), Ottawa, Ontario	10
Figure 2.2	Typical Stone Masonry Wall in the Buildings on Parliament Hill, Ottawa	10
Figure 2.3	Compressive Strength of NHL Mortars with different values of initial Flow (Hanley and Pavia, 2008)	16
Figure 2.4	Flexural Strength of NHL Mortars with different values of initial Flow (Hanley and Pavia, 2008)	17
Figure 2.5	Load-displacement Plots for Polypropylene Fibre-reinforced Composite Beams without a Notch: (a) Paste Matrix and (b) Mortar Matrix. (Banthia and Sheng, 1996)	27
Figure 2.6	Load-displacement and Load-CMOD plots for Polypropylene Fibre-reinforced Composite Beams with a Notch: (a) Paste Matrix and (b) Mortar Matrix. (Banthia and Sheng, 1996)	28
Figure 3.1	A Snapshot of a Typical Sandstone Block used for this Study	31
Figure 3.2	Grain Size Distribution of the Fine Aggregate in Mortar	32
Figure 3.3	Polypropylene Microfibres used in this Study	32
Figure 3.4	Mortar Mixture Machine	36
Figure 3.5	Workability of Mortar Mixes as Determined by a Flow Table	36
Figure 3.6	Schematic of Prisms for Flexural Testing of (a) Mortar and (b) Masonry Unit	37
Figure 3.7	Quasi-Static Test in Progress for Compression of Mortar	38
Figure 3.8	Quasi-Static Test in Progress for Flexure on Masonry Units	39
Figure 3.9	Drop Weight Impact Tester	42
Figure 3.10	Instrumentation for High Speed Data Acquisition	42
Figure 3.11	Trigger Mechanism for activating High-Speed Data Collection	43
Figure 4.1	Stress-strain Response of Sandstone in Compression	45
Figure 4.2	Time History of Poisson's Ratio for Sandstone	46
Figure 4.3	Failure of a Sandstone Cylinder under Compression	46

Figure 4.4	Load-deflection Response under Quasi-Static Flexure for Sandstone Prisms	48
Figure 4.5	Flexural Load-deflection Response under Impact from Drop Height of 250 mm for Sandstone Prisms	48
Figure 4.6	Flexural Load-deflection Response under Impact from Drop Height of 500 mm for Sandstone Prisms	49
Figure 4.7	Failure of a Sandstone Prism under Flexure	49
Figure 4.8	Flexural Toughness Factor for Sandstone Blocks	50
Figure 4.9	Stress Rate Sensitivity of Flexural Strength of Sandstone Blocks	51
Figure 5.1	Compressive Response of Type S Mortar	55
Figure 5.2	Time History of Poisson's Ratio for Type S Mortar	55
Figure 5.3	Failure of Cylinder for Plain Type S Mortar under Compression	56
Figure 5.4	Failure of Cylinder for Fibre-reinforced Type S Mortar under Compression	56
Figure 5.5	Load-deflection Response under Quasi-Static Flexure for Type S Mortar	59
Figure 5.6	Failure of Masonry Unit for Plain Type S Mortar under Flexure. Note Failure Plane at the Stone-mortar Interface.	59
Figure 5.7	Failure of Masonry Unit for Fibre-reinforced Type S Mortar under Flexure. Note Failure Plane passes through the Stone Block.	60
Figure 5.8	Flexural Load-deflection Response under Impact from Drop Height of 250 mm for Type S Mortar	60
Figure 5.9	Flexural Load-deflection Response under Impact from Drop Height of 500 mm for Type S Mortar	61
Figure 5.10	Load-deflection Response under Quasi-Static Flexure for Masonry Units bound with Type S Mortar	61

Figure 5.11	Flexural Load-deflection Response under Impact from Drop Height of 250 mm for Masonry Units bound with Type S Mortar	62
Figure 5.12	Flexural Load-deflection Response under Impact from Drop Height of 500 mm for Masonry Units bound with Type S Mortar	62
Figure 5.13	Flexural Toughness Factor for Masonry Unit and Type S Cement Mortar	64
Figure 5.14	Stress Rate Sensitivity of Flexural Strength of Type S Mortar Shown for Various Fibre Contents	67
Figure 5.15	Stress Rate Sensitivity of Bond Strength of Masonry Unit with Type S Cement Mortar Shown for Various Fibre Contents	67
Figure 6.1	Compressive Response of Hydraulic Lime Mortar	70
Figure 6.2	Failure of Cylinder for Plain Hydraulic Lime Mortar under Compression	70
Figure 6.3	Failure of Cylinder for Fibre-reinforced Hydraulic Lime Mortar under Compression	71
Figure 6.4	Time History of Poisson's Ratio for Hydraulic Lime Mortar	71
Figure 6.5	Load-deflection Response under Quasi-Static Flexure for Hydraulic Lime Mortar	73
Figure 6.6	Failure of masonry unit for plain Hydraulic Lime Mortar under flexure	74
Figure 6.7	Flexural Load-deflection Response under Impact from 500 mm for Hydraulic Lime Mortar	74
Figure 6.8	Flexural Load-deflection Response under Quasi-Static for Masonry Unit with Hydraulic Lime Mortar	75
Figure 6.9	Flexural Load-deflection Response under Impact from 250 mm for Masonry Unit with Hydraulic Lime Mortar	75
Figure 6.10	Flexural Load-deflection Response under Impact from 500 mm for Masonry Unit with Hydraulic Lime Mortar	76

Figure 6.11	Failure of Masonry Unit at the Stone-Mortar Interface	76
Figure 6.12	Failure of Masonry Unit within the Mortar	77
Figure 6.13	Flexural Toughness Factor for Masonry Unit and Ty Hydraulic Lime Mortar	79
Figure 6.14	Stress Rate Sensitivity Shown for Various Fibre Contents for Flexural Strength of Hydraulic Lime Mortar	80
Figure 6.15	Stress Rate Sensitivity Shown for Various Fibre Contents for Bond Strength of Masonry Units with Hydraulic Lime Mortar	80
Figure 7.1	Premixed Fibre-reinforced Mortar M25 used to apply the CTRM	84
Figure 7.2	Carbon textile C10 used to prepare the CTRM	84
Figure 7.3	Flow Test with Fibre-reinforced Mortar as per ASTM 1437	85
Figure 7.4	Example of Failed Masonry Units after Testing as described in Section 3.4.1.2 and Section 3.4.2 The broken Unit was re-assembled prior to Strengthening.	86
Figure 7.5	Masonry Units under Repair using CTRM	87
Figure 7.6	Sample Stored for Curing	87
Figure 7.7	Compressive Response of the Binder used in preparing the CTRM	88
Figure 7.8	Mode of failure of Composite Sandstone/CTRM Specimen Unit-R-0	90
Figure 7.9	Flexural Load-deflection Responses under Quasi-static Loading for Composite Sandstone/CTRM Specimen Unit-R-0	91
Figure 7.10	Mode of Failure of Composite Sandstone/CTRM Specimen Unit-R-2	92
Figure 7.11	Flexural Load-deflection Responses under Quasi-static Loading for Composite Sandstone/CTRM Specimen Unit-R-2	93
Figure 7.12	Impact Test: Composite Sandstone/CTRM Specimen (Unit-R-0; 250 mm Drop)	95

- Figure 7.13 Impact Test: Composite Sandstone/CTRM Specimen (Unit- 95
R-2; 250 mm Drop)
- Figure 7.14 Impact Test: Composite Sandstone/CTRM Specimen (Unit- 96
R-0; 500 mm Drop)
- Figure 7.15 Impact Test: Composite Sandstone/CTRM Specimen (Unit- 96
R-2; 500 mm Drop)

LIST OF SYMBOLS

A	= area under the load-deflection curve up to a deflection of δ_{max} (N-mm)
$a_o(t)$	= midspan acceleration at time t
b	= effective width of the specimen (mm)
DIF	= dynamic impact factor
$d_o(t)$	= midspan displacements at time t
f'_c	= compressive strength of concrete
f'_{co}	= 10 MPa
h_e	= effective depth at notch (mm)
L	= beam span (mm)
l	= clear span of the beam
$P_i(t)$	= inertial load on specimen during the impact
ov	= length of overhanging portion of the beam
$v_o(t)$	= midspan velocity at time t
T_f	= flexural toughness factor (MPa)
$\dot{\epsilon}$	= strain rate in the range of 3×10^{-6} to 300 s^{-1}
$\dot{\epsilon}_s$	= $3 \times 10^{-6} \text{ s}^{-1}$ (static strain rate)
δ	= correction factor
$\dot{\sigma}$	= stress rate

$\dot{\sigma}_s$ = static stress rate
 ρ = mass density for the beam material
 δ_{max} = deflection equal to $L/150$ (mm)

CHAPTER 1 INTRODUCTION

1.1 General

Lime-sand mortars were used widely in Canada and elsewhere in the world until the late 1800s. In Canada, three types of mortar are currently being used for repointing historic masonry projects: lime mortars, hydraulic lime mortars, and Portland cement/masonry cement-lime mortars. Mortar used for historic structures must comply with good conservation principles and be compatible with the historic fabric as far as feasible; it must also be appropriate for the material to be bonded and remain durable under service conditions. Good conservation principles dictate that the mortar be somewhat flexible so that it can act as the sacrificial material saving the masonry unit. The three current types of mortar can differ in their properties significantly. Hydraulic lime mortar (HLM) was the most common binder in Canadian masonry until late in the 19th century. With the rapid development in building materials, natural hydraulic lime mortars suffered because of their variable performance, and cement-based mortars became popular due to their rapid strength development with time. For the restoration and rehabilitation of historic structures, however, hydraulic lime mortar is still preferable due to good adhesion, ductility, and reasonably high values of porosity and permeability. Hydraulic lime mortar also resembles the original mortar of the rehabilitated structures. In the framework of the restoration and rehabilitation process, the compatibility of the new repair mortars and original components of the structures are emphasized. The key considerations for

restoration and rehabilitation of historic masonry structures, like compressive strength, wetting and drying potential, bond, appearance, resistance to frost action and resistance to salts (e.g., chlorides, sulphates) make the richer cement-lime mortar preferable for this purpose.

On the other hand, Type S mortar, a modern cement-based building material with a proven high performance, possesses high compressive strengths, and low deformability, which make it unsuitable for the restoration and rehabilitation of historic masonry assemblies. However, these make it more suitable for the construction of modern masonry structures.

There are many ways in which the rehabilitation and restoration of heritage masonry buildings can be done, and one such way is rehabilitation with the help of carbon fibre that is applied to the side of a masonry building with the help of a special adhesive. Since carbon fibre itself possesses high tensile strength, in general the strength of the repaired structure depends on the bond between the masonry building and the carbon fibre layer. The drawbacks of using carbon fibre reinforcement with epoxy resins, such as lack of transpirations, are eliminated by using a premixed mortar as a binder between the carbon fibre and masonry. A combination of mortar and carbon fibre produces Carbon Textile Reinforced Mortar (CTRM). CTRM possesses the same fire resistance as the rest of the masonry building, retains workability at a high range of temperatures, bonds in the presence of water, and does not require pre-treatment of the masonry surface (Buoizzi, 2006). Using mortar is also more environmentally friendly than using epoxy resins. This information will not only help to

understand the behaviour of a given material, but also provide us with information on the dynamic bond behaviour to explore the application of CTRM in active seismic zones.

The main focus of this study is to characterize materials for the rehabilitation, restoration and retrofitting of historic masonry structures that lie within seismic zones of Canada. This research project was designed to rehabilitate the stone masonry wall in the West Block of Parliament Hill in Ottawa, Canada. Under the aegis of Public Works and Government Services, Canada, This project was divided in to three parts; evaluation of the masonry units and components was conducted at the University of Alberta, the testing and a masonry wall finite element analysis was carried out at the University of Calgary and the anchorage design was examined at the University of Manitoba.

To better understand masonry, one needs to be familiar with the necessary properties of blocks, mortar and units. Blocks and mortar have different quasi-static and dynamic properties. In masonry, they come together as an assembly whose properties are likely different than each of its components. As will be discussed in Chapter 2, currently there is very limited literature available about the relationship between quasi-static and dynamic properties of blocks and mortar, whether individually or as a unit. To the author's knowledge, the present study is the first on the dynamic response of the flexural bond in a masonry unit with sandstone blocks and fibre-reinforced mortar. The addition of fibres in concrete is well-known to improve certain properties. But the effect of discrete fibres in masonry mortar still needs characterization. This study evaluates the

quasi-static and dynamic properties of sandstone blocks, hydraulic lime mortar, Type S mortar, and carbon textile-reinforced mortar. Thus materials are examined individually, and also the constitutive behaviour of these components is described when taken together as a masonry unit.

1.2 Objective and Scope

The core objectives of this study are as follows:

- ❖ To study the quasi-static and dynamic response of Type S mortar and hydraulic lime mortar, with and without fibre reinforcement.
- ❖ To investigate the quasi-static and dynamic response of sandstone blocks from the Paskapoo formations.
- ❖ To inspect the quasi-static and dynamic response of masonry units and to determine the effect of loading rate and fibres on bond strength.
- ❖ To gather knowledge about quasi-static and dynamic responses of broken masonry units externally strengthened with carbon textile-reinforced mortar.

The scope of this study includes the following aspects of building materials and restoration technology:

- ❖ Rehabilitation of historic masonry structures, especially those which fall in the seismic activity zones within Canada.
- ❖ Building of modern masonry structures with traditional and modern materials.

- ❖ Dynamic response of controlled low-strength and high-strength materials.

1.3 Organization

A lime-Portland cement mortar, classified as Type S mortar as per CSA A179-04 (2004), was investigated first, followed by a study of masonry units bound with this material. In order to ensure against test variability, locally available sandstone blocks were used throughout this program. Commercially available polypropylene microfibres were introduced at 0.25% and 0.50% volume fraction to render three mortar mixes together with a reference plain mix. These mortar mixes were characterized in quasi-static compression to ascertain reference mechanical properties. The stress rate sensitivity of the flexural response of such mortars was established, followed by an evaluation of rate effects on the flexural bond in masonry units. An instrumented drop-weight impact tester was utilized to generate the high stress rates, up to 10^8 kPa/s. The post-peak response of the flexural bond was characterized along the standard guidelines for fibre-reinforced concrete through flexural toughness factors.

This thesis is divided into eight chapters. Chapter 1 describes the objectives, scope of this research, and outline of this thesis. The available literature on Paskapoo sandstone, hydraulic lime mortar, Type S mortar, and carbon textile-reinforced mortar is discussed in Chapter 2. Chapter 3 presents the details about the material and mix composition, available experimental setup and test machines, and steps of mortar preparation. The quasi-static and dynamic study of

sandstone blocks, Type S mortar, and hydraulic lime mortar are discussed in Chapters 4, 5 and 6, respectively. Chapter 7 presents the quasi-static and dynamic response of broken masonry units repaired with carbon textile-reinforced mortar. Finally, these results are summarized in Chapter 8 with recommendations for further research.

CHAPTER 2 LITERATURE REVIEW

2.1 General

Masonry is a widespread building material throughout the world. It is used to construct load bearing or partition walls in building structures. Many historical old stone structures were also built from masonry material. In Canada, there are numerous such structures that were built during the past two hundred years, and most of them were built with lime/sand mortar. These mortars exhibit good workability and high water retention in the plastic state and develop strength slowly with time. After fifteen years of research and field recording starting from 1970, the Canadian Inventory of Historic Building (CIHB) currently holds information about many heritage structures in Canada (Table 2.1). (Cameron, 1986; Jackson, 1979)

Table 2.1 Canadian Inventory of Historic Buildings (Cameron, 1986)

Types	Number of holdings
Exterior recording	200,000 buildings
Interior recording	1,900 buildings
Slide collection	25,000 slides
Historical Photographs	40,000 photographs
Research docketts	5,000 buildings

The majority of these heritage masonry structures were built with lime mortars and they have experienced severe damage during their whole life due to extreme weather and numerous freeze-thaw cycles. Also, they were not designed to withstand seismic loads. The present options for these structures are demolition or rehabilitation. The latter is preferable as these are heritage structures, which

have a historical, cultural, and political significance. In an ideal world, rehabilitation or restoration should be designed to include the least intrusive methods, and, wherever possible, they should also attempt to use materials similar to the original construction and be compatible with the existing masonry in terms of movement accommodation (Jeffs, 2001). It also should not impact the aesthetic quality and physical appearance of the structures. A typical example of historic masonry structures is the Parliament Buildings in Ottawa, as shown in Figure 2.1. The exterior masonry walls of many older Canadian masonry buildings were traditionally built using stone units into double wythes with rubble-filled inner cores, as shown in Figure 2.2. Several factors, such as the inherent high porosity of hydraulic lime mortar, change in loading conditions, and differential settlement can cause bulging, displacement, and/or cracking of masonry units (Jeffs, 2001). Among the ingredients of masonry units, mortar is always the easiest to replace. Hence, any interaction must retain the sacrificial nature of the mortar.

There are several types of masonry mortars available for construction and repair of masonry structures. The conservation of historic masonry structures requires mortar Type N, O, and K as per CSA A179. But in the current version of CSA A179-04, these three types are no longer available and hence have no proper legal standing as part of contract documents unless specialized clauses address this issue. Mortar Types S and N are high-strength mortars and are not suitable for restoration of the heritage structures. In the restoration of heritage stone masonry in Canada, hydraulic lime mortar is preferred over Portland cement

mortar (Maurenbrecher *et al*, 2007), as the former is intentionally weaker than the stone blocks and also allows for their movement over the first few months. The current Canadian standard does not have any guidelines for lime mortar. The European Standard EN 459 (2001) is one of the few standards that describe different types of building limes. Due to reasons discussed in the following section, hydraulic lime mortars are preferable over modern masonry materials for the restoration of historic masonry structures, and Type S mortar and carbon textile-reinforced mortar is best suited for the design and repair of modern masonry structures.

Parliament Hill, home of the Parliament of Canada, was built in 1875 with further additions constructed in the last century. It has three edifices called Central Block, East Block and West Block. In order to ensure the preservation of this national heritage building, extensive restoration was required including the rehabilitation of the masonry and exterior walls, dismantling and rebuilding deteriorated areas of masonry and repointing of mortar joints.



Figure 2.1 Parliament Buildings (West Block), Ottawa, Ontario

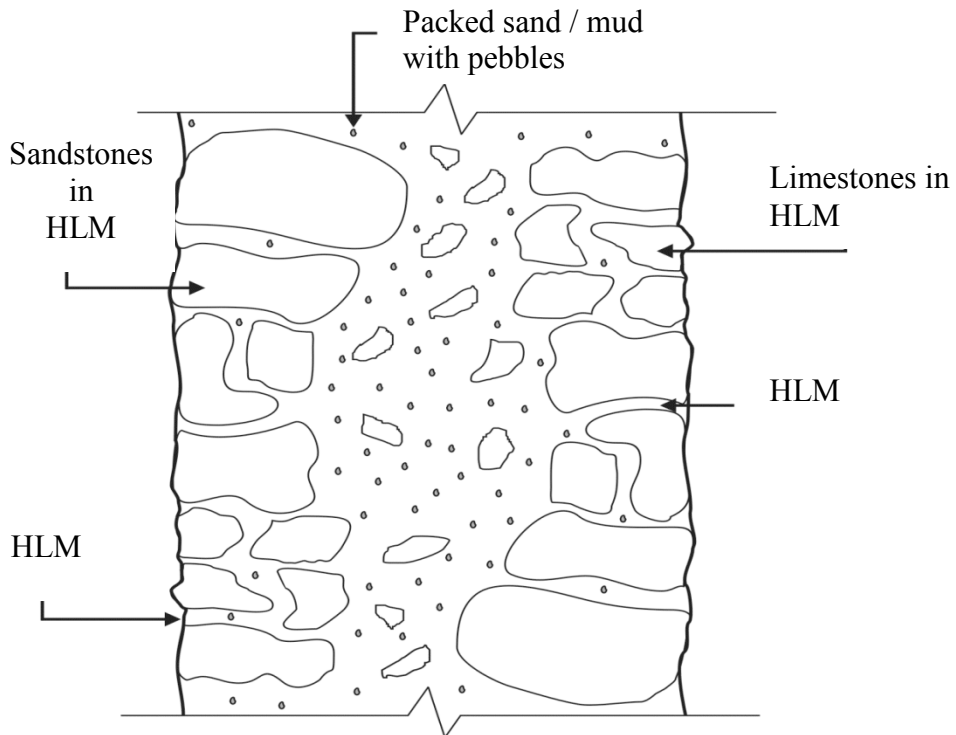


Figure 2.2 Typical Stone Masonry Wall in the Buildings on Parliament Hill, Ottawa

2.2 Type S Mortar

As per CSA A179-04, Type S mortar is a mixture of aggregates, water, and Type S cement binder, which is suitable for general use and recommended particularly when high lateral strength of masonry is desired. It can also be used for below-grade applications. Type S mortar is a cement-rich mortar that has a high compressive strength and relatively poor workability in comparison with lime-based mortar. The proportions of Type S mortar as per CSA A179-04 are listed in Table 2.2, where different proportions of ingredients are indicated by volume. As shown, it may be produced using Type S binder or Type N binder. The minimum 28-day cube compressive strength of Type S mortar is 12.5 MPa, as mentioned in Table 2.3. However, there is no indication in CSA standards of the maximum compressive strength of mortar, which is crucial for the repair and restoration of heritage structures. The mortars described in CSA A179-04 are batched by volume and have a two to three times higher compressive strength than the code-specified minimum compressive strength (Beall, 1997). Such strength is not desirable for historic structures as it might limit deformability and also damage the masonry units. Therefore, Type S mortar is suitable for the construction and repair of modern masonry structures only.

Table 2.2 Proportion Specification for Type S Mortar (CSA A179-04)

Mortar type	Parts by volume			
	Portland cement	Type N mortar cement	Type S mortar cement	Aggregate measured in damp, loose state
S	1/2	1	--	3-1/2 to 4-1/2
S	0	--	1	2-1/4 to 3

Table 2.3 Proportion Specification: Compressive Strength of Mortar Cubes (CSA A 179-04)

Preparation	Mortar Type	Minimum compressive strength, MPa	
		7-day test	28-day test
Laboratory prepared, mixed to a flow of 100 to 115%	S	7.5	12.5

2.3 Hydraulic Lime Mortar (HLM)

Lime was the most versatile building material until late in the 19th century. With the advent of modern Portland cement, the use and popularity of hydraulic lime declined. Currently, there has been a move towards the use of lime mortars in Canada and also throughout the world, and lime has become one of the principal materials used in the conservation and restoration of historic structures. The performance of hydraulic lime mortars used on major Canadian heritage structures over the past five years was monitored on a sample of projects and its performance was satisfactory (Suter *et al.*, 2001).

Lime is derived from the Latin *limus*, meaning mud, and *linere*, meaning to smear. It is acquired from limestone, a sedimentary rock composed mainly of calcium carbonate (Maurenbrecher, 2004). Lime mortars are generally non-hydraulic but they can be given hydraulic properties by adding pozzolanic admixtures containing reactive silicate and aluminates. Hydraulic and non-hydraulic lime mainly differ in the manner by which they harden. The hardening properties of non-hydraulic lime is due to a reaction between CaO in the mix and atmospheric CO₂, through a carbonation process, whereas the hardening properties of hydraulic lime are due to a chemical reaction between active clay

particles, lime, and water (Vicat, 1997; Cowper, 1998). Compared to non-hydraulic lime, hydraulic lime possesses lower permeability and flexibility and a better resistance to moisture, frost, and salt attack (Holmes, 1997). Masonry Types M, O, and K, which are basically lime-based masonry mortars, are no longer recognized by the current version of Canadian standard CSA A179-04. At present, only Types N and S mortars are recognized by CSA A179-04, where Type N and S are high-strength Portland cement-lime mortars, and hence are not suitable for the restoration of heritage structures. The European Standard EN 459 (2001) classifies building lime into three classes: calcium lime (CL), dolomite lime (DL), and hydraulic lime (HL). The first two are further classified according to their oxide content (CaO + MgO), and hydraulic lime is classified as per its compressive strength at 28 days, which is listed in Table 2.4. Natural hydraulic limes (NHL) are those hydraulic limes that are derived completely from argillaceous limestone after slaking. Hydraulic limes can be feebly, moderately, or eminently hydraulic, whereas the new European Standard EN 459 (2001) classifies them by strength as listed in Table 2.5. Natural hydraulic lime is classified as NHL2, NHL3.5 and NHL5 with compressive strengths of 2 MPa, 3.5 MPa, and 5 MPa respectively (Maurenbrecher *et al.*, 2007). The physical properties of hydraulic lime are described in Table 2.6, and the chemical composition of NHL2 is addressed in Table 2.7. As per EN 459 (2001), the initial flow of NHL should be 185 for the best workability, whereas as per ASTM C1437 (2007), the flow should be 100 to 115. The discrepancy is due to the fact that the two test methods are different. The EN 459 (2001) specifies the

dropping at a rate of once per second for 15 s. On the other hand, ASTM C1437 (2007) indicates to drop the table 25 times in 15 s. Hanley and Pavia (2008) conducted extensive research on the workability of natural hydraulic lime mortars and its influence on strength. Figure 2.3 and Figure 2.4 illustrate the outcome of the research where the compressive strength and flexural strength variations are shown with time for various natural hydraulic limes. It was suggested to use a different flow value for different NHL mortars instead of using a fixed flow value for all NHL mortars. Hydraulic limes still contain a high proportion of non-hydraulic lime, which gains strength by carbonation. The strength gain by hydraulic reaction is much slower than for Portland cement; after a year the mortar strength could be three times the 28-day strength. Testing for compressive strength at 28 days is therefore not appropriate for non-hydraulic and hydraulic lime mortars (Portland cement-lime mortars also continue to increase in strength, but the proportionate increase is much less) (Maurenbrecher, 2004).

Many old stone masonry structures in Canada are located in areas of seismic activity. The proper rehabilitation of such buildings requires a quantitative knowledge of the dynamic response of the masonry unit and its components. In particular, the bond between the stone blocks and the binding mortar is of concern (Burnett *et al.*, 2007). The quasi-static response of masonry joints is well-established (Rao *et al.*, 1996; Van Der Pluijm, 1997; Gemert *et al.*, 2003). It is known to depend upon the type of mortar and to possess post-peak residual bond strength (Van Der Pluijm, 1997).

Most recently, Chan and Bindaganavile (2010) carried out research on hydraulic lime mortar with and without fibre reinforcement. NHL2 was used for this purpose. The results showed that the addition of polymeric micro fibres to hydraulic lime mortar improved the compressive, flexural, and shear strength, and the fibre efficiency was most evident for flexural toughness factor. Also there was an optimum dosage of fibre-reinforcement beyond which the fibres did not improve mortar efficiency.

Table 2.4 Composition and Strengths of Masonry Lime Mortars

Type of mix	Descriptions	Composition by volume	Cube strength (MPa)
Hydraulic lime	<ul style="list-style-type: none"> ❖ Low-strength ❖ Performs well and exhibits adequate frost resistance ❖ Used for restoring old masonry structures 	<ul style="list-style-type: none"> ❖ Hydraulic lime: 1 ❖ Aggregate: 2-3 	1-10
Lime	<ul style="list-style-type: none"> ❖ Very low-strength ❖ Used in repointing older thicker masonry structures 	<ul style="list-style-type: none"> ❖ Hydraulic lime: 1 ❖ Aggregate: 2-3 	0.5-2

Table 2.5 Compressive Strength of Hydraulic Limes

Type of hydraulic lime	Compressive strength (MPa)	
	7 day	28 day
HL 2	-	1.5-10
HL 3.5	≥ 1.5	2.7-14
HL 5	≥ 2	4.0-20

Table 2.6 Physical Properties of Hydraulic Limes

Type of hydraulic lime	Bulk density (kg/m ³)	Fineness ⁽¹⁾		Soundness ⁽²⁾ (mm)	Free water content ⁽³⁾ (%)	Penetration ⁽⁴⁾ (mm)	Air content ⁽⁵⁾ (%)	Setting time ⁽⁶⁾ (hour)
		(%)						
			0.09 mm	0.2 mm				
HL 2	400 - 800	≤ 15	≤ 5	≤ 20	≤ 2	20 and < 50	≤ 20	1 and ≤ 15
HL 3.5	400 - 800				≤ 1			
HL 5	400 - 800							

In accordance with test methods:

⁽¹⁾ 5.2 of EN 459-2

⁽²⁾ 5.3.3 of EN 459-2

⁽³⁾ 5.11 of EN 459-2

⁽⁴⁾ 5.5 of EN 459-2

⁽⁵⁾ 5.7 of EN 459-2

⁽⁶⁾ 5.4 of EN 459-2

Table 2.7 Chemical Composition of NHL2 (percentages related to original dry lime) (Lanas, 2004)

Compound	CaO	LOI	SiO ₂	MgO	Al ₂ O ₃	SO ₃	K ₂ O	Fe ₂ O ₃	Na ₂ O
% by mass	54.26	15	12.57	7.65	5.42	2.13	1.35	1.16	0.34

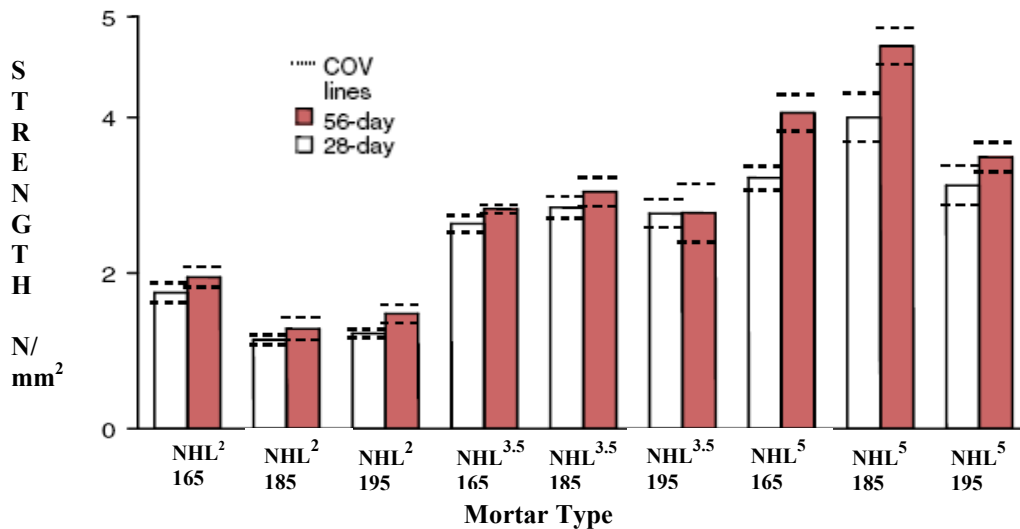


Figure 2.3 Compressive Strength of NHL Mortars with different values of initial Flow (Hanley and Pavia, 2008)

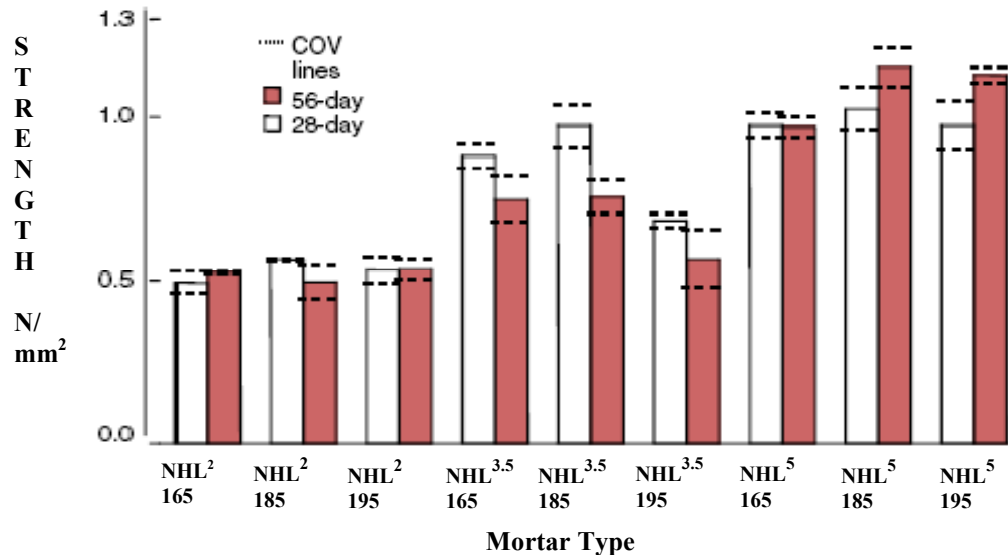


Figure 2.4 Flexural Strength of NHL Mortars with different values of initial Flow (Hanley and Pavia, 2008)

2.4 Carbon Textile-Reinforced Mortar (CTRM)

Over the years, the rehabilitation of aging masonry buildings has become quite a significant issue in Canada. As the buildings get older, they are exposed to an increasing number of freeze-thaw cycles and tend to develop cracks. Those cracks, if left untreated, can result in a catastrophic failure of key components of a building.

In some cases, the buildings can be demolished and re-built, but in most cases this solution is not viable. Generally, a complete rebuild cannot be performed because of safety issues related to demolition in a densely populated area (Witterhold, 1985). Also, in general, many masonry buildings represent historical and cultural value for the community and thus cannot be demolished. The financial side of full reconstruction is another reason why it is deemed not viable (Xue, 2009).

The points described above represent the reasons why rehabilitation of a masonry building is almost always a preferred option to full reconstruction. There are many ways in which such rehabilitation can be done, one of them being application of carbon fibre on the side of a masonry building with the help of a special adhesive. Since carbon fibre itself possesses high tensile strength, in general the strength of the repaired structure depends on the bond between the masonry building and the fibre layer.

Until now the most common way to apply carbon fibre on the side of a building has been achieved with the help of epoxy resins. In this case, the layer of carbon fibre reinforcement is bonded to the masonry structure using epoxy. Even though this method ensures a strong bond, it has several disadvantages:

- i. Epoxy resins are not fire-proof and lose their mechanical properties at elevated temperatures. In case of fire, the bond provided by epoxy resins is destroyed and masonry failure can occur (Buoizzi, 2006).
- ii. Epoxy resins seal the pores in masonry, thus altering the hydrothermal nature of the original building.
- iii. Fibre-reinforced plastics (FRP) applied to damp surfaces have poor adhesion (Buoizzi, 2006).
- iv. FRP requires a specific temperature range for successful application since the workability time of epoxy greatly decreases as the temperature goes up.

The downsides of using carbon fibre reinforcement and epoxy resins are eliminated when mortar is used as a binder between carbon fibre and masonry. A

combination of mortar and carbon fibre produces Carbon Textile Reinforced Mortar (CTRM). Due to the fact that CTRM use is a fairly novel technique, the combined scope of the research done is not complete.

The behaviour of columns reinforced using a TRM jacketing technique was precisely analysed, and the conclusion was made that TRM jacketing significantly improves column response to a cyclic lateral load that imitates seismic activity (Bournas *et al.*, 2009). Similar results were achieved in an experiment where a masonry wall reinforced with TRM was subjected to cyclic loading. When subjected to cyclic loading, the TRM wall specimens exhibited a substantially increased strength, a stable hysteresis behaviour, low stiffness and strength degradation with number of cycles, and considerable energy absorption and dissipation capacity, leading to a substantially improved seismic performance when compared to unreinforced masonry walls (URM) (Harajli *et al.*, 2010). In the same study, static response of masonry walls reinforced with TRM was evaluated as well and proven to be significantly higher than that of an unreinforced masonry wall. As well, TRM proved to greatly increase both shear (Triantafillou and Papanicolaou, 2002) and bending capacity of a concrete beam subjected to a static loading (Buozzi, 2006).

However, the response of masonry units retrofitted with TRM and subjected to dynamic (impact) loading is not covered in the research conducted up to date and has to be evaluated based on the present study.

2.5 Paskapoo Sandstone

Referred to as “Paskapoo Sandstone”, this formation consists of sand grains eroded from the Rocky Mountains and transported by rivers approximately 60 million years ago. The sandstone outcrop is thought to have formed over time with successive layers buried under hundreds of metres of younger sediment, cemented with minerals precipitated from groundwater and gradually exposed by erosion along the river valleys of Alberta, Canada (Geoscape Canada, 2008).

The material is known to vary in compression from 25-50 MPa and in tension from 2.5-4.5 MPa (Parks, 1916) which is shown in Table 2.8 along with other physical properties of samples from the Paskapoo Formation in Alberta.

Table 2.8 Physical Characteristics of Sandstone from the Paskapoo Formation (Parks, 1916)

Characteristic	1	2	3	4	5
Specific gravity	2.678	2.665	2.672	2.677	2.679
Weight per cubic foot (lbs.)	131.48	134.19	136.24	144.66	137.54
Pore space (%)	21.72	19.34	18.26	12.83	17.66
Coefficient of saturation	0.69	0.68	0.72	0.76	0.72
Dry crushing strength (lbs/sq. in.)	5985	7631	9617	11119	8306
Wet crushing strength (lbs/ sq. in.)	3874	5640	7007	7224	5613
Frozen crushing strength (lbs/sq. in.)	2782	3896	4212	6524	4065
Transverse strength (lbs/sq. in.)	398	554	658	582	521
Shearing strength (lbs/sq. in.)	431	497	642	586	531
Loss on corrosion (grams/sq. in.)	0.0675	0.0430	0.0503	0.0419	0.0456
Drilling factor (mm)	25.2	21.0	26.6	17.8	22.7
Chiselling factor (grams)	9.44	6.87	14.66	4.72	11.16

Stone types:

1. Yellow Calgary stone (Wm. Oliver and Co. and J.A. Lewis, Calgary)
2. Grey-yellow Glenbow stone, Alberta Provincial Legislature building (C. de Lavergne, Calgary)
3. Grey-yellow Cochrane stone (Shelly Quarry Co., Calgary)
4. Grey Macleod-Brocket stone (Porcupine Hills and Crowsnest Stone Co. Ltd., Fort Macleod)
5. Average of the above six commercial stones

The Paskapoo Formation was historically Alberta's most productive formation for building stone. This formation consists of a series of thick, tabular, buff-coloured sandstone beds with interbedded siltstone and mudstone layers. The sandstone beds can be in excess of 15 m thick and are commonly stacked into successions greater than 60 m thick (Glass, 1990). Rivers and streams in a fluvial environment deposited the Paskapoo sediments. Fluvial environments transport and deposit coarse to fine-grained sediments. Landforms associated with fluvial environments include deltas, flood plains, point bars, and braided streams. These landforms may develop sedimentary structures such as crossbedding, bedding planes, laminations, ripple marks, and variations in grain size, all of which will give different characteristics to the rock (e.g., appearance and strength) (Crocq, 2010).

2.6 Quasi-Static Response of Masonry Units

Masonry is a layered composite consisting of mortar and masonry units. The bond between mortar and masonry units dictates the performance of masonry and determines how the masonry transfers and resists stresses due to different applied loads (Venkatarama and Vyas Uday, 2008). For very low unit-mortar bond strengths, masonry failure is normally accompanied by bond failure. A study of the relationship between masonry compressive strength and bond strength by Sarangapani *et al.* (2005) indicates that the increase of bond strength

results in an increase of compressive strength of the masonry prisms, while keeping mortar strength constant. The failure of masonry prisms using weak mortar leads to bond failure between the mortar and units, while in the case of stronger mortar, failure is due to splitting of bricks produced by the internal stresses (Costigan and Pavia, 2009; Gumeste and Venkatarama, 2006). For masonry prisms with units stronger than mortar, masonry compressive strength is not sensitive to bond strength (Venkatamara and Vyas Uday, 2008; Costigan and Pavia, 2009), and mortars with distinctly different compressive strengths but same bond strengths result in similar masonry compressive strengths (Rao *et al.*, 1995).

2.7 Impact Response of Masonry Units

The rehabilitation of stone masonry buildings for seismic resistance requires a quantitative knowledge of the dynamic response of the masonry unit and its components. There is much evidence of strain rate sensitivity in the tensile strength of concrete (ACI-446.4R, 2004) and rocks (Zhao and Li, 2000; Kubota *et al.*, 2008; Asprone *et al.*, 2009) at high strain rates. As mentioned earlier, the quasi-static response of masonry joints is well-established. However, very little is known as to the rate sensitivity of masonry joints. Burnett *et al.* (2007) conducted the first such study using clay bricks bonded with lime-Portland cement mortar and found a dynamic impact factor of 3. They carried out a Split Hopkinson Pressure Bar test on masonry joints for the response of masonry joints to dynamic tensile loading. There were three 100 mm diameter and 50

mm length (20 mm brick + 10 mm mortar + 20 mm brick) specimens and five 45 mm diameter and 50 mm length specimens. The strain rate varied from 0.89 to 1.52/s. The test on eight specimens indicated an apparent dynamic enhancement of the bond strength, dynamic increase factor (DIF) = 3.1. Subsequently, Hao and Tarasov (2008) quantified the response of similar mortar and clay bricks under dynamic compression. Recently they conducted an experimental study of the strain rate effects on clay brick and cement-based mortar. Uniaxial compression tests were carried out on brick and mortar specimens at different strain rates ranging from quasi-static (10^{-6} /s) to dynamic up to a strain rate of 200/s. There were 30 brick specimens (38 mm diameter and 78 mm height) and 30 mortar specimens of the same size. From the tests, it was concluded that the strain rate effects on brick and mortar material are in general similar to the strain rate effects on other materials such as concrete and rock. The ultimate and yield strength and strain increased with the strain rate. It was found that the strain rate is more significant on the yield strength and corresponding strain than that of ultimate strength and corresponding strain. The Young's modulus of mortar decreased with the strain rate, but it was the opposite for brick. To the author's knowledge, the present study is the first on the dynamic response of the flexural bond in a masonry unit, particularly with sandstone block and hydraulic lime mortar. From the recent study of Chan and Bindiganavile (2010), it was evident that hydraulic lime mortar is sensitive to strain rates, and the current modified CEB model overestimates the dynamic impact factor for this low-strength material. To the author's knowledge, the present study is also the first on the

stress rates sensitivity of the flexural bond in a masonry unit, particularly with stone block and fibre-reinforced mortar. Given the limited data on the stress rate sensitivity of lime-based mortars, the author drew lessons from existing literature on the dynamic response of Portland cement concrete. The Comité Euro-International du Béton has described the strain rate sensitivity of concrete in tension as a bilinear model (CEB-FIP, 1990) with a high strain rate response beyond 30/s. Malvar and Ross (1998) reported that the CEB-FIP model underestimates the dynamic impact factor (DIF) for strain rates below 30/s and modified the rate sensitivity model as follows:

$$DIF = \left(\frac{\dot{\varepsilon}}{\varepsilon_s}\right)^\delta \text{ for } \dot{\varepsilon} \leq 1\text{s}^{-1} \quad \text{Equation 2.1a}$$

$$DIF = \gamma \left(\frac{\dot{\varepsilon}}{\varepsilon_s}\right)^{1/3} \text{ for } \dot{\varepsilon} \geq 1\text{s}^{-1} \quad \text{Equation 2.1b}$$

where, $\varepsilon_s = 10^{-6}/\text{s}$, $\log \gamma = 6\delta - 2$, $\delta = \frac{1}{1 + \frac{8f'_c}{f'_{co}}}$ with $f'_{co} = 10 \text{ MPa}$

For lime-cement mortars such as Type S masonry mortar, the modulus of elasticity as evaluated from quasi-static testing was shown to drop by 10% at the higher strain rates in the range examined here (Hao and Tarasov, 2008). In the absence of comparable data for hydraulic lime mortars, the quasi-static measure of elastic modulus was considered acceptable to generate the bilinear expression on a semi-log scale for the stress rate sensitivity from Equation (2.1). Thus, the dynamic impact factor for the flexural strength of sandstone and mortar mixes was compared with the following equations:

$$DIF = \left(\frac{\dot{\sigma}}{\dot{\sigma}_s}\right)^\delta \text{ for } \dot{\sigma} \leq E_m s^{-1} \quad \text{Equation 2.2a}$$

$$DIF = \gamma \left(\frac{\dot{\sigma}}{\dot{\sigma}_s}\right)^{1/3} \text{ for } \dot{\sigma} > E_m s^{-1} \quad \text{Equation 2.2b}$$

where, f'_c is taken from Tables 5.1, and 6.1, and δ, γ are the same as in Equation (2.1).

While a lot of effort has been spent on studying fibre-reinforced cement, no one has carried out research in this field with mortar. The existing literature of concrete could be a valuable guideline for masonry structures. Masonry structures behave similarly to that of concrete in many aspects. The bond behaviour and load transfer mechanism of FRP bonded to masonry were found to be similar to FRP bonded to concrete (Wills *et al.*, 2009).

2.8 Role of Fibre in Cement/Hydraulic Lime Mortar Composites

The role of fibres in improving the mechanical properties of concrete is well-known (ACI-544.R1, 1996) namely significant improvement to the tensile strength and post-crack residual strength in mortars under impact loading (Glinicki, 1994; Bharatkumar and Shah, 2004). Fibre improves the energy absorption capacity of concrete by enhancing its post-peak stress-transfer capability and hence is an effective way of improving concrete's resistance to impact load. However, the choice of fibre type, length, and shape greatly influences the composite performance. There are various types of fibre, such as metallic, mineral, polymeric, or natural. Short, discrete, polymeric fibres increase the energy dissipated by concrete under impact loading (Mindess and

Vondran, 1988), sometimes exceeding in DIF over steel fibres (Bindiganavile and Banthia, 2001). However, very little is known about their performance in mortars used for masonry. In what appears to be the first such study, Polyvinyl Acetate (PVA) fibres were investigated for flexural bond with clay bricks by Armwood *et al.* (2008). They found that although the post-peak response in mortars improves with an increase in the fibre content, the strain at failure in a masonry unit was smaller, so that the flexural bond failed sooner and the benefits from the post-peak response of fibre reinforcement in mortars were not seen in the flexural response of the masonry unit. Their study concluded that the total fibre content should be restricted to an upper limit of 0.6% volume fraction. Recently Chan and Bindiganavile (2010) studied the effect of polypropylene micro-fibres on the behaviour of hydraulic lime mortar up to 0.5% volume fraction. Clearly, while microfibres may enhance the aggregate-paste interface in a stone masonry joint (Bentur and Alexander, 2000), it is not just the strength but also the possible changes to the failure mechanism that define the composite response. This paper describes the dynamic response of stone masonry joints with particular emphasis on the flexural bond. A typical flexural load deflection response of paste and mortar with polypropylene micro-fibres is shown in Figure 2.5 and Figure 2.6 for beam without notch and with notch, respectively. Banthia and Sheng (1996) conducted a study where cement paste and cement mortar were reinforced at 1, 2 and 3% by volume of carbon, steel, and polypropylene microfibres. By four point flexural testing of both notched and unnotched beams,

considerable strengthening, toughening, and stiffening was observed due to the incorporation of microfibre into the matrix.

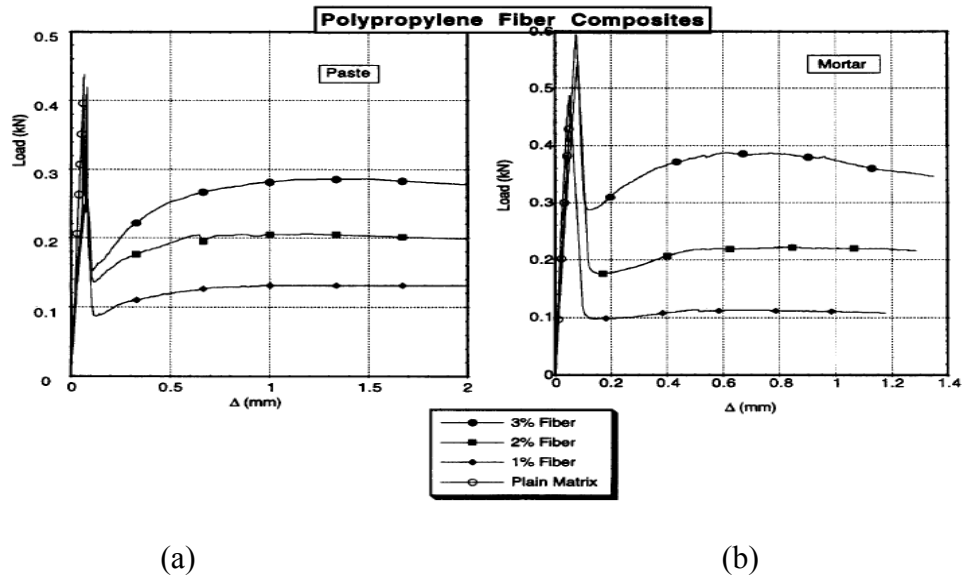


Figure 2.5 Load-displacement Plots for Polypropylene Fibre-reinforced Composite Beams without a Notch: (a) Paste Matrix and (b) Mortar Matrix (Banthia and Sheng, 1996)

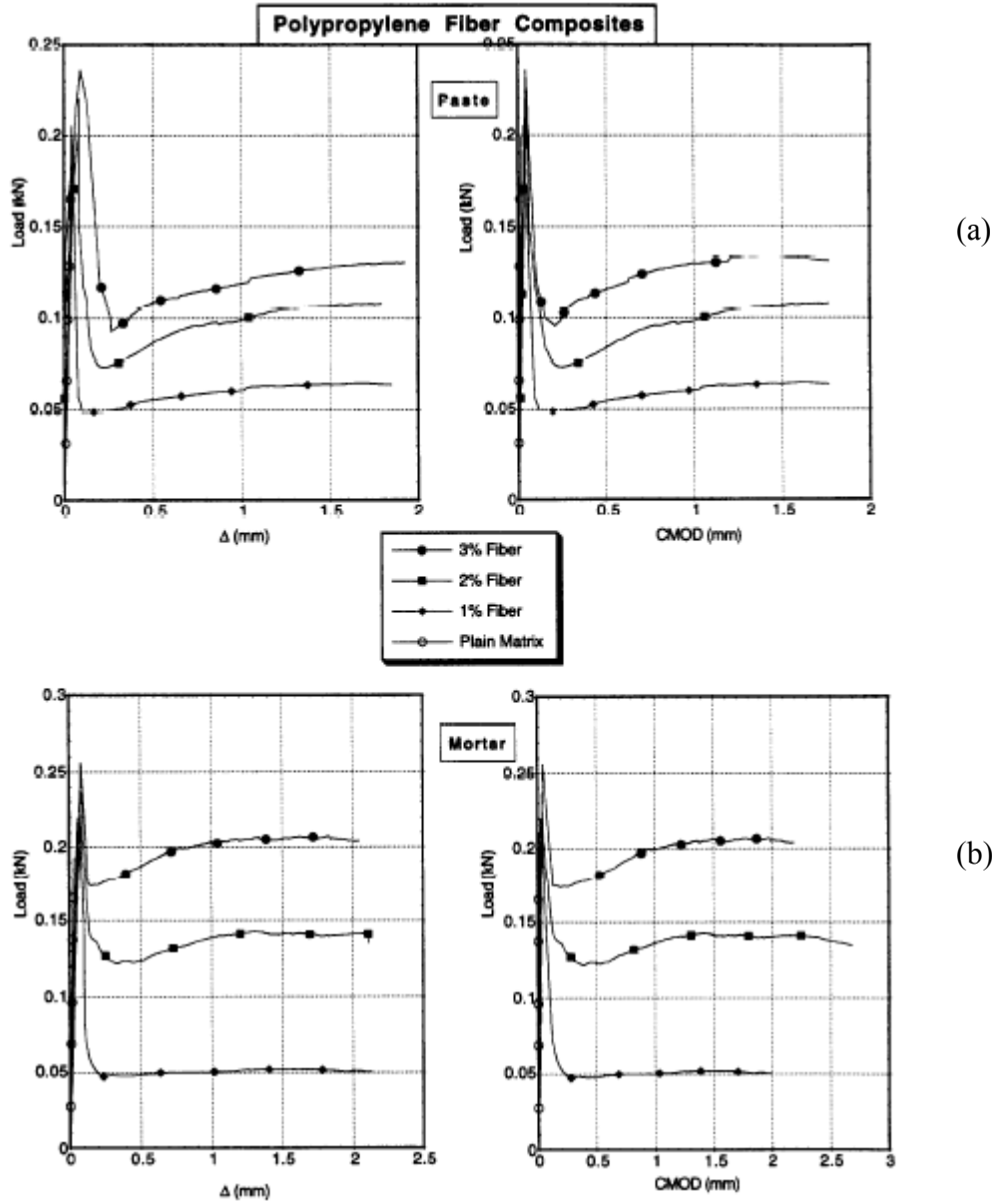


Figure 2.6 Load-displacement and Load-CMOD plots for Polypropylene Fibre-reinforced Composite Beams with a Notch: (a) Paste Matrix and (b) Mortar Matrix (Banthia and Sheng, 1996)

CHAPTER 3 EXPERIMENTAL DETAILS

3.1 Introduction

In this research program, tests on plain and fibre-reinforced Type S mortar and hydraulic lime mortar were carried out to investigate the compressive and flexural strength, flexural toughness, and stress rate sensitivity. Also quasi-static and dynamic tests on stone blocks and repaired broken masonry units were conducted. The materials were selected to fulfill the requirements of rehabilitation of masonry structures suitable for the Canadian environment. For quasi-static tests, ASTM standards were followed and available test set ups and machines also conformed to the standards. For the dynamic test, an instrumented drop-weight impact machine was used. This chapter describes the raw materials that were used in this study along with the specimen preparation, the test machines, the test setup, and the test program.

3.2 Materials and Composition

3.2.1 Type S Mortar

The sandstone blocks from the Paskapoo Formation (Figure 3.1) were bound using a Type S mortar designed to achieve a 28-day compressive strength of 15 MPa. The chemical composition of the Type S cement binder as adapted from the manufacturer is shown in Table 3.1. The mortar was designed as per CSA A179-04 (2004). The Type S mortar was proportioned with water, Type S cement binder and fine aggregates in a ratio of 1:2:6 by mass and was in

accordance with ASTM C144 (2004). The mix design of the Type S mortar is shown in Table 3.3. The water-to-binder ratio was suitably adjusted to achieve a slump flow in plain mortars within 100-115% in order to meet the workability criterion per CSA A179-04 (2004). A blended sand was used as the fine aggregate to meet the grading criterion as shown in Figure 3.2. This gradation is particularly designed to ensure superior durability in the context of historic stone masonry (Maurenbrecher et al., 2001). Polypropylene microfibres were introduced as the discrete reinforcement at dosage rates of 0.25% and 0.50% by volume fraction. These fibres are illustrated in Figure 3.3, and Table 3.2 lists their salient features.

3.2.2 Hydraulic Lime Mortar (HLM)

The same sandstone used earlier with Type S mortar (Figure 3.1) was used to prepare the masonry units. A natural hydraulic lime (NHL2) with a targeted compressive strength of 2 MPa (at 180 days) was sourced from France. Its chemical composition was shown earlier in Table 2.6. Polypropylene microfibres with properties as listed in Table 3.2 were introduced as the discrete reinforcement at dosage rates of 0.25% and 0.50% by volume fraction (V_f). The plain mortar was prepared as per CSA A179-04 (2004) and the mix design for both plain and fibre-reinforced mixes is shown in Table 3.4. For the plain mortar, the water-to-binder ratio was suitably adjusted to achieve a flow between 100-115% in order to meet the workability criterion per CSA A179-04 (2004). No change was made to the mix design to adjust slump flow with fibres, so as to

maintain proportions. The fine aggregate was the same blended sand (Figure 3.2) that was used for the Type S mortar.

3.2.3 Paskapoo Sandstone

Sandstone blocks from the Paskapoo Formation, local to Alberta, were used to prepare the masonry units reported in this paper. The nominal variation of compressive strength of this sandstone is 25-50 MPa, as discussed in Section 2.5. The blocks were 100 mm x 100 mm x 150 mm and were used for preparing masonry units to be tested under flexure. Subsequently, cylinders were cored from intact sandstone blocks for quasi-static compression tests.

Table 3.1 Chemical Composition of Type S Binder (% mass)

CaCO ₃	SiO ₂ (Crystalline silica)	Ca(OH) ₂	CaSO ₄	MgO	CaO	Portland Cement
20-50	<10	0-20	5-10	0-4	0-1	30-75



Figure 3.1 A Snapshot of a Typical Sandstone Block used for this Study

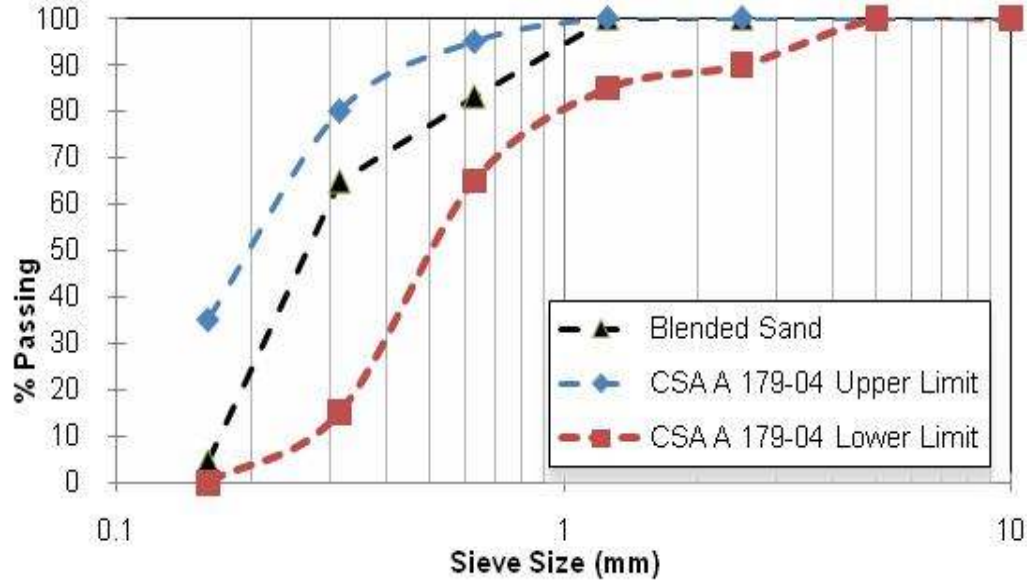


Figure 3.2 Grain Size Distribution of the Fine Aggregate in Mortar



Figure 3.3 Polypropylene Microfibres used in this Study

Table 3.2 Properties of Polypropylene Microfibres

Specific Gravity	0.91
Fibre Length (mm)	20
Density (kg/m ³)	910
Tensile Strength (MPa)	450
Modulus of Elasticity (MPa)	3450
Denier	3

3.3 Specimen Preparation

As mentioned earlier, the mix proportions for the plain and fibre-reinforced mortars are listed in Table 3.3 for Type S binder and Table 3.4 for hydraulic lime. They were mixed in a mortar mixer (as shown in Figure 3.4) with rotation about the horizontal axis to ensure satisfactory blending of the fine aggregates, binder, water, and microfibres. The mixing sequence, crucial to achieving the desired workability, was as follows: First, 2/3 of the mix water was added to the mixer with half the fine aggregates and the entire binder. After 2-3 minutes of mixing, the remaining sand and water was added with an additional 8-10 minutes of mixing. At this point, for the fibre-reinforced mortars, polypropylene microfibres were added to the mixture. These fibres were fluffed through an air-jet to ensure maximum dispersion in the mix. After 2-3 minutes of further blending, the workability of the fresh mortar was determined by using a flow table as per ASTM C1437 (2007), and shown in Figure 3.5. Whereas the slump flow in plain mortars was as required by the standard, introducing fibres led to a significant drop (Table 3.3 and Table 3.4). However, no change was made to the mix composition or the proportion to restrict the number of variable parameters during analysis. A certified mason helped supervise the preparation of mortars in this research program.

The mortar mixes were cast into cylinders (with 100 mm diameter and 200 mm height) and prisms with dimensions of 100 mm x 100 mm x 350 mm. The masonry units were built to have the same dimensions as the mortar prisms to simplify the test setup (Figure 3.6). Two sandstone blocks (100 mm x 100 mm x

150 mm) were joined with mortar to produce each masonry unit. While the blocks were sawn to ensure plane faces and straight edges, one square face was chiselled to produce a rough surface on each block, and the masonry unit was prepared to measure 350 mm in length and have dimensions identical to the mortar beams. Care was taken to moisten the chiselled stone surface prior to applying the mortar. Three cylinders were cast for each mortar mix, along with 3 prisms as flexural specimens per mix. Further, with each mortar mix, three masonry units were cast to test the flexural bond. Each stone block was “battered” with mortar prior to laying the rest of the binder to form the prism. In order to ensure consistency in test conditions, the cylinders, prisms, and masonry units were cast from the same batch of mortar every time. The specimens were left in their moulds at room temperature and humidity to be demoulded after 7 days, at which time they were stored under ambient temperature and humidity (18-24°C and 30-50% relative humidity) for another 28 days before testing. Sandstone cylinders were obtained through coring to obtain 50 mm x 100 mm specimens for quasi-static compression testing. The test protocol is described in Table 3.5 for both Type S mortar and hydraulic lime mortar.

Table 3.3 Mix Design of Type S Mortar

Mix & Designation	Fibre Content (% V_f)	Type S Cement (kg/m^3)	Sand (kg/m^3)	Water (kg/m^3)	Slump Flow (%)
0.00% V_f Fibre (SF0)	0	400	1200	200	106
0.25% V_f Fibre (SF1)	0.25	400	1200	200	37
0.5% V_f Fibre (SF2)	0.5	400	1200	200	23

Table 3.4 Mix Design of Hydraulic Lime Mortar

Mix & Designation	Fibre Content (% V_f)	NHL-2 (kg/m^3)	Sand (kg/m^3)	Water (kg/m^3)	Slump Flow (%)
0.00% V_f Fibre (LF0)	0	400	1200	400	103
0.25% V_f Fibre (LF1)	0.25	400	1200	400	48
0.5% V_f Fibre (LF2)	0.5	400	1200	400	39

Table 3.5 List of Specimens

Test	Standard	Type	Size	Quantity	Comments
Compression	ASTM C469	Sandstone Cylinder	50 mm diameter 100 mm height	2	For Paskapoo Sandstone Specimen
Flexural (Quasi-static)	ASTM C1609	Sandstone Beam	40 mm width 40 mm depth 140 mm length	3	
Flexural (Impact – drop height of 250 mm)	-	Sandstone Beam	40 mm width 40 mm depth 140 mm length	3	
Flexural (Impact – drop height of 500 mm)	-	Sandstone Beam	40 mm width 40 mm depth 140 mm length	3	
Compression	ASTM C469	Mortar Cylinder	100 mm diameter 200 mm height	6	For each mix of Type S mortar and hydraulic lime mortar, i.e. mix with 0% fibre, 0.25% fibre and 0.5% fibre
Flexural (Quasi-static)	ASTM C1609	Mortar Beam	100 mm width 100 mm depth 350 mm length	3	
		Masonry Unit	100 mm width 100 mm depth 350 mm length	3	
Flexural (Impact – drop height of 250 mm)	--	Mortar Beam	100 mm width 100 mm depth 350 mm length	3	
		Masonry Unit	100 mm width 100 mm depth 350 mm length	3	
Flexural (Impact– drop height of 500 mm)	--	Mortar Beam	100 mm width 100 mm depth 350 mm length	3	
		Masonry Unit	100 mm width 100 mm depth 350 mm length	3	



Figure 3.4 Mortar Mixture Machine



Figure 3.5 Workability of Mortar Mixes as Determined by a Flow Table

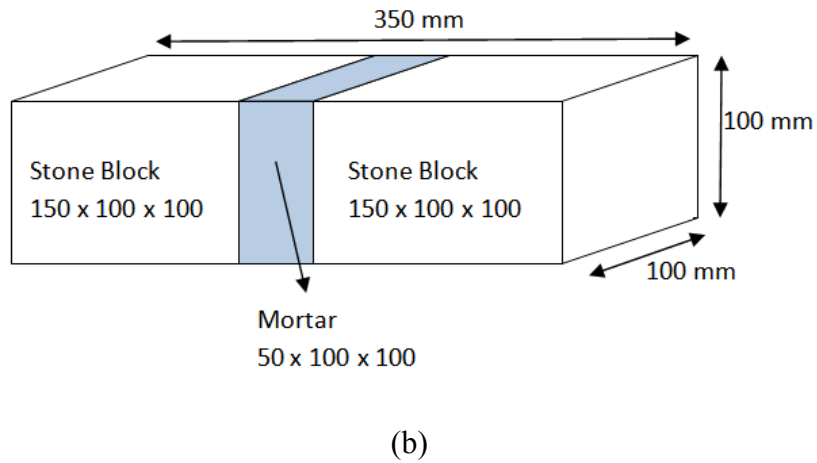
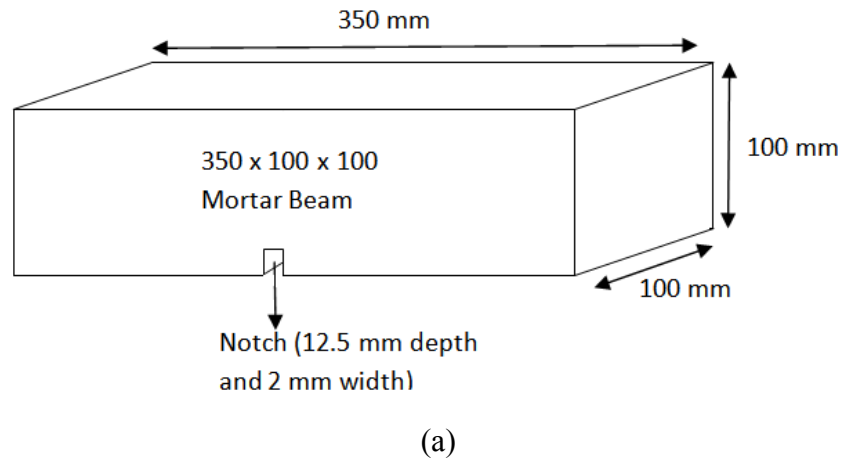


Figure 3.6 Schematic of Prisms for Flexural Testing of (a) Mortar and (b) Masonry Unit

3.4 Test Setup

3.4.1 Quasi-Static Testing

3.4.1.1 Compression Test

The sandstone and mortar cylinders were tested in a universal testing machine with a built-in load cell of 1000 kN capacity (MTS 1000). Three replicates were tested in each case. The cylinders were instrumented as shown in Figure 3.7 to derive the compressive stress-strain response together with axial and transverse

strain histories as per ASTM C469 (2001). The loading surface was kept plane and parallel through sulphur capping.

Three linear variable displacement transducers (LVDTs) were arranged at 120° about the longitudinal axis. Two others were placed diametrically along the radial direction at mid-height to evaluate Poisson's ratio. The data acquisition system obtained load, stroke, and LVDT measurements at 5 Hz. The test was conducted using a fixed rate of displacement at 1.25 mm/min as per ASTM C469 (2001).

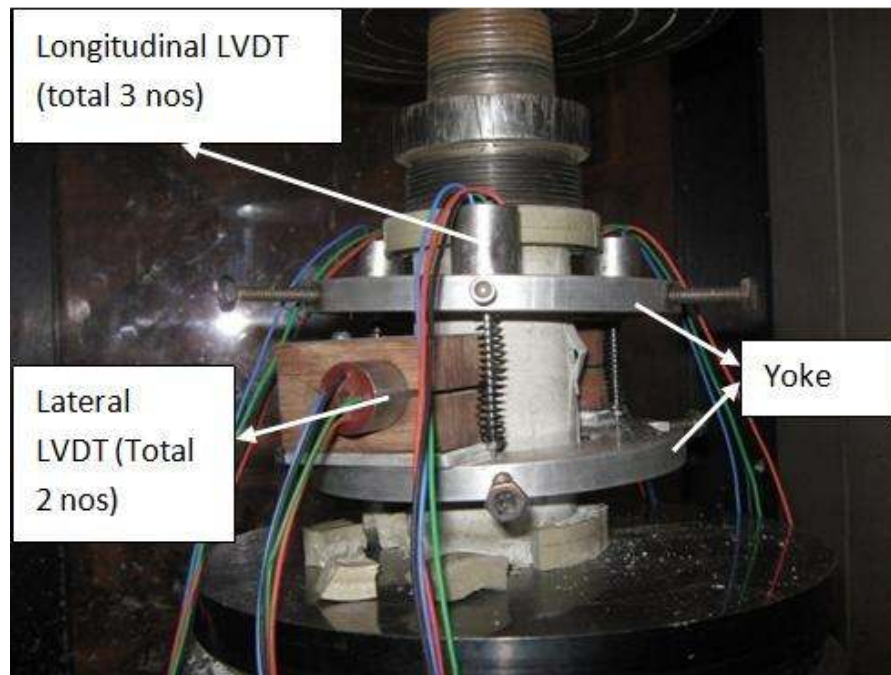


Figure 3.7 Quasi-Static Test in Progress for Compression of Mortar

3.4.1.2 Flexural Test

The mortar prisms and masonry units were tested under 4 point flexure as per the configuration shown in Figure 3.8 based on ASTM C1609 (2007). Three replicates were tested for each mortar mix. A clear span of 300 mm was

maintained for both mortar and masonry specimens. In order to ensure a known failure path, the mortar prisms were sawn to create a notch 12.5 mm deep and 2 mm wide at mid-span. Two LVDTs were attached on either side of the beam specimen onto a yoke, according to the JSCE-G 552-1999 (2005), in order to obtain the deflection of the neutral axis and account for support settlement, if any. The quasi-static flexural tests were conducted at a constant displacement rate at 0.1 mm/min. A data acquisition system was used to record the load, stroke, and midspan displacement at 5 Hz.

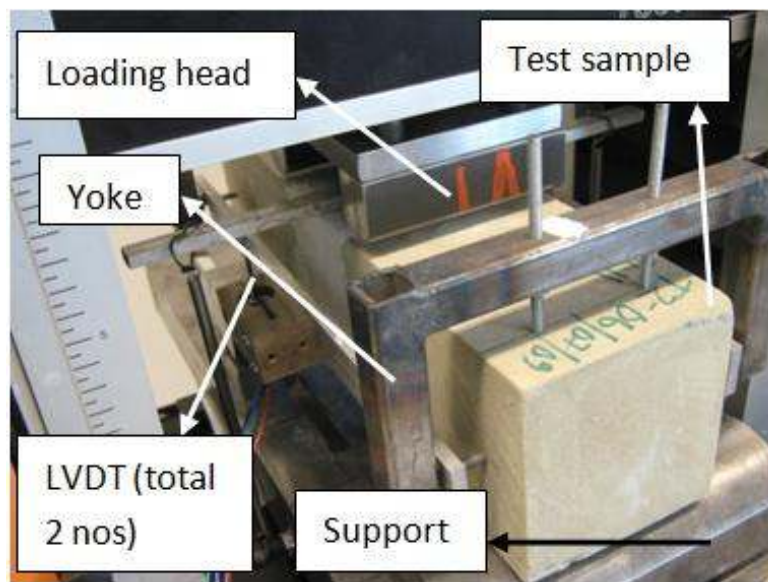


Figure 3.8 Quasi-Static Test in Progress for Flexure on Masonry Units

3.4.2 Impact Testing

An instrumented drop-weight impact tester, as shown in Figure 3.9, was employed to generate high rates of flexural loading. This test machine consists of a 62 kg hammer that may be raised to 2.5 m so as to generate a maximum impact energy of 1000 J. With each mortar mix, three mortar beams and three masonry

units were examined under impact from two separate heights, namely 250 mm and 500 mm. Ignoring friction, these drop heights were expected to generate an impact velocity of 2.20 m/s and 3.10 m/s, respectively. Such velocities correspond to low velocity impact loading and generate strain rates associated with seismic loading (CEB-FIP, 1990).

Since 4-point flexure is impossible to achieve under drop-weight impact, the dynamic tests were conducted in 3-point bending. The difference in shear response due to the altered load configuration was neglected. The striking edge of the impacting hammer, i.e. the loading tup, was instrumented with eight strain gauges to form the load cell. A piezoelectric accelerometer was attached below each specimen at midspan (adjacent to the notch) to gather the acceleration history, as shown in Figure 3.10. The data from the load cell and the accelerometer were recorded by a data acquisition system at 100,000 Hz. There is a load cell, equipped with a Wheatstone bridge mounted on a tup, as shown in Appendix A.7, by which it is possible to gather load history. In addition to this load and acceleration data collection system, the high strain-rate test facility drop weight impact machine is equipped with two high-speed cameras through which a stereoscopic dynamic record of the dynamic event can be obtained. Together, both cameras were set to capture images at a rate of 10,000 frame/s and these images were analyzed later with image-processing software called TEMA (TEMA, 2009) to obtain deflection, velocity, and acceleration history with time. The entire system is synchronized internally with a trigger mechanism system, as shown in Figure 3.11, through which all the data collection starts at a single time

stamp. The trigger system is equipped with an optical system that is placed a few millimetres above the specimens. When the hammer passes the sensor and cuts the infra red ray, the voltage drops from 5 V to 0 V, which automatically triggers the data collection system at that instant. While the image data was intended for future fracture evaluation, not included in this document, all analysis was based on acceleration history from the accelerometer and load history from the load cell.

Since a suddenly applied load generates an inertial response from the specimen, the inertial effects must be accounted for to evaluate the true stress load experienced by the material (Chen and Sih, 1977). The equivalent static response was derived based on the single-degree-of-freedom approach. The generalized inertial load on the specimen during impact, $P_i(t)$, was evaluated as follows (Banthia et al., 1989):

$$P_i(t) = \rho A a_o(t) \left[\frac{1}{3} + \frac{8(ov)^3}{3l^2} \right] \quad \text{Equation 3.1}$$

Where, $a_o(t)$ is acceleration at midspan of the beam at time t ; ρ is mass density for the beam material; A is cross-sectional area of the beam; l is clear span of the beam; and ov is length of overhanging portion of the beam. Also, the velocity, $v_o(t)$, and displacements histories, $d_o(t)$, at the load-point were obtained by integrating the acceleration history with respect to time.

$$v_o(t) = \int a_o(t) dt \quad \text{and} \quad d_o(t) = \int v_o(t) dt \quad \text{Equation 3.2}$$

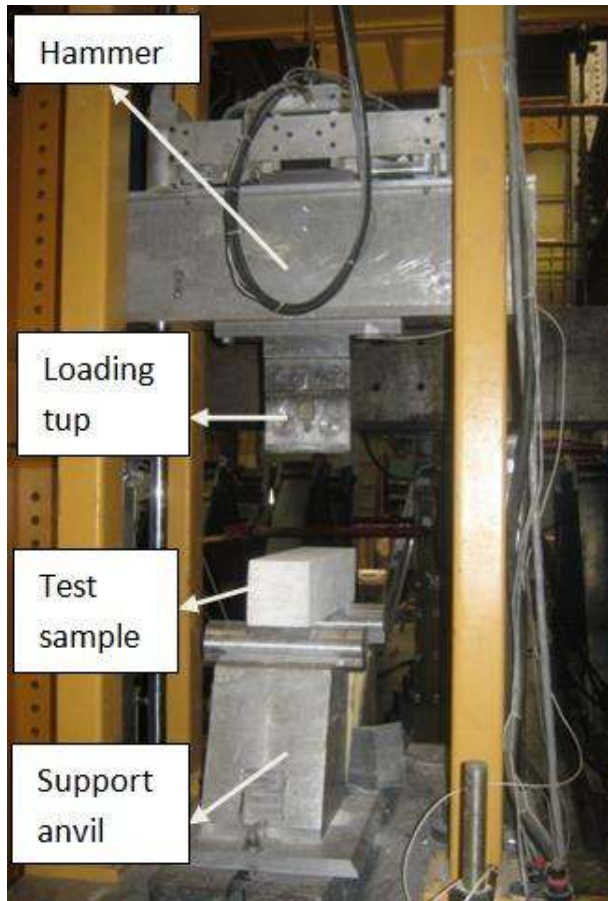


Figure 3.9 Drop-Weight Impact Tester

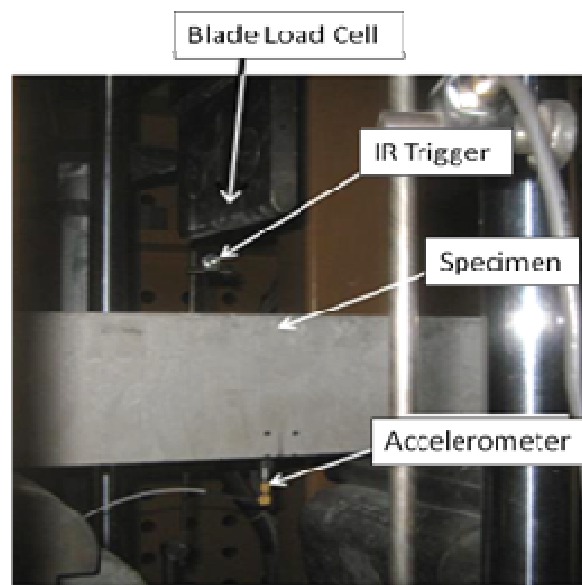


Figure 3.10 Instrumentation for High-Speed Data Acquisition

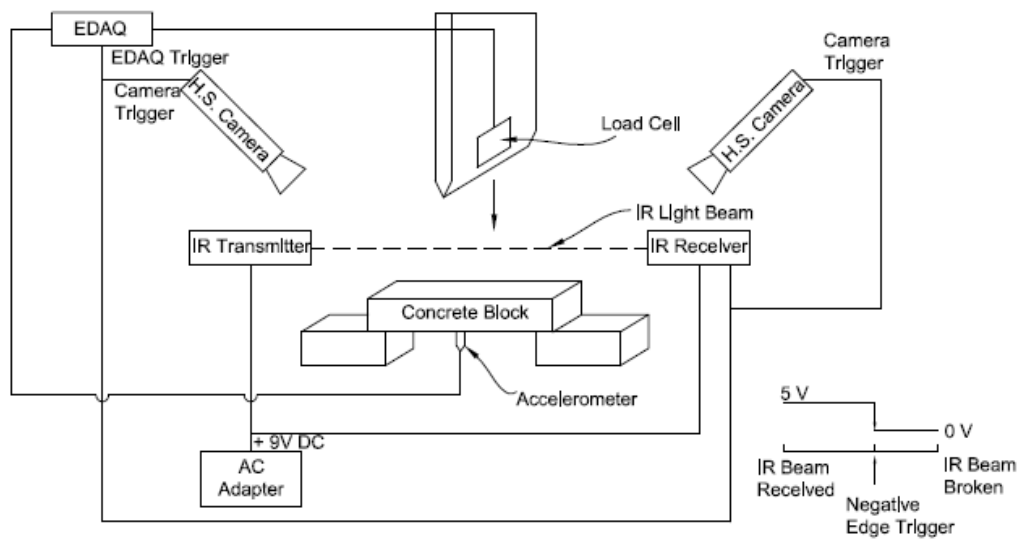


Figure 3.11 Trigger Mechanism for activating High-Speed Data Collection

CHAPTER 4 QUASI-STATIC AND IMPACT RESPONSE OF SANDSTONE BLOCKS

4.1 Introduction

The sandstone blocks that were used in this study were extracted from the Paskapoo Formation, which is local to Alberta. Three test samples for each loading rate were obtained from the batch of sandstone blocks similar to those used for testing of the masonry units. For the compression tests, two cylinders with a 50 mm diameter and 100 mm height were cored, and for the flexural tests, three beams of size 40 mm x 40 mm x 140 mm long were sawn from the sandstone blocks for each test protocol. The samples were tested as per test methods described in Chapter 3, Section 3.4. The representative curves were averaged over at least three specimens for compression, quasi-static flexure, and impact testing. The mechanical properties are summarized in Table 4.1.

4.2 Compressive Response

Two cored cylinders of size 50 mm diameter and 100 mm height were tested as per ASTM C469 (2001) by using a MTS 1000 material testing system with the use of LVDTs and an electronic data acquisition system, as discussed in Section 3.4.1.1. As seen in Figure 4.1, the compressive strength of sandstone was about 27 MPa. Although only two sandstone cylinders were examined, note that the response was very nearly identical and provides sufficient confidence as to the properties of the sandstone blocks used in this study. The elastic modulus and Poisson's ratio were 3800 MPa and 0.22, respectively. The time history for

Poisson's ratio is shown in Figure 4.2, and values in the relatively constant, middle third portion of the response were taken to represent the tested Paskapoo sandstone. A representative failure sample under quasi-static compression is shown in Figure 4.3.

Parks (1916) conducted research on different types of sandstone, locally available within Alberta. The study on Yellow Calgary sandstone, Grey-yellow Glenbow sandstone, Grey-yellow Cochrane sandstone, and Gray Macleod-Brocket sandstone revealed that the compressive strength varied from 25 MPa to 50 MPa. The compressive strength of Paskapoo sandstone that was found from this research is within this range.

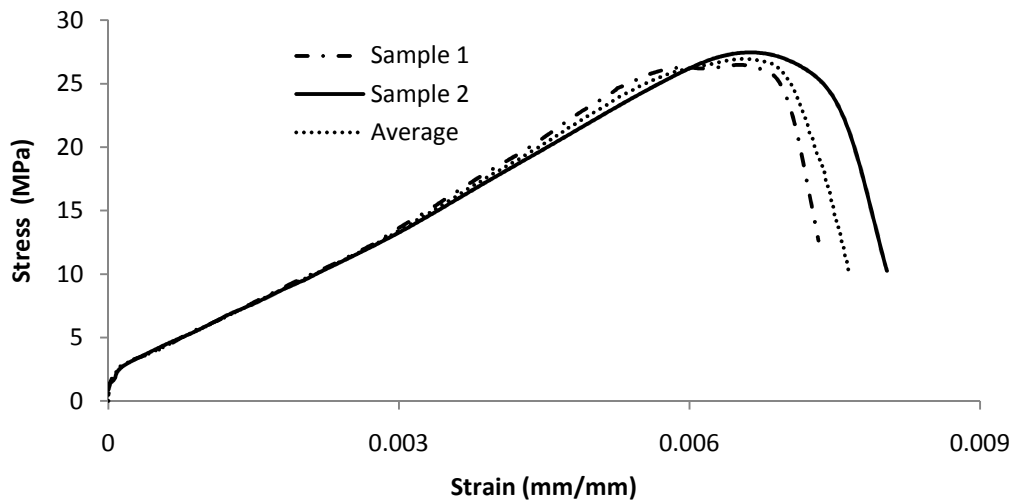


Figure 4.1 Stress-strain Response of Sandstone in Compression

Table 4.1 Mechanical Properties of Paskapoo Sandstone

Compressive strength (MPa)	Elastic modulus (MPa)	Poisson's ratio	Quasi-static flexural strength (MPa)
27	3800	0.22	5.4

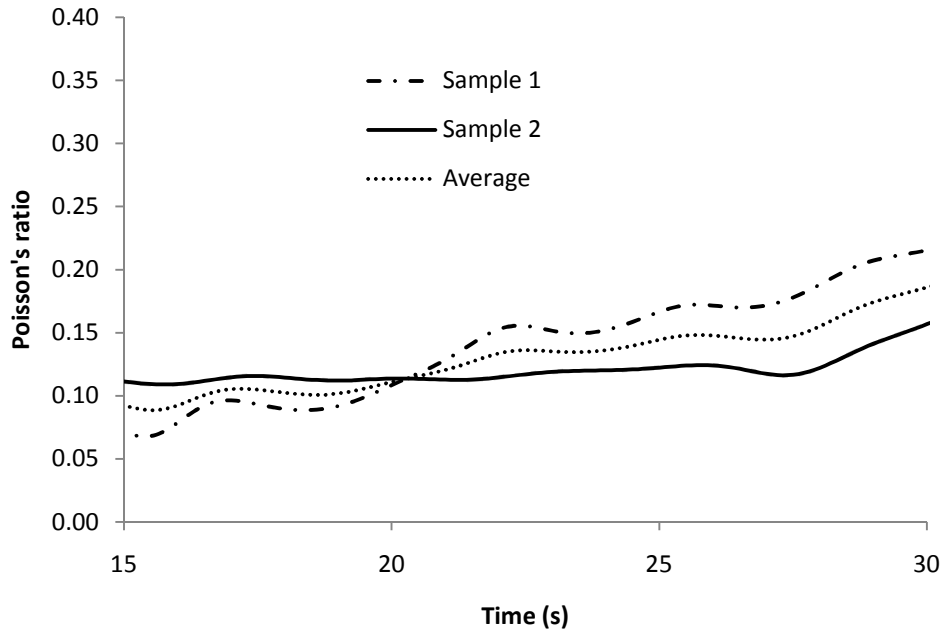


Figure 4.2 Time History of Poisson's Ratio for Sandstone



Figure 4.3 Failure of a Sandstone Cylinder under Compression

4.3 Flexural Response

Quasi-static flexural testing was done under 4-point loading on four beams of size 40 mm x 40 mm x 140 mm long with a 120 mm clear span between supports and an overhanging portion of 10 mm on each of the supports. The quasi-static flexural response of the sandstone blocks is shown in Figure 4.4. The modulus of rupture (MOR) of the sandstone blocks was found to be 5.4 MPa. The flexural strength as evaluated from the compressive strength using a standard relationship (CSA A23.3, 2004) equalled to 3.1 MPa, which was lower than that obtained from test results. Further testing is required in order to develop a suitable relationship similar to that of concrete.

For impact testing, three beams of size 40 mm x 40 mm x 140 mm long were prepared for each loading rate. The span between supports was 120 mm and the overhanging portion was 10 mm on each side of the support. The dynamic flexural responses are presented in Figure 4.5 and Figure 4.6 for 250 mm and 500 mm drop of height respectively. From these results, it is clearly evident that the flexural strength of sandstone blocks increases with the increment of loading rate. A typical failure pattern under flexural loading condition is shown in Figure 4.7. As this is the first known study on the dynamic flexural response of sandstone, there was no literature available to compare this result with others of the same kind.

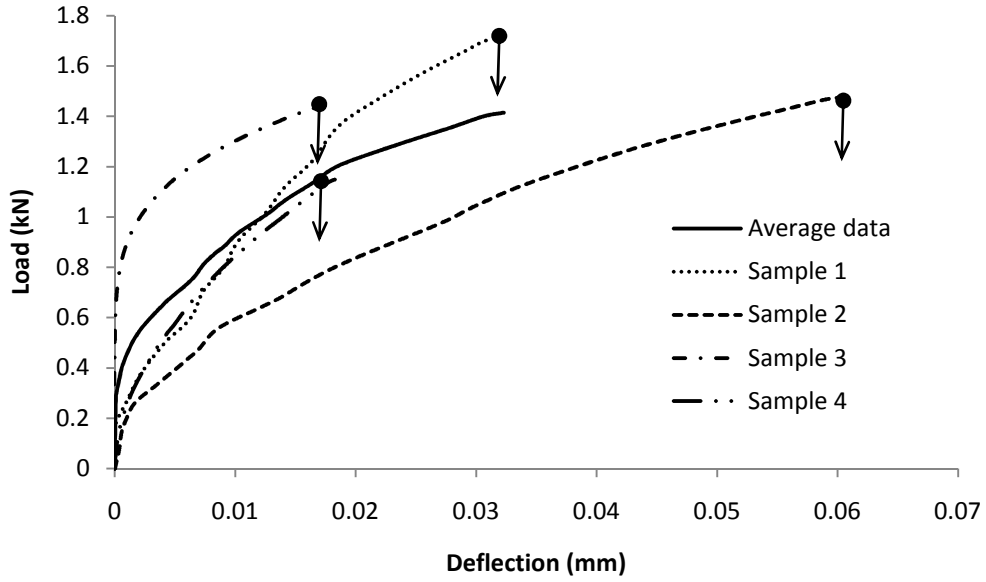


Figure 4.4 Load-deflection Response under Quasi-Static Flexure for Sandstone Prisms

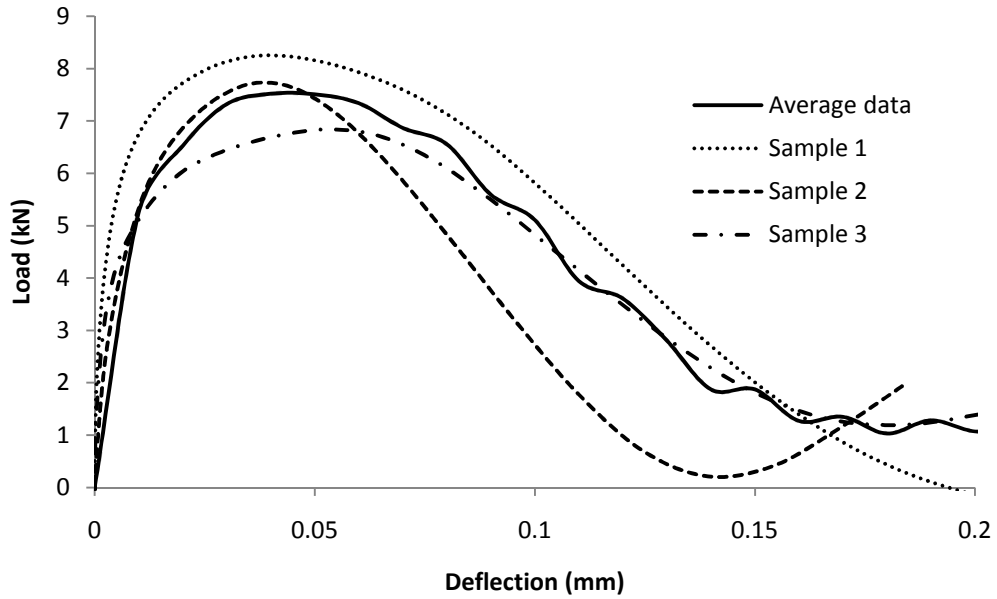


Figure 4.5 Flexural Load-deflection Response under Impact from Drop Height of 250 mm for Sandstone Prisms

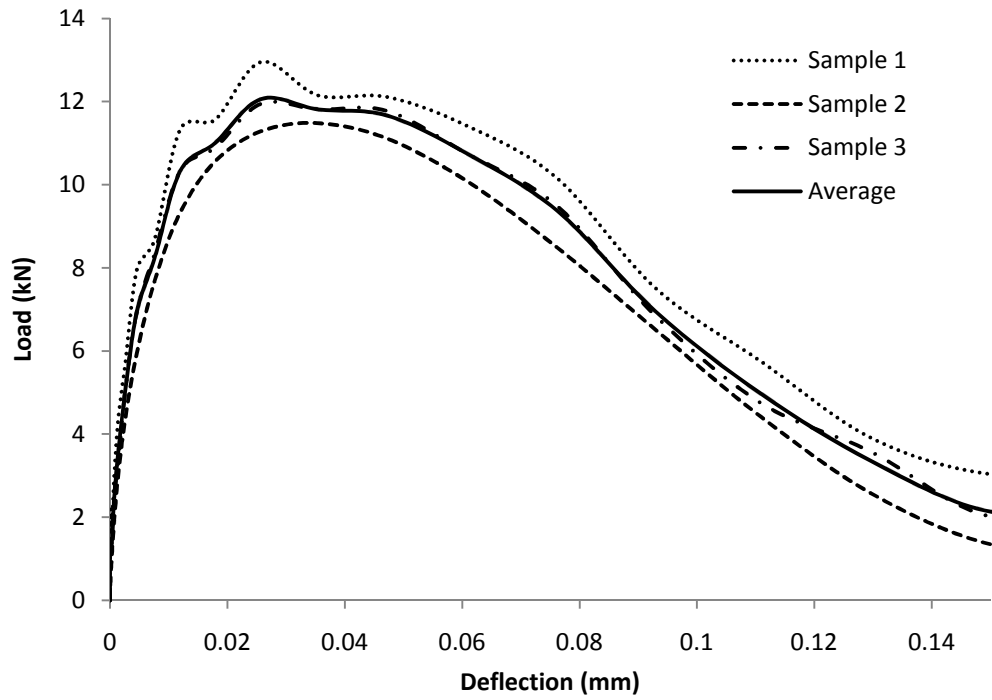


Figure 4.6 Flexural Load-deflection Response under Impact from Drop Height of 500 mm for Sandstone Prisms



Figure 4.7 Failure of a Sandstone Prism under Flexure

4.4 Flexural Toughness Factor

The flexural toughness factor (FTF) values were calculated for different loading rates using JSCE G-552 (2005). The FTF values for sandstone are presented in Figure 4.8. As expected, the sandstone blocks exhibit increased toughness with an increase in the loading rate. It can be seen that sandstone tested under impact with a drop height of 250 mm absorbs five times energy as much as quasi-static loading configuration. A 60% increment in FTF was observed when the loading rate changed from 250 mm drop height to 500 mm drop height.

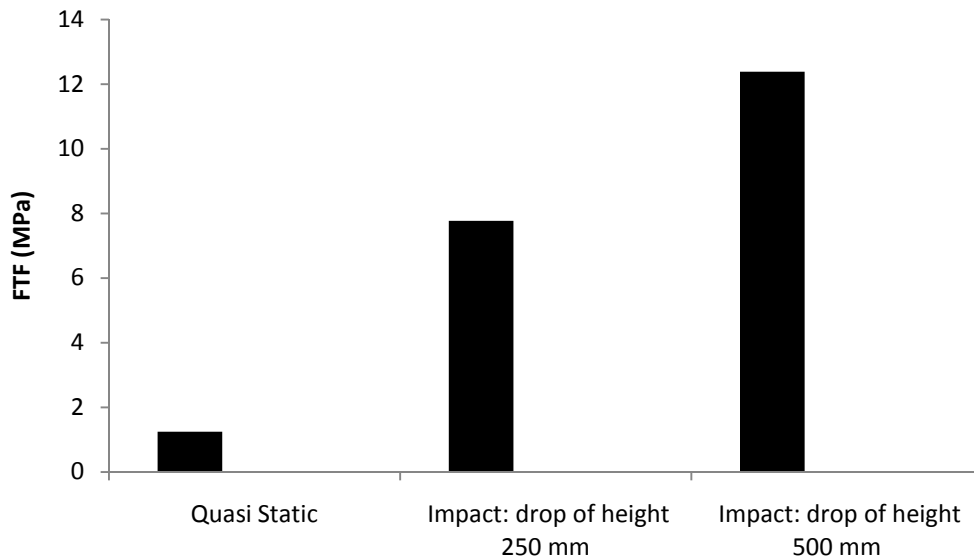


Figure 4.8 Flexural Toughness Factor for Sandstone Blocks

4.5 Rate Effects

The stress-rate sensitivity was expressed in terms of the dynamic impact factor (DIF), defined as the ratio of the dynamic to static strength (flexural and/or bond strength), and is shown for the flexural strength of sandstone blocks in Figure 4.9. The stress-rate was calculated by assuming a constant loading rate, although

the actual stress history was non-linear. The DIF depends on the stress-rate and not only on the quasi-static strength of material. The Malvar-Ross modification to the CEB-FIP model expressed in Equation (2.2) is shown alongside. From this it can be concluded that the Paskapoo sandstone block is stress rate sensitive and its sensitivity is more or less equal to that provided by the modified CEB-FIP expression. This agrees with Kubota *et al.* (2008), who found that the Japanese sandstone also obeyed the CEB-FIP expression shown in Equation 2.1. On the other hand, Zhao & Li (2000) found that granite displayed a lower rate sensitivity.

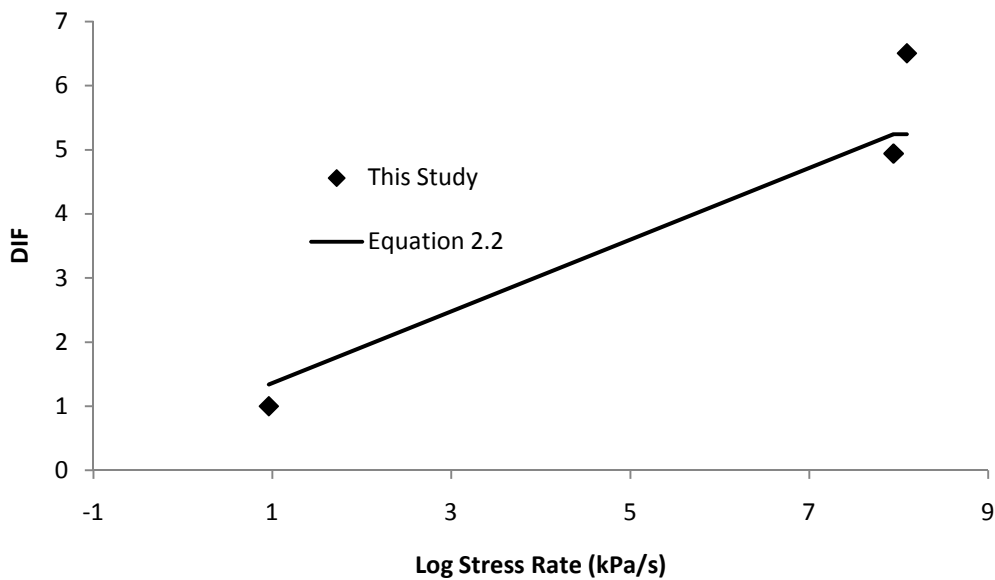


Figure 4.9 Stress Rate Sensitivity of Flexural Strength of Sandstone Blocks

4.6 Conclusions

Based on this study of sandstone blocks, the following conclusions can be made:

- ❖ The flexural strength of Paskapoo sandstone is sensitive to higher loading rates, and this stress rate sensitivity conforms to the model developed for concrete (Modified CEB-FIP model).
- ❖ The flexural toughness factor of this local sandstone increases with an increase in the loading rate.

CHAPTER 5 QUASI-STATIC AND IMPACT RESPONSE OF SANDSTONE MASONRY UNITS BOUND WITH TYPE S MORTAR

5.1 Introduction

This chapter describes the first phase involving tests on mortar and masonry units based on plain and fibre-reinforced Type S cement-lime mortars. As discussed in Chapter 3, Section 3.3, commercially available polypropylene microfibres were introduced at 0.25% and 0.50% volume fraction to render three mortar mixes together with a reference plain mix. These mortar mixes were characterized in quasi-static compression to establish reference mechanical properties. The stress rate sensitivity of the flexural response of such mortars was established, followed by an examination of rate effects on the flexural bond in masonry units. The post-peak response was characterized along the standard guidelines for fibre-reinforced concrete through flexural toughness factors as per JSCE G-552 (2005).

5.2 Compressive Response

The stress-strain response in compression for the Type S masonry mortars is shown in Figure 5.1, with their mechanical properties evaluated as listed in Table 5.1. Although the Type S mortars were cast to have a compressive strength of 15 MPa, they were found to be 40% stronger. It brings to the fore that in mixing masonry mortar, flexibility in the mix design is advised so that a desired compressive strength may be achieved. Strictly adhering to a mix design may result in significantly overshooting the target strength. Nevertheless, with

consistency across mixes, the higher compressive strength was accepted for this study. This chapter therefore evaluates stone masonry, where the compressive strength of the mortar and the stone are comparable. The quasi-static tests were conducted at 500 kPa/s. The time history for Poisson's ratio is shown in Figure 5.2, and values in the relatively constant, middle third portion of the response were taken to represent each of the three mortar types. The data indicates a drop in value with higher fibre content. Three specimens were tested and averaged to get each data point corresponding to every mortar mix. Whereas the sandstone was only 30% stronger in compression than the mortars, the modulus of elasticity of the mortar was approximately 2.5 times that of the sandstone. The elastic modulus of the specimens with fibres was significantly less than that of plain mortar. However, the latter matched the findings by Hao and Tarazov (2009).

The shear modulus as evaluated from the modulus of elasticity and Poisson's ratio were in the range of 3500 – 4000 MPa, as shown in Table 5.1. A representative specimen that failed under compression is shown in Figure 5.3 for plain mortar and in Figure 5.4 for fibre-reinforced mortar.

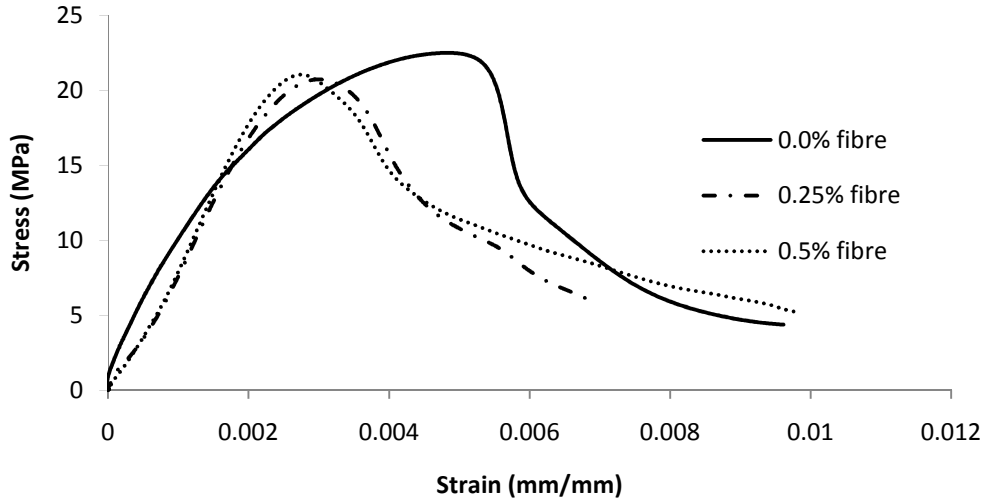


Figure 5.1 Compressive Response of Type S Mortar

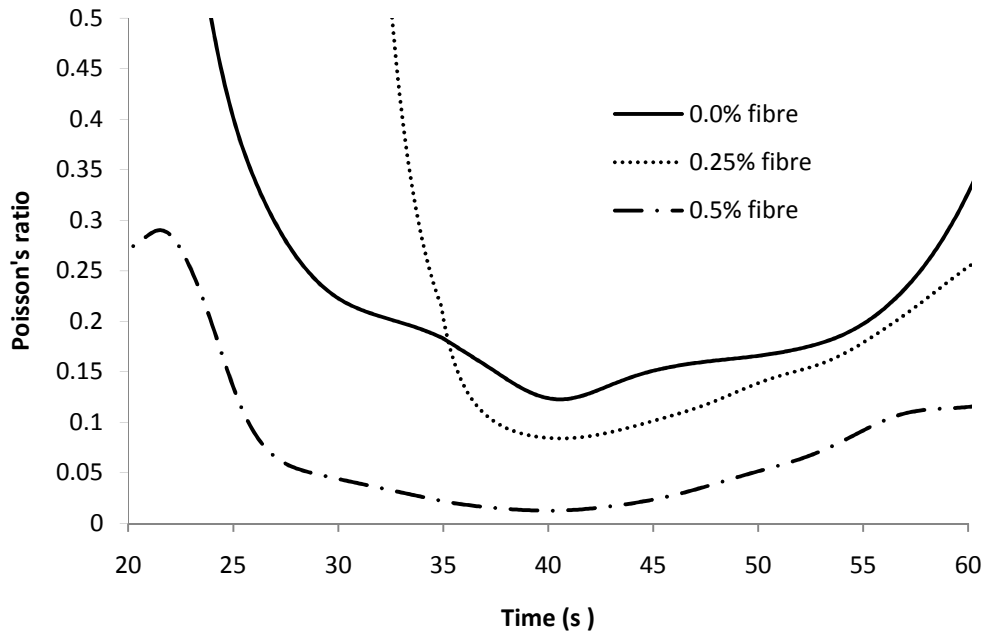


Figure 5.2 Time History of Poisson's Ratio for Type S Mortar



Figure 5.3 Failure of Cylinder for Plain Type S Mortar under Compression



Figure 5.4 Failure of Cylinder for Fibre-reinforced Type S Mortar under Compression

Table 5.1 Compressive Response of Plain and Fibre-reinforced Type S Mortar

Mix	f'_c (MPa)			E_c (MPa)			Poisson's ratio			G (MPa)
	Value	σ^*	C_v^{**} (%)	Value	σ^*	C_v^{**} (%)	Value	σ^*	C_v^{**} (%)	
0.00 % V_f	22	0.87	3.99	9280	286	3.0	0.17	0.013	7.79	3970
0.25 % V_f	21	2.70	12.98	7535	1147	15.2	0.09	0.019	21.35	3460
0.5% V_f	21	3.21	15.39	7900	862	10.9	0.04	0.010	25.37	3800

* Standard Deviation; ** Coefficient of Variation

5.3 Flexural Response

The flexural responses of mortar and masonry units under quasi-static and impact loading presented here were taken as the average of at least three specimens. The statistical variations were evaluated in terms of standard deviation and coefficient of variation.

5.3.1 Mortar

The quasi-static flexural response of the Type S mortars is shown in Figure 5.5, while their flexural impact response is shown in Figure 5.8 for drop height of 250 mm and in Figure 5.9 for drop height of 500 mm. Under quasi-static loading, note that there was no post-peak residual strength carrying capacity for either the plain or fibre-reinforced mortars. Further, whereas the compressive strength for the three mixes was within a 10% spread, there was a 33% reduction in the flexural strength when the fibre content was raised from 0.25% to 0.50% volume fraction. This is likely due to variation in fibre dispersion, which manifests itself due to lower workability in masonry mortar. However, under

impact loading, the flexural strength was highest for the mix containing fibres at 0.50% volume fraction. The mechanical properties as evaluated from the flexural response of Type S mortar and masonry units are summarized in Table 5.2.

5.3.2 Masonry Units

The quasi-static flexural response of the masonry units is shown in Figure 5.10, while the response under impact loading is shown for a drop height of 250 mm and 500 mm in Figure 5.11 and Figure 5.12, respectively. It is clear that fibre reinforcement consistently improved the flexural bond strength under all rates of loading. Of considerable significance was the failure mode in each case. Whereas those units bound with plain mortar failed at the mortar-block interface (Figure 5.6), the masonry units bound with fibre-reinforced mortars consistently failed through fracture in the stone block (Figure 5.7). This transition in the mode of failure implies an improvement in the stone-mortar interface in the presence of discrete microfibres. The exact cause for the stronger interface is not clear. Such an improvement is likely due to the improved packing of hydration products at the paste-rock interface through modified wall effect and moisture dispersion, which lead to a densified transition zone (Bentur and Alexander, 2000). The failure patterns confirm the results obtained by Sarangapani *et al.* (2005) and Costigan and Pavia (2009), in that a stronger mortar led to block failure. Banthia and Dubeau (1994) believe this happens due to the reduction in paste shrinkage. So that, the weakest section is no longer at the stone-mortar interface but moves to within the stone block.

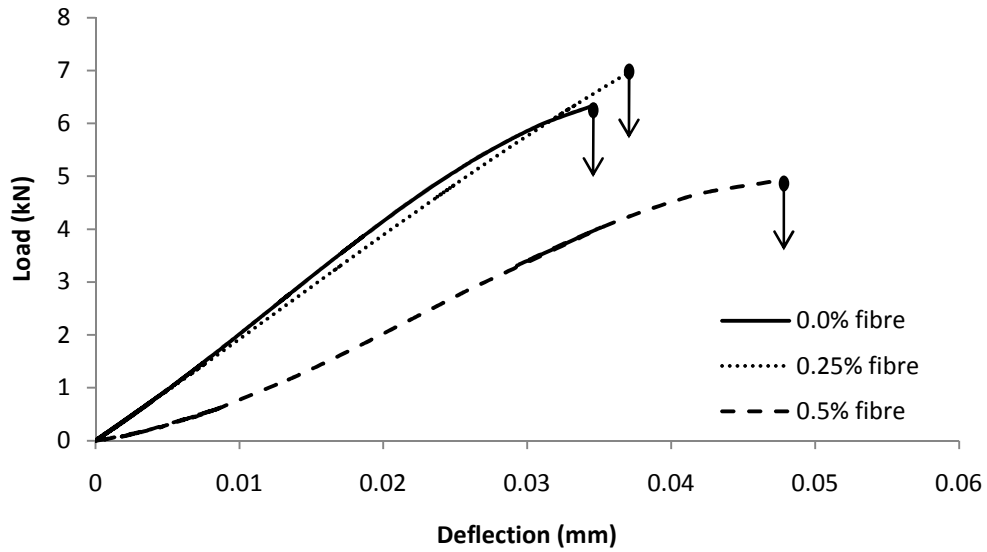


Figure 5.5 Load-deflection Response under Quasi-Static Flexure for Type S Mortar



Figure 5.6 Failure of Masonry Unit for Plain Type S Mortar under Flexure. Note Failure Plane at the Stone-mortar Interface.



Figure 5.7 Failure of Masonry Unit for Fibre-reinforced Type S Mortar under Flexure. Note Failure Plane passes through the Stone Block.

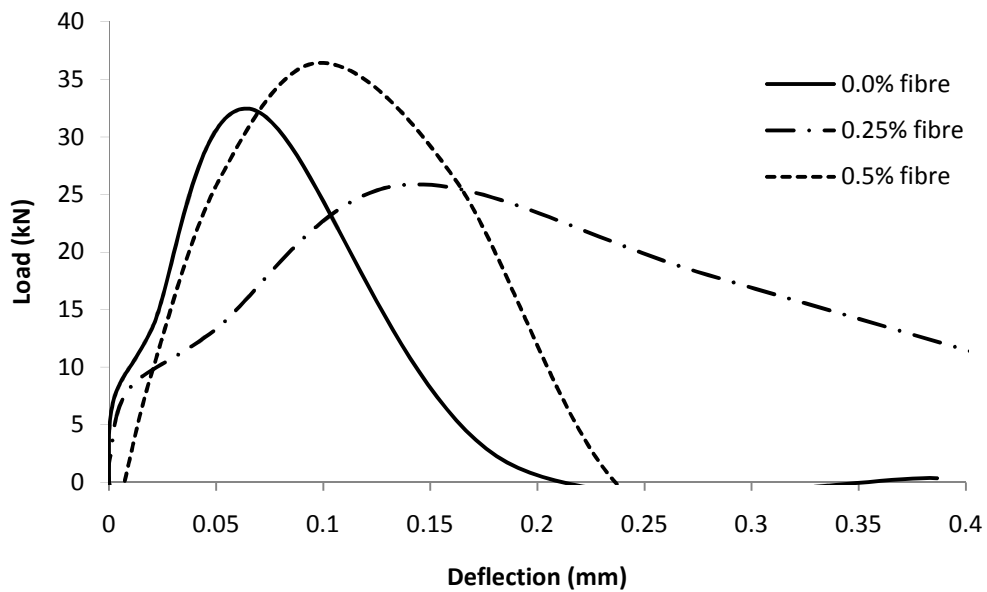


Figure 5.8 Flexural Load-deflection Response under Impact from Drop Height of 250 mm for Type S Mortar

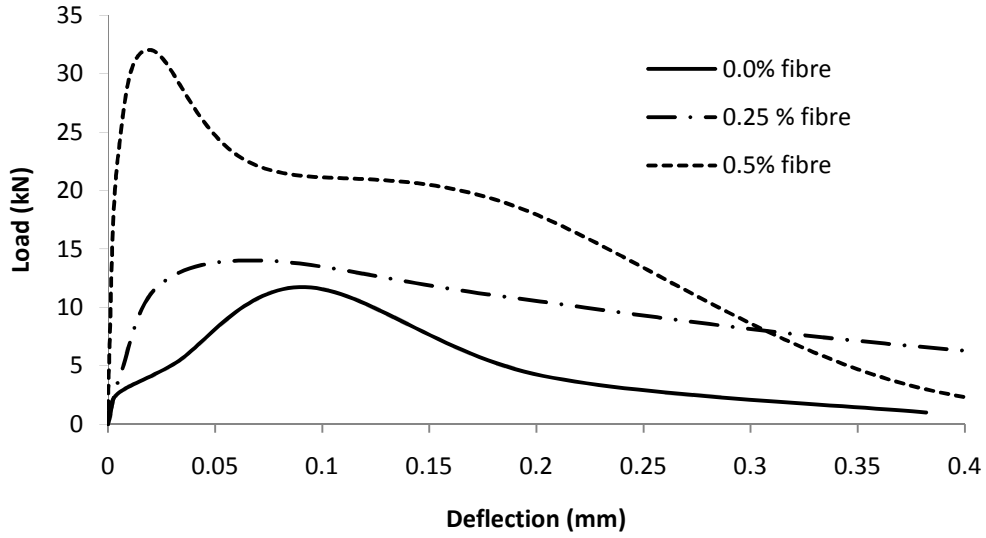


Figure 5.9 Flexural Load-deflection Response under Impact from Drop Height of 500 mm for Type S Mortar

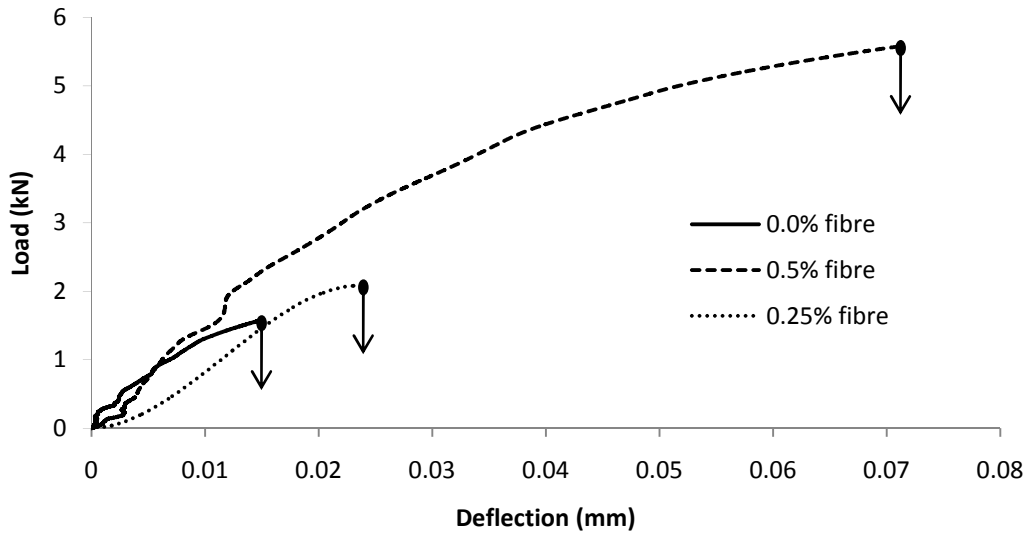


Figure 5.10 Load-deflection Response under Quasi-Static Flexure for Masonry Units bound with Type S Mortar

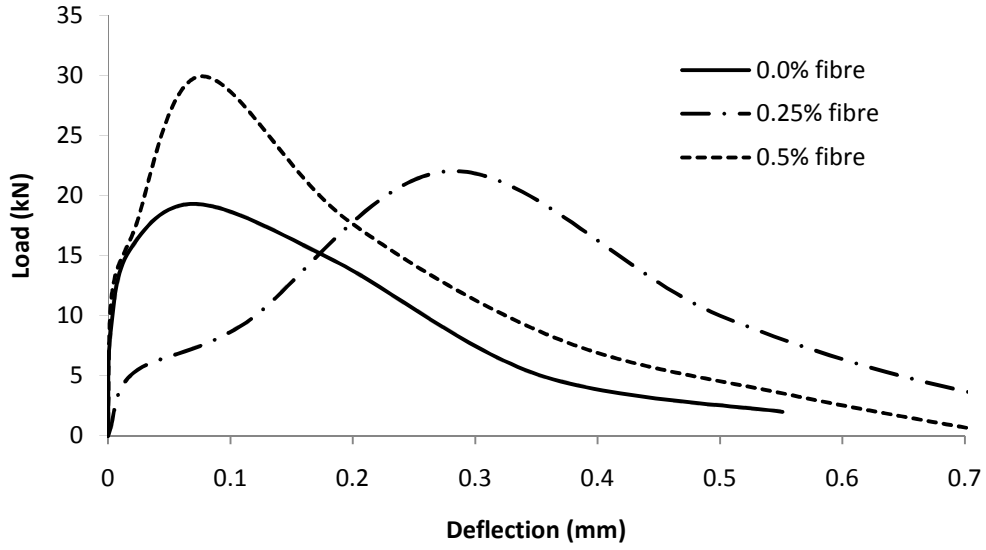


Figure 5.11 Flexural Load-deflection Response under Impact from Drop Height of 250 mm for Masonry Units bound with Type S Mortar

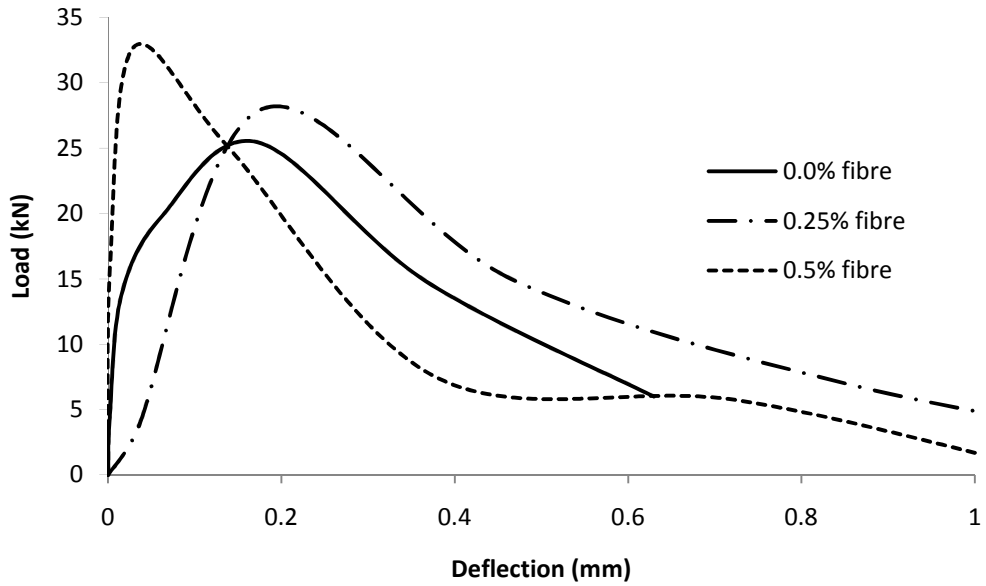


Figure 5.12 Flexural Load-deflection Response under Impact from Drop Height of 500 mm for Masonry Units bound with Type S Mortar

Table 5.2 Flexural Response of Mortar Beams and Masonry Units for Type S Mortar

Specimen	Tests	Fibre (%)	Peak Load (kN)			FTF (MPa)		
			Value	σ^*	C_V^{**} (%)	Value	σ^*	C_V^{**} (%)
Mortar Beam	Quasi Static Tests	0	6.52	0.18	2.88	1.3	0.29	22.54
		0.25	7.40	0.34	4.59	1.24	0.37	30.24
		0.5	4.95	0.46	9.40	1.08	0.15	13.85
	Impact Tests Drop height = 250 mm	0	32.30	9.20	39.02	3.06	0.26	8.59
		0.25	25.79	3.43	15.58	5.09	0.73	14.38
		0.5	36.44	9.67	37.98	8.06	1.28	15.92
	Impact Tests Drop height = 500 mm	0	11.74	2.93	24.95	1.93	0.27	14.15
		0.25	14.00	13.99	30.84	1.52	0.29	19.54
		0.5	32.05	7.23	22.56	5.87	0.55	9.51
Masonry Unit	Quasi Static Tests	0	1.58	0.24	15.46	0.25	0.05	23.68
		0.25	2.08	0.10	4.76	0.35	0.06	18.51
		0.5	5.58	1.07	18.70	1.09	0.15	14.37
	Impact Tests Drop height = 250 mm	0	19.29	4.08	21.16	2.64	0.92	35.15
		0.25	22.04	4.04	18.31	3.29	0.72	22.16
		0.5	29.94	5.35	17.9	2.42	0.27	11.49
	Impact Tests Drop height = 500 mm	0	25.47	10.21	40.10	3.50	0.39	11.37
		0.25	28.00	6.63	23.68	3.63	0.55	15.40
		0.5	32.76	9.87	30.12	3.34	0.59	17.72

* Standard Deviation; ** Coefficient of Variation

5.4 Flexural Toughness Factor

The energy dissipated during flexure was evaluated through flexural toughness factors (FTF) as per JSCE-G 552 (2005) as follows:

$$T_f = \frac{A.L}{\delta_{max}bh_e^2} \quad \text{Equation 5.1}$$

Where, T_f is the flexural toughness factor (MPa); A is the area under the load-deflection curve up to a deflection of δ_{max} (N-mm); L is the beam span (mm); δ_{max} is equal to $L/150$ (mm); b is the effective width of the specimen (mm); and h_e is the effective depth at notch (mm).

While the FTF was always higher in fibre-reinforced mortars, this was more apparent under impact from the higher drop height (Figure 5.13). However, for the masonry units, the FTF values revealed an optimal fibre content, in this case at 0.25% volume fraction. Note that the addition of fibres consistently increased the flexural bond strength in the masonry units at all loading rates. Clearly, there lies a trade-off when it comes to improving the bond between the mortar and the stone block – as the fracture plane switched from the mortar-block interface to within the stone block, the masonry unit became more brittle.

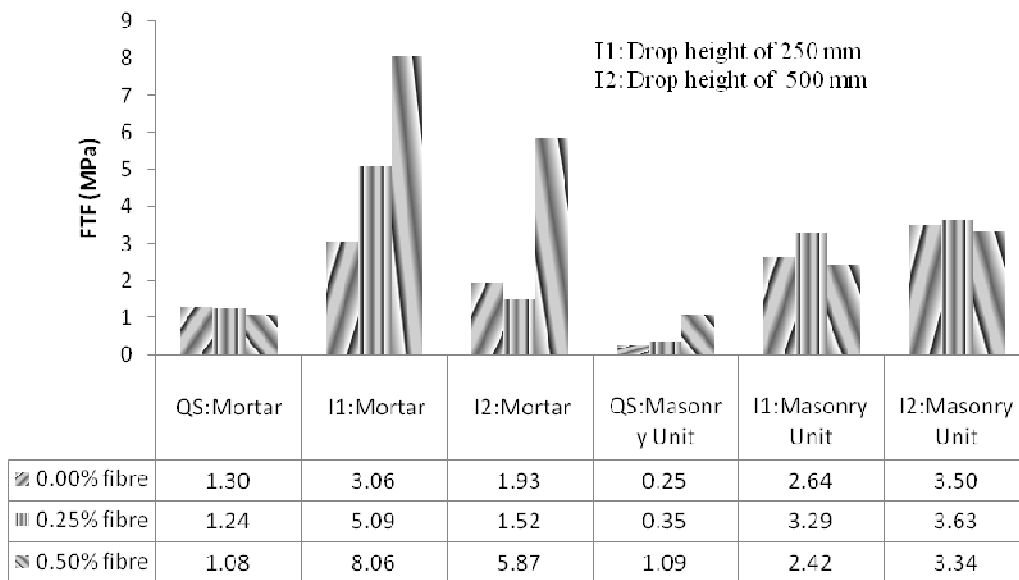


Figure 5.13 Flexural Toughness Factor for Masonry Unit and Type S Mortar

5.5 Rate Effects

The stress rate sensitivity was expressed in terms of the dynamic impact factor (DIF) defined in Section 2.7, as the ratio of flexural strength under any stress rate to that obtained from ASTM C1609 (2007) and is shown for the flexural strength of mortars in Figure 5.14. The Malvar-Ross modification to the CEB-FIP model expressed in Equation (2.2) is shown alongside. Research by Hao and Tarazov (2008) has shown a 10% drop in the quasi-static modulus of elasticity in cement- lime mortar for the range of strain rates in the present study. Nevertheless, the quasi-static measure of the elastic modulus from Table 3 was considered acceptable to generate the bilinear expression for stress rate sensitivity from Equation (2.2), shown in Figure 5.14 for $f'_c = 21$ MPa (to correspond to the compressive strength of the mortars). In past research reports, a DIF of 2 was obtained by Glinicki (1994) for mortars and by Bindiganavile (2003) for concrete, when examined at 10^5 kPa/s. Note from Figure 5.14 that the plain Type S mortar and the mix reinforced with 0.25% fibre volume fraction were in agreement with the modified CEB-FIP expression, whereas the mix with 0.5% fibre volume fraction was significantly more stress rate sensitive. However, the role of fibres on stress rate sensitivity of the mortar strength was not clear from this study, as the flexural strength of the material dropped with the increase in loading rate. The possible reason could be the effect of fibre dispersion onto mortar.

The dynamic impact factors for the flexural bond strength of masonry units are shown in Figure 5.15. Note that the stress rate sensitivity of the flexural bond

strength was higher than that for the flexural strength of the mortar alone. For the three mortar mixes investigated, it is clear that adding fibres decreased the rate sensitivity of the bond. Since the failure plane in the presence of fibres was through the sandstone, it is likely that the lower stress rate sensitivity of the joint is a reflection of the relatively smaller stress rate sensitivity of brittle rocks when compared with that of fibre-reinforced Type S mortar. This is consistent with the DIF obtained from experimental test results of sandstone, as seen from Figure 4.9, which shows a lower value than that of Type S mortar. The dynamic impact factors in Figure 5.15 were significantly higher than those reported by Burnett *et al.* (2007). This difference is likely due to the difference in test methods, since the drop-weight technique employs larger specimens but smaller velocities to develop the same stress rate. As there is no literature available to compare the two impact test methods, it is recommended to conduct research on the same material with both techniques.

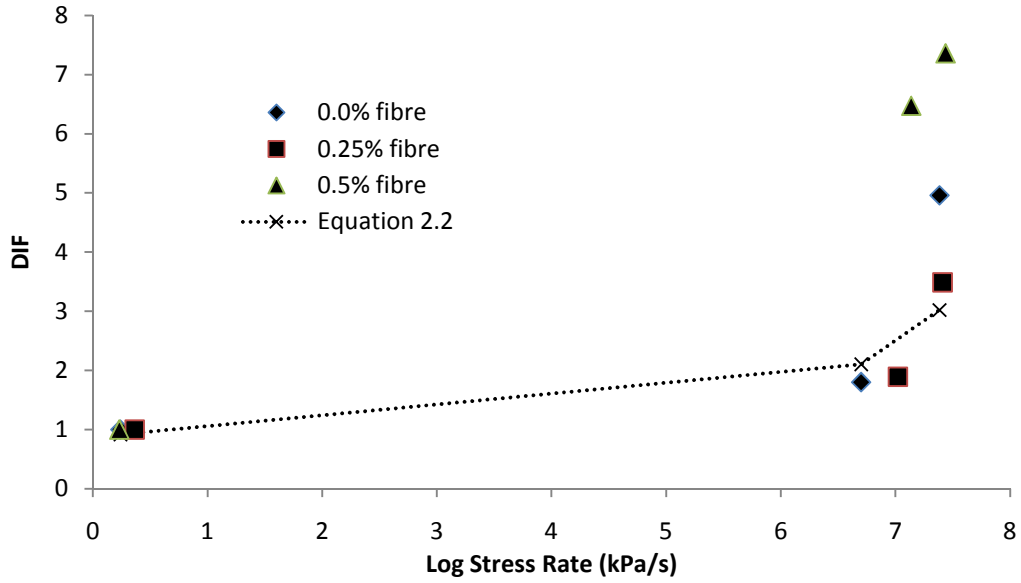


Figure 5.14 Stress Rate Sensitivity of Flexural Strength of Type S Mortar Shown for Various Fibre Contents

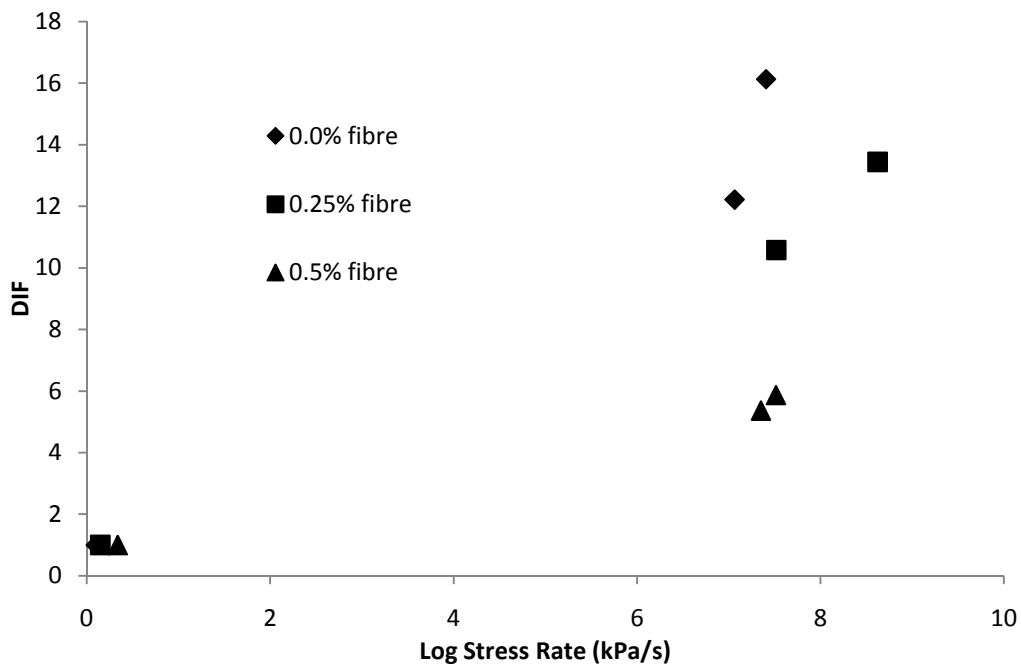


Figure 5.15 Stress Rate Sensitivity of Bond Strength of Masonry Unit with Type S Mortar Shown for Various Fibre Contents

5.6 Conclusions

Based on the results reported here, the following conclusions may be drawn:

- ❖ The dynamic responses of plain and fibre-reinforced Type S mortars are sensitive to high stress rates. While the modified CEB-FIP expression captures the stress rate sensitivity of the flexural strength of plain Type S mortar, it underestimates that with fibre reinforcement.
- ❖ The flexural bond strength is more sensitive to stress rate than the flexural strength of the mortar at similar drop heights. However, the addition of fibres consistently decreases the rate sensitivity of the flexural bond strength.
- ❖ The addition of polypropylene microfibres to the Type S mortar transforms the mode of failure in sandstone masonry units from failure at the stone-mortar interface to fracture within the stone. This is true at all loading rates.
- ❖ Due to the trade-off between higher bond strength and lower flexural toughness factors, there exists an optimal dosage of fibres that may be added to Type S mortars in order to achieve the maximum bond energy at high stress rates.

CHAPTER 6 QUASI-STATIC AND IMPACT RESPONSE OF SANDSTONE MASONRY UNITS BOUND WITH HYDRAULIC LIME MORTAR (HLM)

6.1 Introduction

This chapter describes the second phase involving tests on mortar and masonry units based on plain and fibre-reinforced hydraulic lime mortars. As discussed earlier, commercially available polypropylene microfibres were introduced at 0.25% and 0.50% volume fraction with a reference plain mixture. These mortar mixes were characterized in quasi-static compression, quasi-static and dynamic flexure. The stress rate sensitivity of the flexural response and rate effects on the flexural bond in masonry units are also examined. The post-peak response was characterized through flexural toughness factors as per JSCE G-552 (2005).

6.2 Compressive Response

The stress-strain response in compression for plain and fibre-reinforced HLM is shown in Figure 6.1, with the mechanical properties listed in Table 6.1. The data indicates a drop in elastic modulus with fibre reinforcement. A typical failure specimen under compression is shown for plain HLM in Figure 6.2 and in Figure 6.3 for fibre-reinforced hydraulic lime mortar. It is clear from the pictorial representation that the presence of numerous cracks in fibre-reinforced mortar bears the evidence of some difficulty in workability and hence slightly lower resistance. The elastic modulus, which decreased with fibre reinforcement, was in all cases less than half that of the sandstone. The Poisson's ratio of the HLM was about 0.18 for the plain mortar, and for the fibre-reinforced mortars, it was

0.19 and 0.30 respectively, with 0.25% and 0.5% fibre volume fraction as seen from Figure 6.4. The shear modulus of HLM evaluated from Modulus of elasticity and Poisson's ratio was found to be in the range of 500-800 MPa with the reduced value associated with fibre-reinforced mortar.

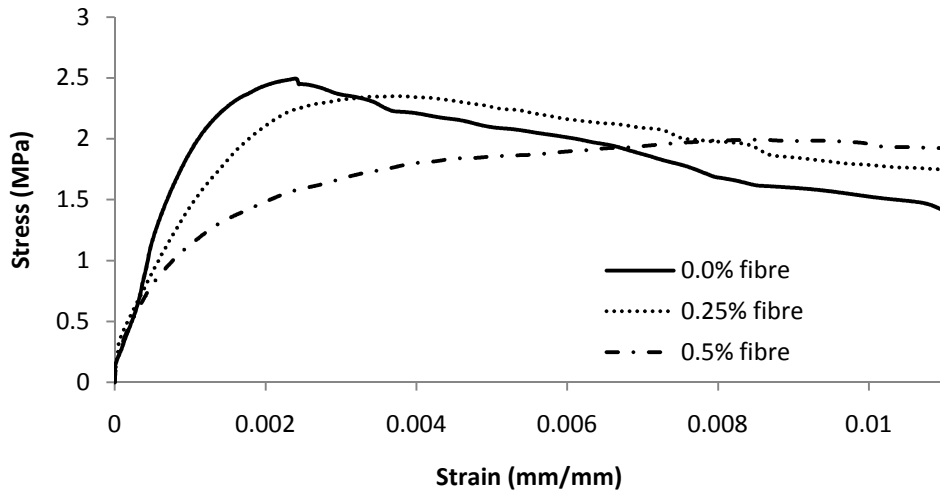


Figure 6.1 Compressive Response of Hydraulic Lime Mortar



Figure 6.2 Failure of Cylinder for Plain Hydraulic Lime Mortar under Compression



Figure 6.3 Failure of Cylinder for Fibre-reinforced Hydraulic Lime Mortar under Compression

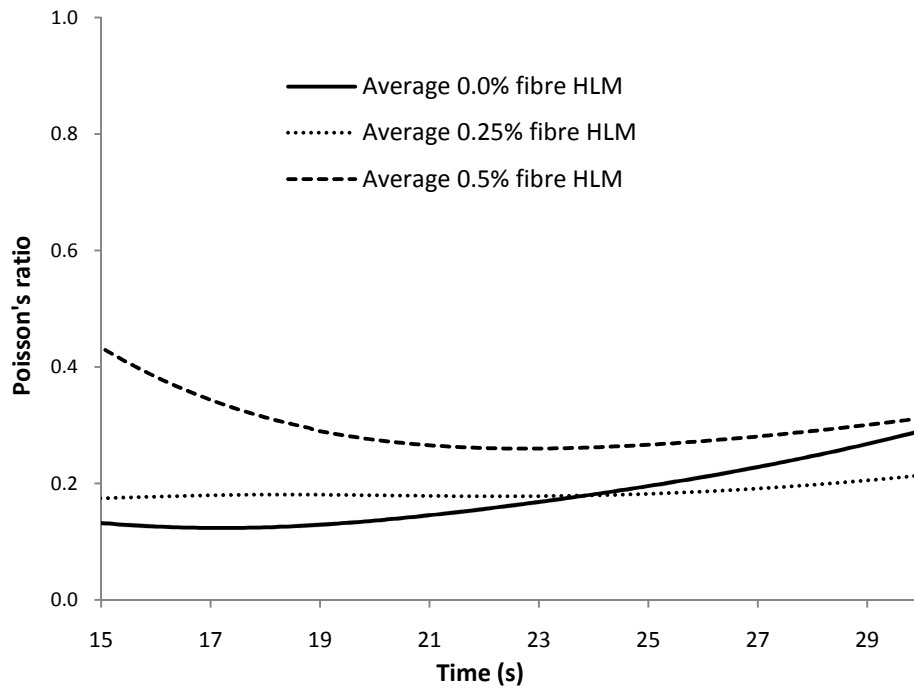


Figure 6.4 Time History of Poisson's Ratio for Hydraulic Lime Mortar

Table 6.1 Compressive Response of Plain and Fibre-reinforced Hydraulic Lime Mortar

Mix	f'_c (MPa)			E_c (MPa)			Poisson's ratio			G (MPa)
	Value	σ^*	C_v^{**} (%)	Value	σ^*	C_v^{**} (%)	Value	σ^*	C_v^{**} (%)	
0.00% V_f Fibre	2.5	0.64	25.4	1930	384	19.8	0.18	0.04	23.7	820
0.25% V_f Fibre	2.4	0.56	23.4	1380	286	20.7	0.19	0.03	15.4	580
0.50% V_f Fibre	2.0	0.05	2.4	1320	388	29.4	0.30	0.06	20.8	510

* Standard Deviation; ** Coefficient of Variation

6.3 Flexural Response

6.3.1 Mortar

The quasi-static responses of plain and fibre-reinforced HLM are shown in Figure 6.5, while their dynamic response is shown in Figures 6.6 and 6.7 for drop heights of 250 mm and 500 mm, respectively. The mechanical properties are listed in Table 6.2. As expected, a post-peak residual strength capacity was witnessed in fibre-reinforced mortars. The addition of fibres increased the flexural strength of the mortar at quasi-static loads, but whereas dynamic loading resulted in an increase in the flexural strength for all mortars, the role of fibres was not clear. There was an optimum fibre dosage (in this case = 0.25% V_f) that resulted in maximum flexural strength for higher drop heights. It was observed that the addition of fibre at a dosage level more than 0.25% volume fraction rendered a less workable mix.

6.3.2 Masonry Units

The quasi-static flexural response of the masonry units is shown in Figure 6.8, while the response under impact loading is shown for a drop height of 250 mm and 500 mm in Figures 6.9 and 6.10, respectively. Note that the addition of fibres led to higher flexural bond strength at quasi-static and low impact loads. However, for the 500 mm drop, the strongest bond performance was with the plain HLM. The role of fibres may be explained through an examination of the failure mode as illustrated in Figure 6.11 and Figure 6.12. Whereas the mode of failure in the masonry units under quasi-static loading was through fracture at the mortar-block interface (Figure 6.11), the failure plane transferred to within the mortar under dynamic loading (Figure 6.12), particularly with fibre reinforcement. This shifting of the failure plane was observed for all fibre-reinforced HLM.

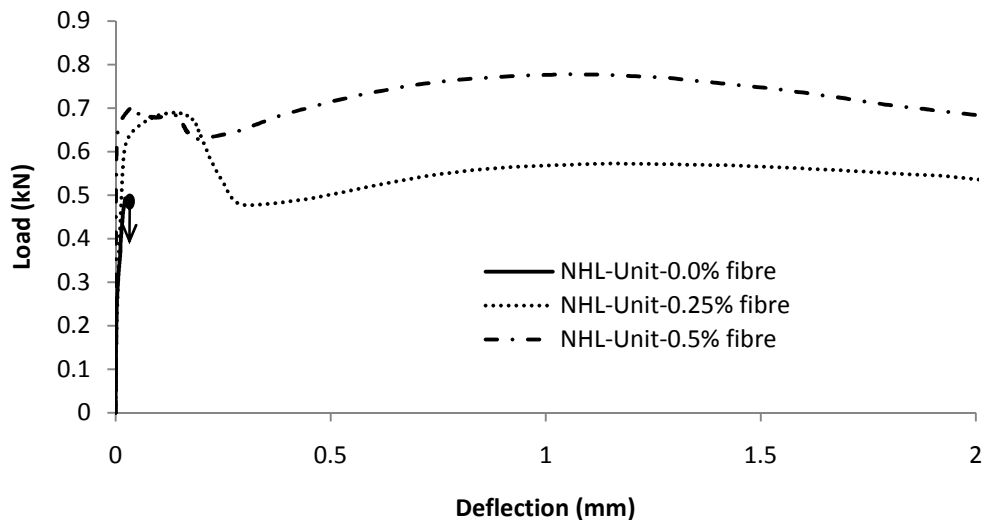


Figure 6.5 Load-deflection Response under Quasi-Static Flexure for Hydraulic Lime Mortar

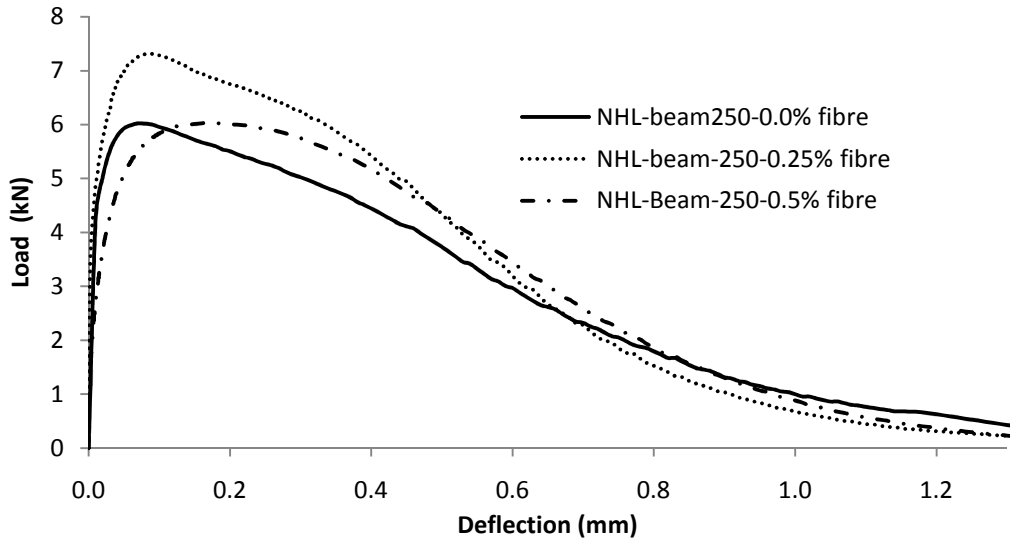


Figure 6.6 Flexural Load-deflection Response under Impact from 250 mm for Hydraulic Lime Mortar

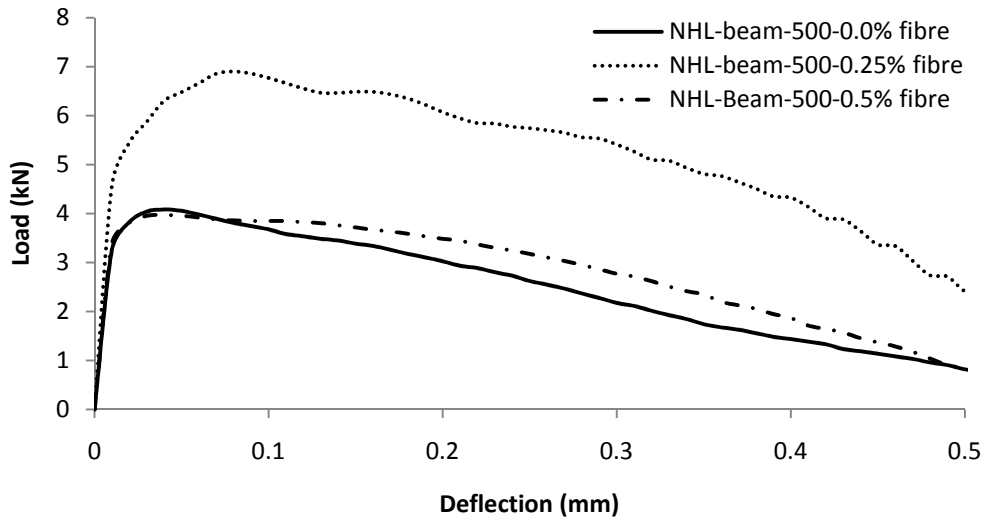


Figure 6.7 Flexural Load-deflection Response under Impact from 500 mm for Hydraulic Lime Mortar

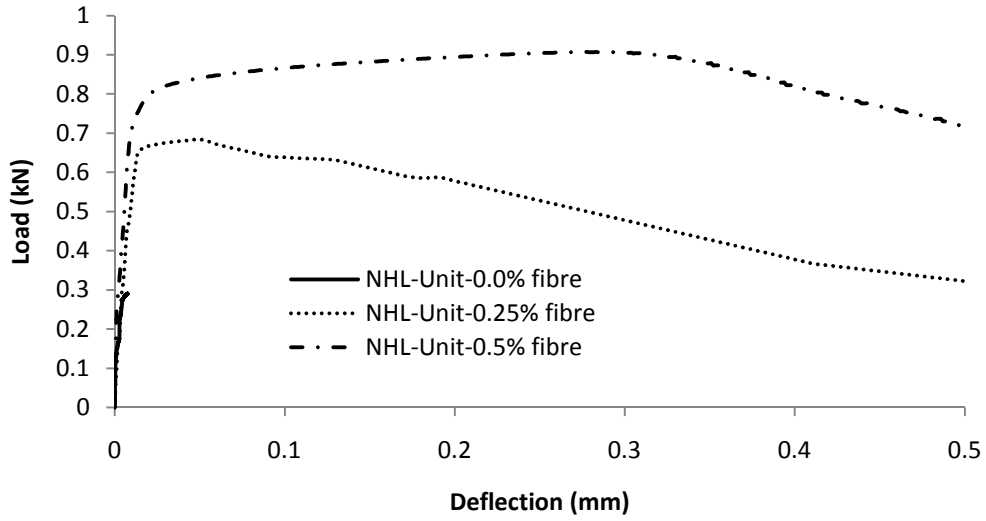


Figure 6.8 Flexural Load-deflection Response under Quasi-Static for Masonry Unit with Hydraulic Lime Mortar

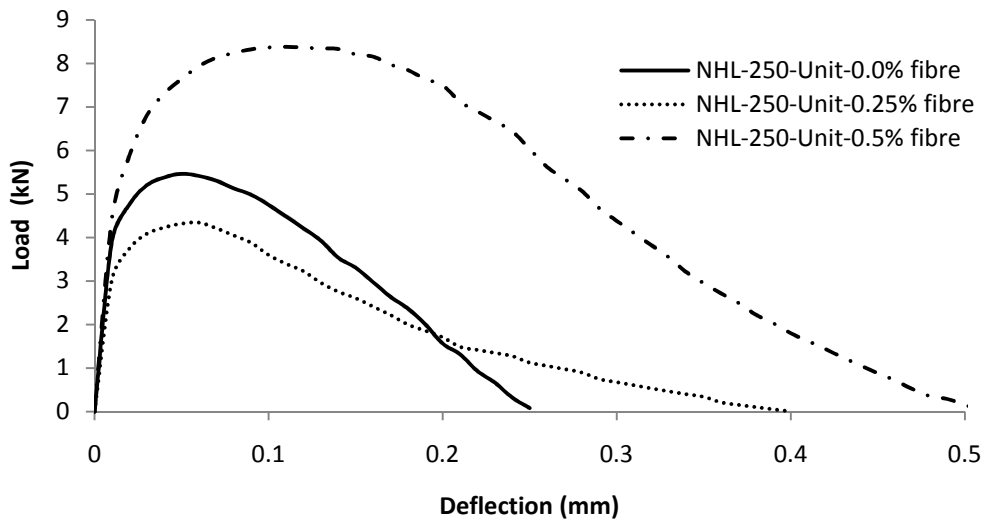


Figure 6.9 Flexural Load-deflection Response under Impact from 250 mm for Masonry Unit with Hydraulic Lime Mortar

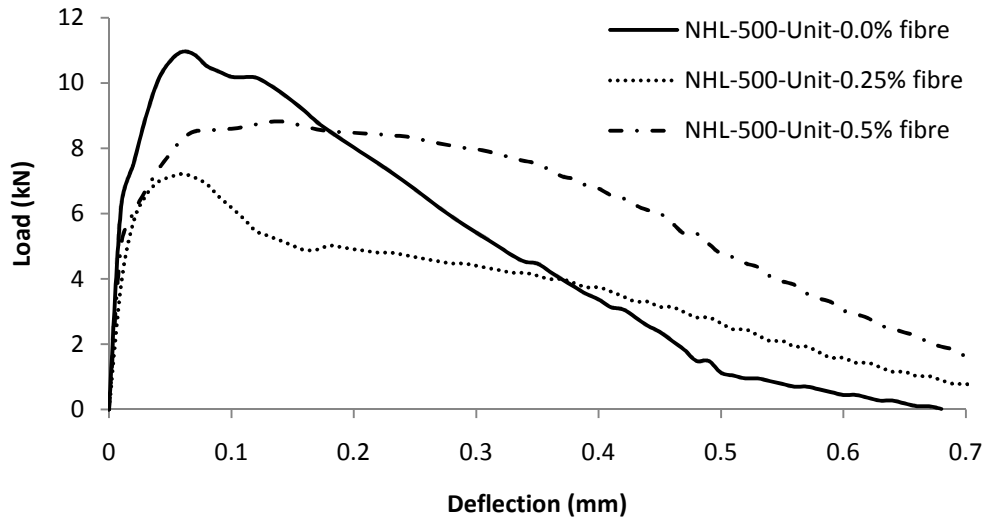


Figure 6.10 Flexural Load-deflection Response under Impact from 500 mm for Masonry Unit with Hydraulic Lime Mortar



Figure 6.11 Failure of Masonry Unit at the Stone-Mortar Interface



Figure 6.12 Failure of Masonry Unit within the Mortar

Table 6.2 Flexural Response of Mortar Beams and Masonry Units for Hydraulic Lime Mortar

Specimen	Tests	Fibre (%)	Peak Load (kN)			FTF (MPa)		
			Value	σ^*	C_v^{**} (%)	Value	σ^*	C_v^{**} (%)
Mortar Beam	Quasi Static Tests	0	0.49	0.04	8.86	0.14	0.005	3.41
		0.25	0.7	0.17	24.35	0.22	0.040	18.38
		0.5	0.8	0.19	23.74	0.28	0.033	11.86
	Impact Tests Drop height = 250 mm	0	6.03	0.51	8.49	1.05	0.166	15.76
		0.25	7.32	0.39	5.26	1.23	0.144	11.74
		0.5	6.16	0.38	6.22	1.11	0.094	8.45
	Impact Tests Drop height = 500 mm	0	4.12	0.41	9.90	0.89	0.069	7.74
		0.25	8.45	6.98	82.57	1.55	0.328	21.16
		0.5	3.98	0.43	10.9	1.29	0.393	30.50
Masonry Unit	Quasi Static Tests	0	0.29	0.07	24.07	0.04	0.006	15.21
		0.25	0.72	0.12	16.72	0.08	0.015	18.97
		0.5	0.92	0.2	22.16	0.12	0.039	31.81
	Impact Tests Drop height = 250 mm	0	5.48	1.61	29.39	1.01	0.282	27.91
		0.25	7.09	1.55	21.84	0.59	0.229	38.84
		0.5	8.61	0.7	8.1	1.47	0.129	8.76
	Impact Tests Drop height = 500 mm	0	11.14	5.95	53.40	1.45	0.276	19.06
		0.25	9.35	5.95	63.64	0.94	0.274	29.13
		0.5	12.85	2.39	18.6	1.53	0.366	23.91

* Standard Deviation; ** Coefficient of Variation

6.4 Flexural Toughness Factor (FTF)

While the FTF was always higher in fibre-reinforced mortars, this was more apparent under impact from the higher drop height (Figure 6.13). Unlike for the masonry units with Type S mortars, the FTF values were higher in fibre-reinforced mortar with 0.5% volume fraction. However, there was a drop with 0.25% volume fraction under dynamic loading. Note that the addition of fibres consistently increased the flexural bond strength in the masonry units. Clearly, in

the case of controlled low-strength mortars such as HLM, the addition of fibres provides higher energy dissipation in the joint without altering the sacrificial nature of the mortar. A sacrificial mortar ensures failure within itself or at the interface, and in the process avoids catastrophic failure within the stone block. Fibre reinforcement in HLM provides higher bond strength which is a welcome addition, but not sufficient; the resulting higher bond energy is the main attraction.

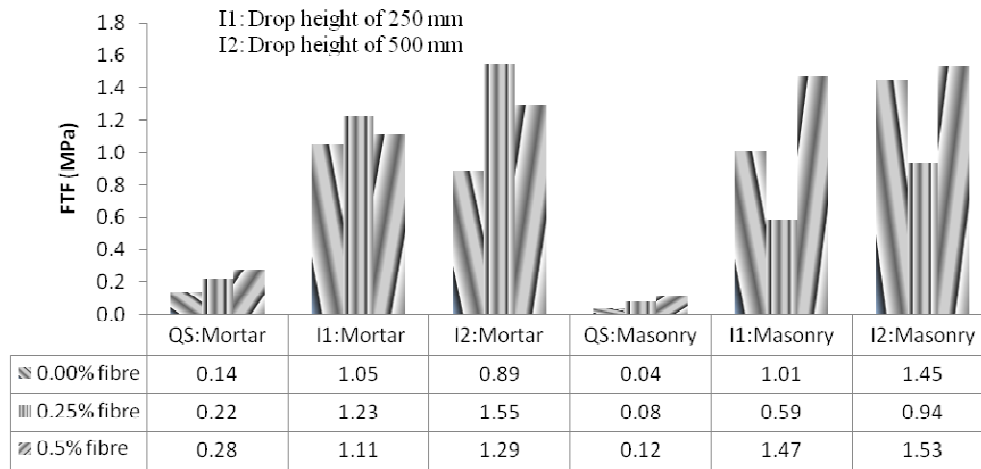


Figure 6.13 Flexural Toughness Factor for Hydraulic Lime Mortar and Masonry Units

6.5 Rate Effects

The stress rate sensitivity was expressed in terms of the dynamic impact factor (DIF) and is shown in Figure 6.14 and Figure 6.15. Note that the addition of fibres led to a decrease in loading rate sensitivity for both the flexural strength of the mortar and the flexural bond strength of the masonry unit. Once again, as with Type S mortar, the sensitivity of the flexural bond was higher than the sensitivity of the flexural strength of the mortar alone. The author notes that the

constitutive laws (CEB-FIB, 1990) formulated for regular concrete vastly overestimate the stress rate effects for HLM.

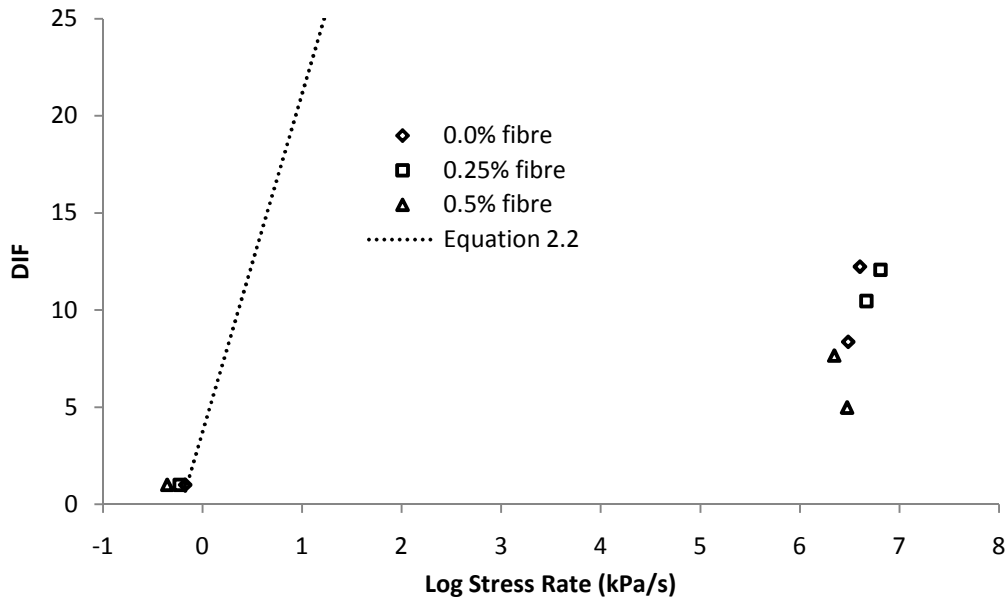


Figure 6.14 Stress Rate Sensitivity Shown for Various Fibre Contents for Flexural Strength of Hydraulic Lime Mortar

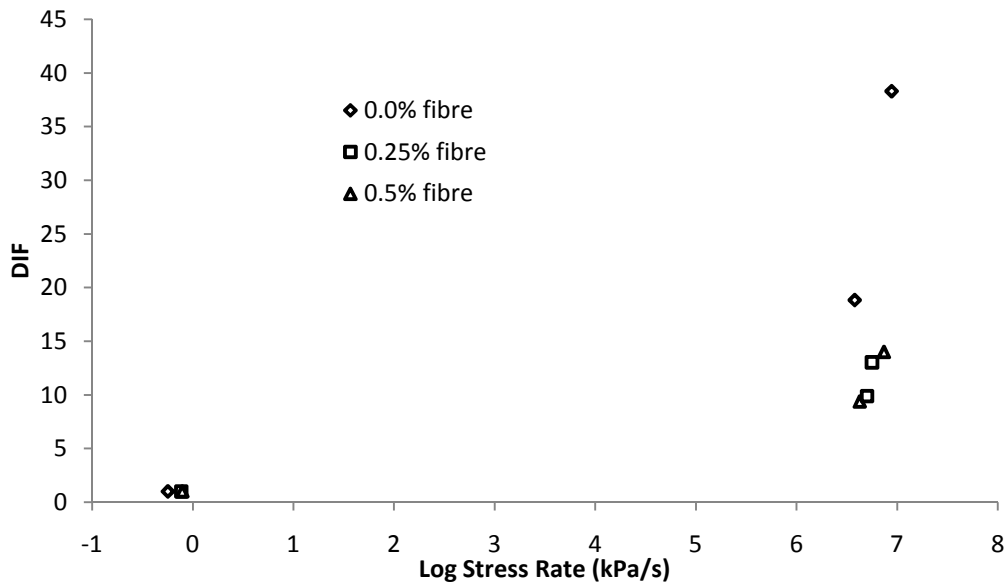


Figure 6.15 Stress Rate Sensitivity Shown for Various Fibre Contents for Bond Strength of Masonry Units with Hydraulic Lime Mortar

6.6 Concluding Remarks

- ❖ Polypropylene fibres in hydraulic lime mortar improve the flexural bond under quasi-static loading.
- ❖ Under dynamic loads, adding polypropylene fibres to HLM transfers the mode of failure from the stone-mortar interface to fracture within the mortar. This was attributed to the improvement in the stone-mortar bond.
- ❖ Hydraulic lime mortar is sensitive to high stress rates under flexure, but the CEB-FIP expression for tensile strength overestimates the dynamic impact factor.
- ❖ The flexural bond strength was more sensitive to stress rate than the flexural strength of the mortar at similar rates of loading. However, the addition of polypropylene fibres consistently decreased the rate sensitivity in both mortars and units.

CHAPTER 7 EXTERNAL STRENGTHENING OF SANDSTONE MASONRY UNITS WITH CARBON TEXTILE-REINFORCED MORTAR (CTRM)

7.1 Introduction

The rehabilitation of masonry buildings using carbon textile reinforced mortar (CTRM) is a novel technique (Triantafillou and Papanicolaou, 2002). While there is a large amount of research material on the external strengthening with carbon fibre-reinforced polymer (CFRP), the dynamic response of stone masonry externally strengthened with CTRM is relatively unknown. It is important to ascertain whether the failure will occur at the bond between CTRM and the stone block or as a tensile failure of the CTRM layer. Recall that any intervention must be reversible. This will have bearing on the reversibility of the repair method. Information on the relative increase in energy absorption of the repaired specimens compared to the original masonry unit is of interest as well. The study of CTRM behaviour under impact loading will provide us data that can be compared to similar applications of conventional CFRP. It will provide us with information on whether the epoxy bond or masonry bond behaves better in an impact loading case. This important information will help us pick the proper reinforcing material for a particular loading regime and application.

This chapter describes a pilot study to explore the feasibility of using a textile-reinforced mortar for external strengthening of stone masonry. Further research is needed in order to ensure its effectiveness. In particular, for application to

heritage masonry, the reversibility and durability of such an intervention must be ensured.

7.2 Materials and Mix Design

The broken masonry units were repaired with a premixed mortar called X Mesh M25 and X Mesh C10. As shown in Figure 7.1, X Mesh M25 is a premixed mortar that is a cementitious matrix, which has to be mixed with water to become like mortar for carbon textile net application on substrate. X Mesh C10 is a carbon fibre net in which the bundles of filaments have a $0^0/90^0$ orientation and are spaced 100 mm apart as shown in Figure 7.2. The physical properties of the carbon textile are given in Table 7.1. Potable water was used in preparing the mix. As specified in the manufacturer's datasheet, the amount of water added to the mortar was 25 kg per 100 kg of premixed mortar. The resulting mortar did not exhibit significant flow when subjected to ASTM C 1437 flow test as shown in Figure 7.3 and achieved 20% spread.



Figure 7.1 Premixed Fibre-reinforced Mortar M25 used to apply the CTRM

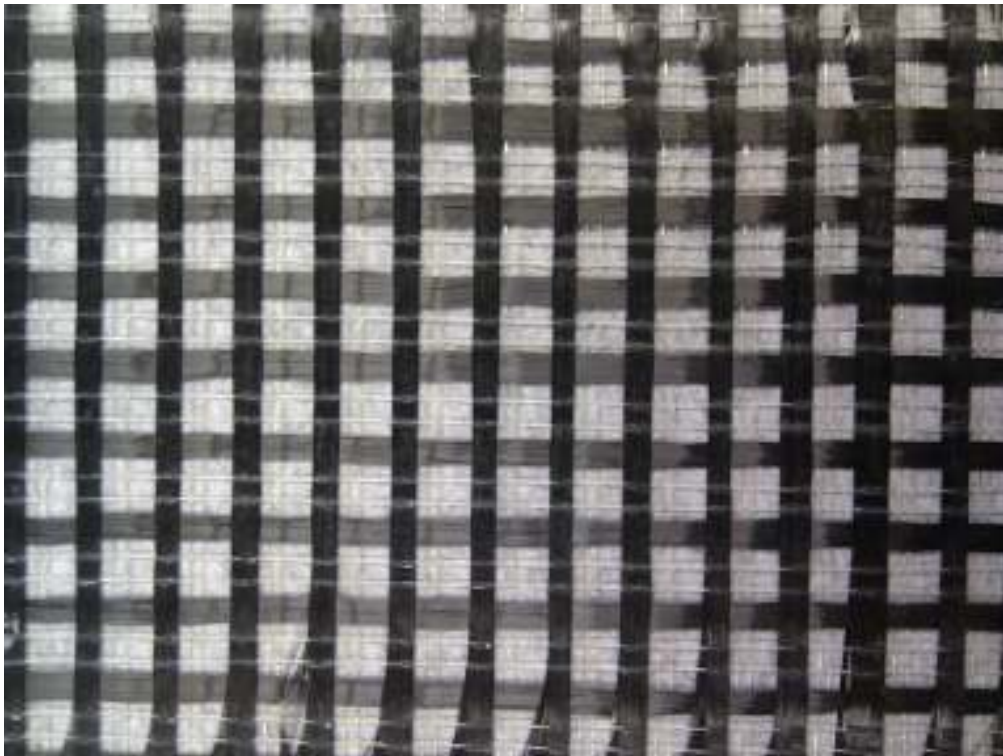


Figure 7.2 Carbon Textile C10 used to prepare the CTRM



Figure 7.3 Flow Test with Fibre-reinforced Mortar as per ASTM 1437

Table 7.1 Physical Properties of Carbon Textile used in the CTRM

Weight of carbon textile in the mesh (g/m^2)	168
Thickness for calculation of carbon section at 0^0 or 90^0 (mm)	0.047
Breaking load in direction 0^0 or 90^0 (Kg/cm)*	≥ 160

* Breaking load refers to a unit width of about 1 cm

7.3 Specimen Preparation

The masonry units tested to failure as described in Chapter 5 and Chapter 6 were salvaged for repair with CTRM. A typical broken masonry unit is shown in Figure 7.4. The steps required to prepare the externally strengthened specimens are presented below. The mortar was prepared by adding 2.5 L of water to 10 kg of the dry M25 premix, while the carbon textile was cut into rectangular pieces, 180 mm x 50 mm. The mortar was mixed using a paint mixer. First the water

was poured into a pan. Then the mortar premix was introduced at regular intervals into the pan, taking care not to form any lumps while the paint mixer was running. Before its application, the mix was left undisturbed for 5-6 minutes, and then it was mixed again for another minute. In the mean time, the sandstone blocks were retrieved and placed together to form the original unit. The length of the unit was buttered with about 3 mm of mortar on its tensile surface. The carbon textile was placed over the mortar approximately in the middle of the block (Figure 7.5) and was gently brushed into the mortar. A distance of 25 mm on the ends of the stone was left exposed and unstrengthened. Over the top of the mesh a second 3 mm layer of mortar was placed. After that the specimens were cured in ambient temperature and humidity (18-24 °C and 30-50% relative humidity) and the specimen was covered with burlap which was further protected with absorbents (Figure 7.6). Curing was done at regular intervals to make sure that the surface of the CTRM was wet at all times for a period of one week.



Figure 7.4 Example of Failed Masonry Units after Testing as described in Section 3.4.1.2 and Section 3.4.2. The broken Unit was re-assembled prior to Strengthening.



Figure 7.5 Masonry units under Repair using CTRM



Figure 7.6 Samples Stored for Curing

7.4 Compressive Response of Binder used in preparing the CTRM

Three cylinders of size 75 mm diameter and 150 mm height were tested as per ASTM C469. The test was conducted as per the procedure described in Chapter 3, subsection 3.4.1.1. The compressive response of the mortar is shown in Figure 7.7, and results are given in Table 7.2. Even though the cylinders were made

from the same batch of mortar and cured in an identical way for 20 days, the tests show non-uniformity in the material properties of the specimens. Specimen 1 had a significantly larger modulus of elasticity than specimens 2 and 3. Ultimate compressive strength varied from 22 to 32 MPa. Randomized fibre distribution in mortar can partially account for the mechanical properties of the specimens. Further investigation is required to explain the compression test results.

The compressive strength of this mortar is very close to regular concrete. The statistical variation of this mortar was found to be equal to that of regular concrete. As per ACI 214 (1957), the standard deviation for regular concrete of this strength should be 3.2 MPa with a coefficient of variation of 12.9%, where as a standard deviation of 2.5 MPa and coefficient of variation of 8.76% was found for mortar used to prepare the CTRM.

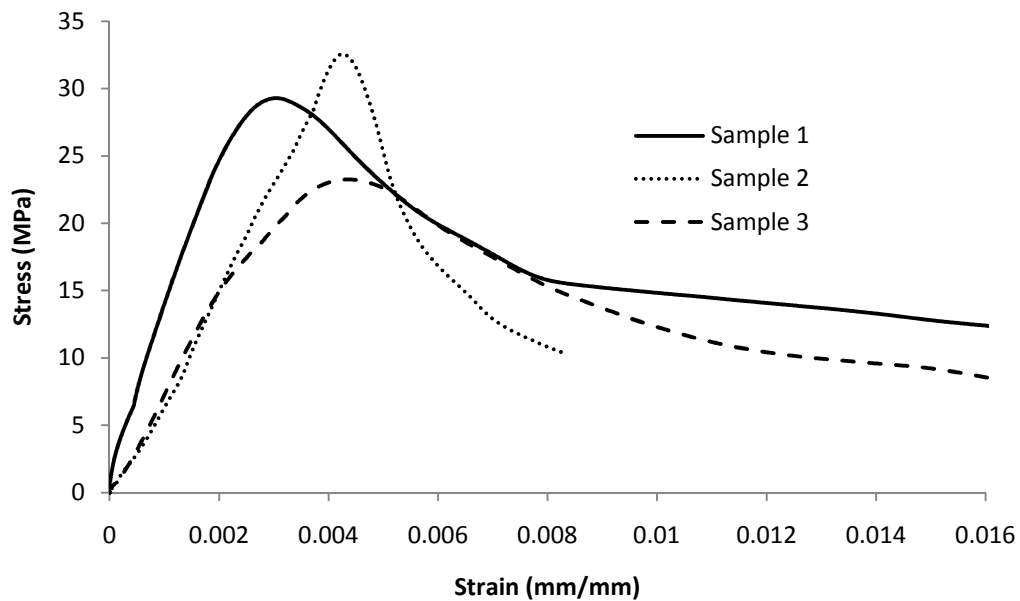


Figure 7.7 Compressive Response of the Binder used in preparing the CTRM

Table 7.2 Compressive results of the binder used in preparing the CTRM

	Compressive strength (MPa)*	Modulus of elasticity (MPa)*
Sample 1	29.53	8676.00
Sample 2	33.07	7362.95
Sample 3	23.28	7451.11
Average	28.62	7830.02
Standard deviation	2.51	928.47
Coefficient of variation (%)	8.76	11.86

* Values shown in table are at 20 days

7.5 Quasi-Static Flexural Testing of Sandstone Masonry Unit Externally Strengthened with CTRM

7.5.1 Introduction

This section contains flexural results for two types of specimen: Unit-R-0 and Unit-R-2. Both types of specimen prior to retrofitting with CTRM were represented by a fractured specimen of two sandstone blocks joined together with mortar. In the case of Unit-R-0, at the end of the original test, fracture occurred at the boundary of mortar and sandstone block. In the case of Unit-R-2 the fracture had occurred through the sandstone block. Recall that this was a result of the presence of fibre in the Type S mortar as discussed in Section 5.3.2. Both types of specimens were cured for 20 days after the CTRM was applied.

7.5.2 Quasi-Static Test Results: Unit-R-0

Four specimens of Unit-R-0 were tested. In all four cases the specimen failed through tensile failure in the CTRM as well as compressive failure of the mortar

binding the sandstone blocks. As seen in the picture (Figure 7.8), the CTRM broke because of the failure of the bond between the carbon fibre and mortar. This pulling out of carbon fibres meant that even after peak load was reached, some specimens were still able to support certain loads and were not subject to abrupt catastrophic failure. The range of maximum load that a masonry unit repaired with CTRM could sustain was 10-13 kN.



Figure 7.8 Mode of Failure of Composite Sandstone/CTRM Specimen Unit-R-0

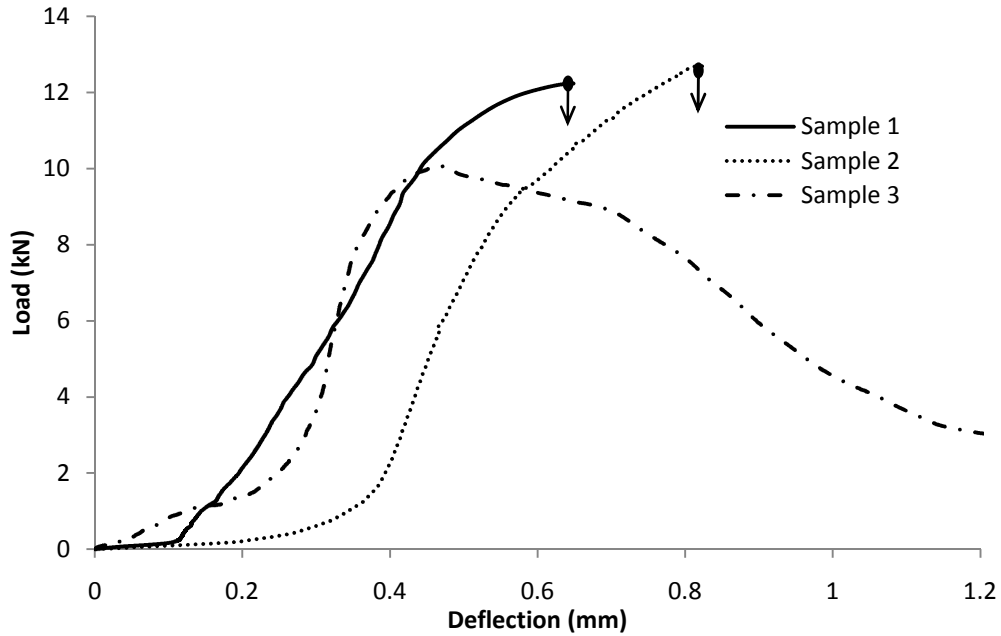


Figure 7.9 Flexural Load-deflection Responses under Quasi-static Loading for Composite Sandstone/CTRM Specimen Unit-R-0

7.5.3 Quasi-static Test Results: Unit-R-2

Four specimens of Unit-R-2 were tested. All four specimens failed through tensile failure of the CTRM. In the case of Unit-R-2, the average peak load, as shown in Figure 7.11, was significantly higher than in the case of Unit-R-0. This can be explained by the fact that Unit-R-2 failure was governed by the tensile strength of CTRM (Figure 7.10); in Unit-R-0, however, failure occurred through both the CTRM and mortar in between two sandstone blocks (Figure 7.8). The mechanical properties of both specimen types tested are significantly better than those of the original masonry units. According to data obtained in tests done on original masonry unit the maximum load it could withstand was in the range of 6 kN, which is significantly lower than results obtained for either type of the fractured specimen.

There is a strength difference that cannot be neglected between the two types of specimens tested. Specimens that originally fractured through sandstone proved to be stronger than specimens that originally failed at the mortar-sandstone boundary. The reason for this lies in the fact that sandstone provides better compressive resistance than mortar during the bending of the specimens.



Figure 7.10 Mode of Failure of Composite Sandstone/CTRM Specimen Unit-R-2

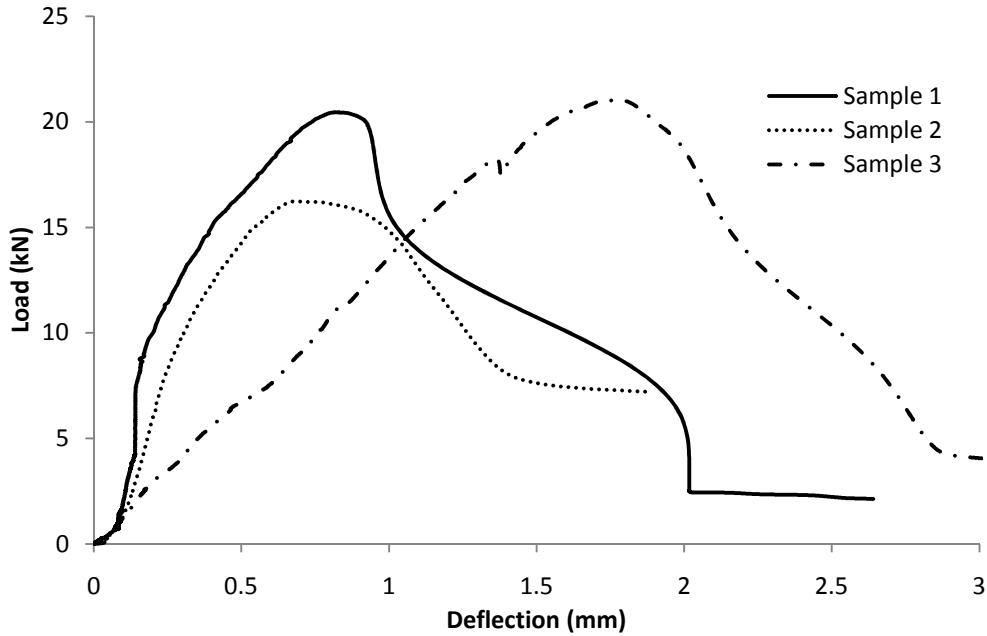


Figure 7.11 Flexural Load-deflection Responses under Quasi-static Loading for Composite Sandstone/CTRM Specimen Unit-R-2

7.6 Impact Testing of Composite Sandstone/CTRM Specimen

7.6.1 Introduction

Two unit types were used to evaluate dynamic response: Unit-R-0 and Unit-R-2 (analogous to the quasi-static test). The specimens were subjected to two types of impact generated via a drop from a height of 250 mm and 500 mm.

7.6.2 Impact Test Results

Figure 7.12 and Figure 7.13 describe the impact response of Unit-R-0 and Unit-R-2 for a drop height of 250 mm, whereas Figure 7.14 and Figure 7.15 illustrate the impact response of Unit-R-0 and Unit-R-2, respectively, for a drop height of 500 mm. The specimens representing Unit-R-0 had a smaller mechanical strength than specimens representing Unit-R-2. The specimens subjected to a

higher energy impact could withstand a higher maximum load than those subjected to the 250 mm drop. The load versus displacement diagrams for all specimen types and energy levels, as well as a table of peak total and bending loads, can be found in Table 7.3.

Table 7.3 Impact Test Results for Composite Sandstone/CTRM Specimens

Specimen ID	Total Load (kN)	Bending Load (kN)	Drop of height (mm)
250-UNIT-R-0-1	16.99	12.11	250
250-UNIT-R-0-2	17.14	12.22	250
250-UNIT-R-0-3	17.69	12.61	250
Avg-250-UNIT-R-0	17.28	12.32	
Standard deviation	0.37	0.26	
Coefficient of variation (%)	2.13	2.13	
250-UNIT-R-2-1	30.02	21.40	250
250-UNIT-R-2-2	14.98	10.68	250
250-UNIT-R-2-3	11.95	8.52	250
Avg-250-UNIT-R-2	18.98	13.54	
Standard deviation	9.68	6.90	
Coefficient of variation (%)	50.97	50.97	
500-UNIT-R-0-1	45.02	32.10	500
500-UNIT-R-0-2	28.08	20.02	500
500-UNIT-R-0-3	24.43	17.42	500
Avg-500-UNIT-R-0	32.51	23.18	
Standard deviation	10.99	7.83	
Coefficient of variation (%)	33.79	33.79	
500-UNIT-R-2-1	31.34	22.35	500
500-UNIT-R-2-2	37.03	27.73	500
500-UNIT-R-2-3	37.03	26.40	500
Avg-500-UNIT-R-2	35.13	25.49	
Standard deviation	3.28	2.80	
Coefficient of variation (%)	9.35	11.00	

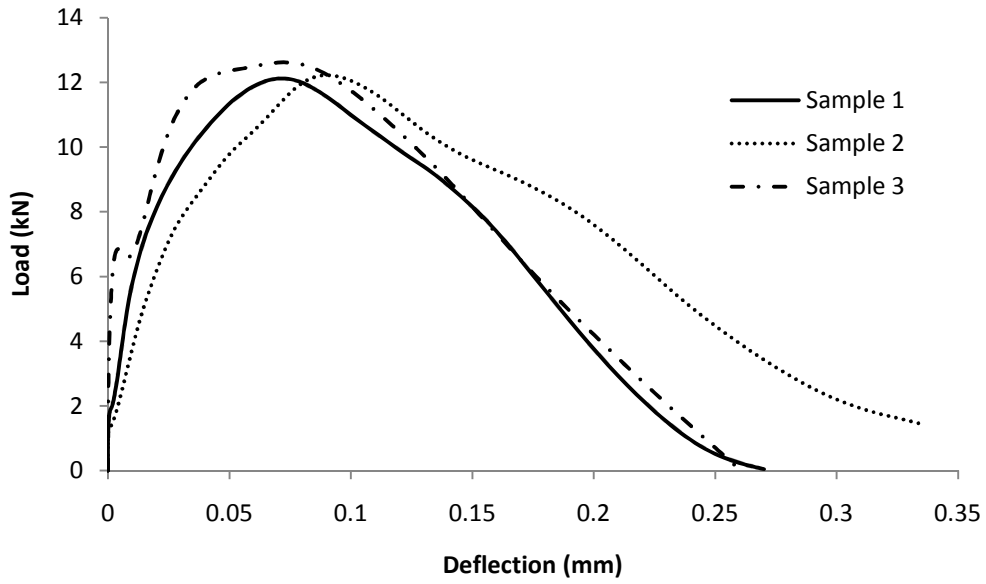


Figure 7.12 Impact Test: Composite Sandstone/CTRM Specimen (Unit-R-0; 250 mm Drop)

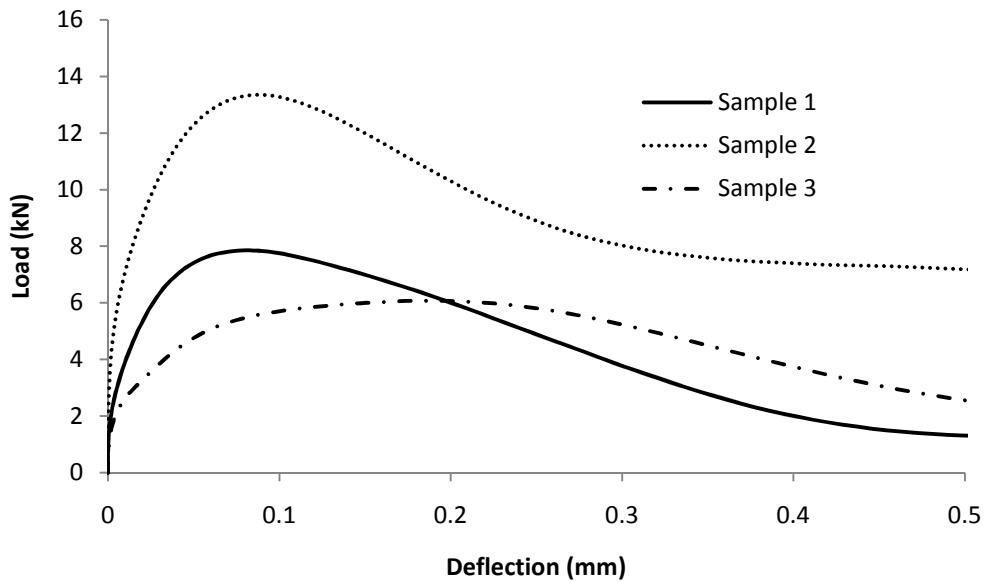


Figure 7.13 Impact Test: Composite Sandstone/CTRM Specimen (Unit-R-2; 250 mm Drop)

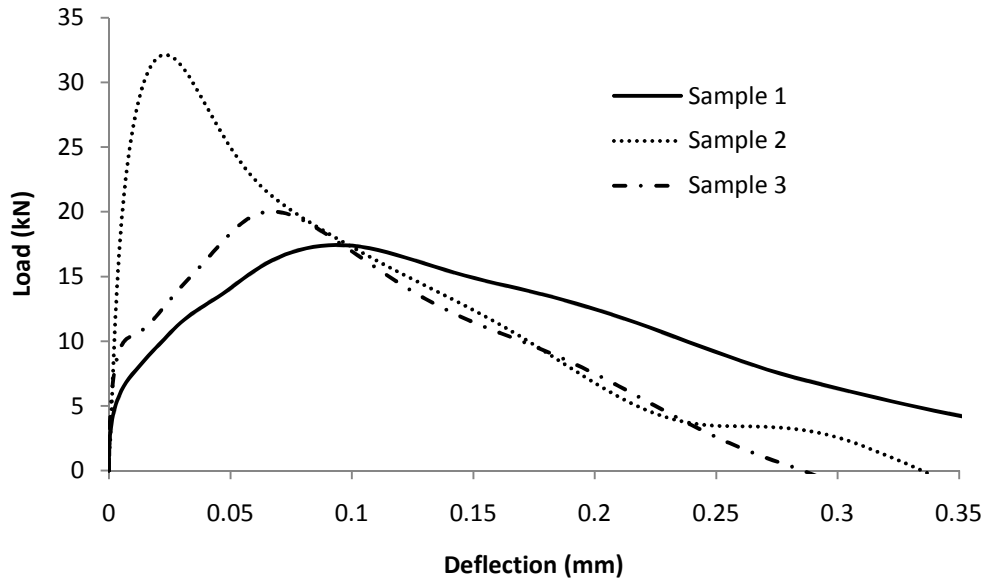


Figure 7.14 Impact Test: Composite Sandstone/CTRM Specimen (Unit-R-0; 500 mm Drop)

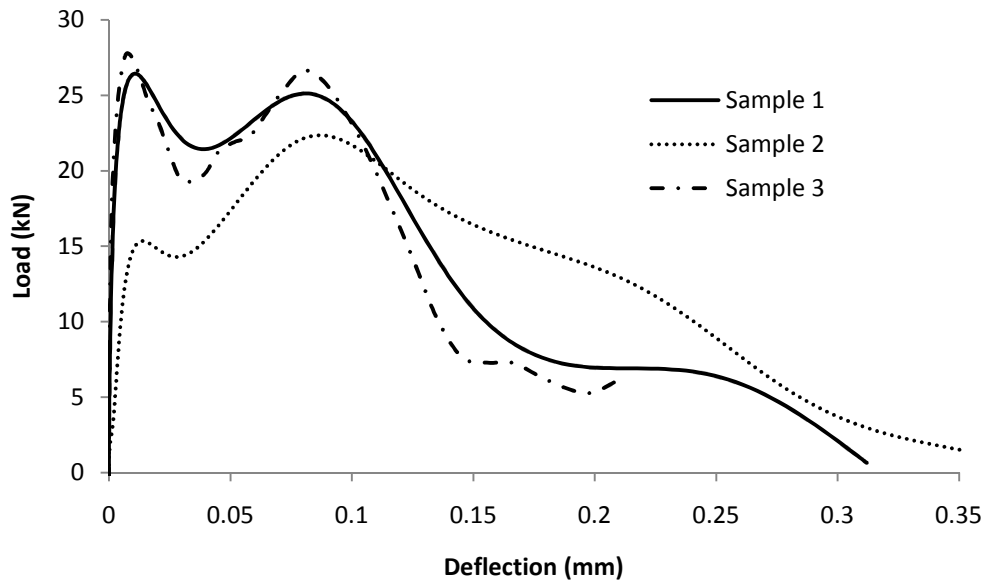


Figure 7.15 Impact Test: Composite Sandstone/CTRM Specimen (Unit-R-2; 500 mm Drop)

7.6.3 Discussion of Results

Compared with the average values of unrepaired specimens subjected to impact load, the peak load of repaired specimens was essentially the same. For the 250 mm drop, the unrepaired specimen had an average total peak load of 19.30 kN, whereas repaired specimens had an average total peak load of 18.13 kN. For the 500 mm drop, the unrepaired specimens had an average total peak load of 25.47 kN, whereas repaired specimens had an average peak total load of 33.82 kN. The reason that the application of CTRM had a small effect on the strength of a specimen is due to following factor: The load applied by the hammer is transferred to one part of the broken masonry unit, and thus there is movement of one part of the unit against another. Such movement creates tensile stress between the masonry unit and CTRM, and the bond fails in a peeling off failure instead of tensile failure in the CTRM.

7.7 Quasi-Static Results of Mortar Beam Specimens

This section includes quasi-static flexural results on mortar beam of dimension 150 mm x 50 mm x 50 mm. The quasi-static flexural responses of this premixed mortar are summarized in Table 7.4.

Table 7.4 Quasi-Static Test Results: Mortar Beam Specimen

Specimen ID	Load (kN)	MOR (MPa)
Mortar beam -1	1.57	6.68
Mortar beam -2	1.36	5.79
Mortar beam -3	1.52	6.50
Average	1.48	6.32
Standard deviation	0.15	0.63
Coefficient of variation (%)	10.01	10.01

7.8 Impact Results of Mortar Beam Specimens

This section includes impact testing results of mortar beam of dimension 150 mm x 50 mm x 50 mm. The results provide us with information on the tensile strength of the mortar subjected to impact.

A mortar beam subjected to impact with a hammer dropped from a 250 mm height could sustain a maximum average total peak load of 13.97 kN with standard deviation of 4.38 kN. A mortar beam subjected to impact with a hammer dropped from a 500 mm height could sustain maximum average total peak load of 20.30 kN, with standard deviation of 0.14 kN. In comparison with the quasi-static results, the premixed mortar that is used for applying CTRM on broken masonry units exhibits a superior impact strength response with an increase in the loading rate.

Table 7.5 Impact Test Results: Mortar Beam Specimen

Specimen ID	Total Load (kN)	Bending Load (kN)	Drop height (mm)
250-UNIT-No-CTRM-1	15.32	11.35	250
250-UNIT-No-CTRM-2	12.04	8.92	250
250-UNIT-No-CTRM-3	19.36	14.34	250
250-UNIT-No-CTRM-4	9.18	6.80	250
Avg-250-UNIT-No-CTRM	13.97	10.35	
Standard deviation	4.38	3.25	
Coefficient of variation (%)	31.37	31.37	
500-UNIT-No-CTRM-1	20.21	14.97	500
500-UNIT-No-CTRM-2	20.40	15.11	500
500-UNIT-No-CTRM-3	20.31	14.97	500
Avg-500-UNIT-No-CTRM	20.30	15.04	
Standard deviation	0.14	0.10	
Coefficient of variation (%)	0.67	0.67	

7.9 Conclusions

The use of CTRM to repair broken masonry provided a significant increase of strength as well as energy absorption over unrepaired/unbroken masonry units. The weakness in the specimen was the bond between the carbon fibre and mortar used in the CTRM. The use of different kinds of fibres with compatible elastic moduli might improve the fibre-mortar bond. However, it is important not to eliminate this weakness as a whole since it is responsible for the higher energy absorption of a specimen. As fibre is pulled out of the CTRM, energy is dissipated slowly and thus this weakness in the bond does not lead to rapid failure.

Under impact loading conditions the use of CTRM for repair of broken masonry units did not provide sufficient benefits over unrepaired/unbroken masonry units. The peel-off mode of failure was the main reason for the lower maximum load that the repaired masonry units could withstand on impact. In order to eliminate such failure mode, the following ways might be attempted:

- ❖ Roughen the surface of the sandstone block in order to improve the sandstone-masonry bond.
- ❖ Use different types of fibres (with compatibility in elastic moduli between mortar and fibre such as glass) in order to achieve better strain compatibility in fibre, mortar and masonry unit.
- ❖ Prevent sandstone blocks from sliding against each other in order to eliminate peel-off failure. This can be done by introducing a binder in

between the sandstone blocks. Epoxy might be a good choice since it has high tensile and shear resistance.

Use of CTRM in retrofitting improves the resistance of repaired masonry units significantly. In order for the CTRM to be efficient in repairing masonry structures, the sandstone blocks need special preparation. The original mortar must be washed away to get a suitable surface for strong bonding and the cavity should be filled with a mortar of higher strength and elastic modulus.

CHAPTER 8 CONCLUSIONS AND RECOMMENDATIONS

This study examined the loading rate effects on the components of sandstone masonry and joint in a stone masonry unit bound with a modern Type S masonry mortar as well as a traditional hydraulic lime mortar. Also, a pilot study was conducted to examine the feasibility of using textile reinforced mortar in external strengthening of such units under variable loading rates. The following conclusion can be drawn on the basis of this study:

- ❖ The dynamic responses of plain and fibre-reinforced mortars are sensitive to high stress rates. However, models developed for concrete, such as the modified CEB-FIP expressions, underestimate the stress rate sensitivity of the flexural strength of mortar.
- ❖ The flexural bond strength is more sensitive to stress rate than the flexural strength of the mortar at similar drop heights. However, the addition of fibres consistently decreases the rate sensitivity of the flexural bond strength.
- ❖ The addition of polypropylene microfibre to the mortar transforms the mode of failure. For Type S mortar, the failure transform from the stone-mortar interface to within the stone blocks, but in the case of hydraulic lime mortar, the mode of failure transforms from the stone-mortar interface to fracture within the mortar.
- ❖ Due to the trade off between higher bond strength and lower flexural toughness factors, there exists an optimal dosage of fibres that may be

added to mortars in order to achieve the maximum bond energy at high stress rates.

- ❖ Repairing masonry with CTRM improves the performance but technique requires a strong repointing mortar.

On the basis of the results reported in thesis, the following recommendations are made for future research work in this field:

- ❖ There is a need to standardize the test methods for lime mortars in North America. It will be better to restore those standards for lime mortars that are no longer recognized by CSA with additional classification of lime mortars suitable for restoration and rehabilitation of historic masonry structures.
- ❖ The present study is the first of its kind studying sandstone masonry units bound with fibre-reinforced mortars. It is recommended to study the fibre effects on compressive strength, Poisson's ratio, flexural strength, DIF, and flexural toughness factor in depth. The use of different types of fibres with variation of lime in the mortar is also recommended. The method of preparation and fibre dispersion that have influence on mortar strength is of further research interest.
- ❖ The current study focuses only on the quasi-static compressive response of mortars. It is required to investigate the compressive behaviour of mortar under dynamic loading conditions.

- ❖ It is highly recommended to gather some comparative results with different types of impact testing for identical building materials like a drop-weight impact machine or the Split Hopkinson Pressure Bar.
- ❖ Petrographic characterization of the building stone used in historic masonry is required for better control of repair options.

REFERENCES

ACI 214. 1957. Recommended Practice for Evaluation of Compression Test Results of Field Concrete. Committee 214, American Concrete Institute, Farmington Hills, MI, 16 pages.

ACI 446.4R. 2004. Report on dynamic fracture of concrete. Committee 446, American Concrete Institute, Farmington Hills, MI, 29 pages.

ACI 544.R1. 1996. Report on fibre reinforced concrete. Committee 544, American Concrete Institute, Farmington Hills, MI, 66 pages.

Armwood, C., Sorensen, A., Skourup, B and Erdogmus, E. 2008. Fibre reinforced mortar mixtures for the reconstruction and rehabilitation of existing masonry structures, Proceedings: AEI 2008-Building Integrated Solutions, ASCE, 10 pages.

Asprone, D., Cadoni, E., Prota, A. and Manfredi, G. 2009. Dynamic behaviour of a Mediterranean natural stone under tensile loading. *International Journal of Rock Mechanics & Mining Sciences*, Vol. 46, pp. 514-520.

ASTM C 1437. 2007. Standard test method for flow of hydraulic cement mortar. ASTM International, West Conshohocken, PA.

ASTM C 144. 2004. Standard specification for aggregate for masonry mortar. ASTM International, West Conshohocken, PA.

ASTM C 1609-07. 2007. Standard test method for flexural performance of fibre reinforced concrete (using beam with third-point loading). ASTM International, West Conshohocken, PA.

ASTM C 469-02. 2001. Standard test method for static modulus of elasticity and Poisson's ratio of concrete in compression. ASTM International, West Conshohocken, PA.

Banthia, N. and Dubeau, S. 1994. Carbon and steel microfiber-reinforced cement-based composites for thin repairs. *ASCE Journal of Materials in Civil Engineering*, Vol. 6. No. 1, pp. 88-99.

Banthia, N.P., Mindess, S., Bentur, A. and Pigeon, M. 1989. Impact testing of concrete using a drop-weight impact machine, *Experimental Mechanics*, Vol. 29, No. 12, pp. 63-69.

Banthia, N. and Sheng, J. 1996. Fracture toughness of micro-fibre reinforced cement composites. *Cement and Concrete Composites*, Vol. 18. No. 4, pp. 251-269.

Beall, C. 1997. *Masonry design and detailing for architects, engineers and contractors*. McGraw-Hill, 4th edition. P.138.

Bentur, A. and Alexander, M.G. 2000. A review of the work of the RILEM TC-159-ETC: Engineering the interfacial transition zone in cementitious composites. *Materials and Structures*, RILEM, Vol. 33, pp. 82-87.

Bharatkumar, B.H. and Shah, S.P. 2004. Impact resistance of hybrid fibre reinforced mortar. *International RILEM Symposium on Concrete Science and Engineering: A Tribute to Arnon Bentur*, e-ISBN: 2912143926, March, 2004.

Bindiganavile, V. 2003. Dynamic fracture toughness of fibre reinforced concrete. PhD thesis, University of British Columbia, Vancouver, BC, Canada, 258 pages.

Bindiganavile, V. and Banthia, N. 2001. Polymer and steel fibre reinforced cementitious composites under impact loading, Part 1: bond-slip response. *ACI Materials Journal*, Vol. 98, No.1, pp. 10-16.

Bindiganavile, V. and Banthia, N. 2001. Polymer and Steel Fibre reinforced Cementitious Composites under Impact Loading, Part 2: Flexural toughness. *ACI Materials Journal*, Vol. 98, no.1, pp. 17-24.

Bournas, D. A., Triantafillou, T. C., M.ASCE, Zygoris, K., & Stavropoulos, F. 2009. Textile-Reinforced Mortar versus FRP Jacketing in Seismic Retrofitting of RC Columns with Continuous or Lap-Spliced Deformed Bars. *Journal of Composites for Construction*.

Buozzi, B. 2006. Ultra high mechanical performance Polyparaphenylene benzobisoxazole (PBO) fibre mesh, with a stabilized inorganic matrix, for structural reinforcement of concrete. 1 -20097, San Donato Milanese, Technical Management – October 2006.

Burnett, S., Gilbert, M., Molyneaux, T., Tyas, A., Hobbs, B. and Beattie, G. 2007. The response of masonry joints to dynamic tensile loading. *Materials & Structures*, RILEM 40, pp. 517-527.

Cameron, C. 1986. Canadian inventory of historic building. Bulletin of the Association for Preservation Technology, Environment Canada, 18(1):49.

CEB-FIP, CEB-FIP Model Code 90. 1990. Comité Euro-International du Beton – Federation Internationale de la Precontrainte, Redwood Books, Trowbridge, Wiltshire, UK.

Chan, R. and Bindiganavile, V. 2010. Toughness of fibre reinforced hydraulic lime mortar. Part-1: Quasi-static response. *Materials and Structures*. DOI 10.1617/s11527-010-9598-4.

Chan, R. and Bindiganavile, V. 2010. Toughness of fibre reinforced hydraulic lime mortar. Part-2: Dynamic response. *Materials and Structures*. DOI 10.1617/s11527-010-9599-3.

Chen, E.P. and Sih, G.C. 1977. Transient response of cracks to impact loads, *Mechanics of Fracture*, 4: Elastodynamic crack problems, pp. 1-58.

Costigan, A. and Pavia, S. 2009. Compressive, flexural and bond strength of brick/lime mortar masonry. Proceedings of PROHITEC 09.

Cowper, A. 1998. Lime and Lime Mortars. Donhead Publishing Ltd, Dorset (1998) [first published in 1927 for the Building Research Station by HM Stationery Office, London].

Crocq, C.S. 2010. Building Stone in Alberta. Energy Resources Conservation Board, Alberta Geological Survey, ERCB/AGS Open File Report 2010-01.

CSA A 179-04. 2004. Mortar and grout for unit masonry. Canadian Standards Association.

CSA A 23.3. 1994. Design of concrete structures. Canadian Standards Association.

EN 459-2001. 2001. Building lime. Part 1: Definitions, specifications and conformity criteria. Part 2: Test methods. European standard available from the British Standards Institution.

Gemert, D.V, Rickstal, F.V., Ignoul, S., Toumbakari, E.E. and Balen, K.V. 2003. Structural consolidation and strengthening of masonry: historical overview and evolution. MSR VI International Conference Materials Science and Restoration, Karlsruhe, Seminar on “Consolidation of Masonry”, Advances in Materials Science and Restoration AMSR 1, pp. 1-20.

Geoscape Canada. 2008.

http://geoscape.nrcan.gc.ca/calgary/topics/sandstone_e.php.

Glass, D.J. 1990. Lexicon of Canadian stratigraphy, volume 4: Western Canada, including eastern British Columbia, Alberta, Saskatchewan and southern Manitoba. Canadian Society of Petroleum Geologists, Calgary, Alberta, p. 772.

Glinicki, M.A. 1994. Toughness of fibre reinforced mortar at high tensile loading rates. *ACI Materials Journal*, Mar-Apr, Vol. 91 no. 2, pp. 161-166.

Green, M. F., Bisby, L. A., Beaudoin, Y., & Labossière, P. 2000. Effect of freeze-thaw cycles on the bond durability between fibre reinforced polymer plate reinforcement and concrete. *Canadian Journal of Civil Engineering*, **27**(5): 949-959.

Gumeste, K.S. and Venkatarama, R.B.V. 2006. Strength and elasticity of brick masonry prisms and wallettes under compression. *Materials & Structures*– 29: 241-253.

Hanley, R. and Pavia, S. 2008. A study of the workability of natural hydraulic lime mortars and its influence on strength. *Material & Structures*. 41(2):373–381.

Harajli, M. H., Elkhatib, H., & San-Jose, T. J. 2010. Static and Cyclic Out-of-Plane Response of Masonry Walls Strengthened Using Textile-Mortar System. *Journal of Materials in Civil Engineering*. doi:10.1061/(ASCE)MT.1943-5533.0000128.

Hao, H. and Tarasov, B.G. 2008. Experimental study of dynamic material properties of clay brick and mortar at different strain rates. *Australian Journal of*

Structural Engineering, Vol. 8, no. 2, Special issue on masonry, ISSN 1328-7982, pp. 117-131.

Holmes S. and Wingate M. 1997. *Building with lime: A practical introduction*, 2nd Edition. ITDG, London.

Jackson, S. 1979. Canadian inventory of historic building. *Archivaria*, 8: 157-160.

Jeffs, P.A. 2001. Core consolidation of heritage structure masonry walls & foundation using grouting techniques— Canadian case studies. In: *Proceedings of the 9th Canadian masonry symposium*, University of New Brunswick, Canada, 4–6 June 2001.

JSCE-G 552-1999. 2005. Method of test for flexural strength and flexural toughness of steel-fibre reinforced concrete. *Test Methods and Specifications*, Japan Society of Civil Engineers.

Kubota, S., Ogata, Y., Wada, Y. Simangunsong, G., Shimada, H. and Matsui, K. 2008. Estimation of the dynamic tensile strength of sandstone. *International Journal of Rock Mechanics and Mining Sciences*, Vol. 45, pp.397-406.

Lanas, J. Perez Bernal, J.L. Bello, M.A. Alvarez Galindo, J.I. 2004. Mechanical properties of natural hydraulic lime based mortars. *Cement and Concrete Research*, Vol.34 no. 12, pp. 2191-2201.

Malvar, L.J. and Ross, C.A. 1998. Review of strain rate effects for concrete in tension. *ACI Materials Journal*, Vol. 95 no. 6, pp. 735-739.

Maurenbrecher, A.H.P., Trischuk, K. and Rousseau, M.Z. 2001. Review of factors affecting the durability of repointing mortars for older masonry. 9th Canadian Masonry Symposium, Fredericton, N.B., pp. 1-12.

Maurenbrecher, A.H.P. 2004. Mortars for repair of traditional masonry. National Research Council. NRCC-46903. V.9, no.2, May 2004, pp. 62-65.

Maurenbrecher, A.H.P., Trischuk K., Rousseau M.Z., Subercaseaux M.I. 2007. Key considerations for repointing mortars for the conservation of older masonry. Institute for Research in Construction Research Report 225, National Research Council Canada, Ottawa, Canada.

Mindess, S. and Vondran, G. 1988. Properties of concrete reinforced with fibrillated polypropylene fibres under impact loading. *Cement and Concrete Research*, Vol. 18 no. 1, pp. 109-115.

Parks, W.A. 1916. Report on the building and ornamental stones of Canada Vol IV: Provinces of Manitoba, Saskatchewan and Alberta. No. 388, 333 pages.

Rao, K.V., Reddy, B.V.V. and Jagadish, K.S. 1996. Flexural bond strength of masonry using various blocks and mortars. *Materials and Structures*, Vol. 29, March, pp 119-124.

Sarangapani, G. Venkatarama, R.B.V. Jagadish K.S. 2005. Brick–mortar bond and masonry compressive Strength. *Journal of Material & Civil Engg.* (ASCE) 17(2):229–237.

Suter, G.T., Borgal C.P. and Blades K. 2001. Overview of mortars for Canadian historic structures. In proceedings of the 9th *Canadian Masonry Symposium*. University of New Brunswick, Canada. 4-6 June.

Triantafillou, T., & Papanicolaou, C. 2002. Textile Reinforced Mortars (TRM) versus Fibre reinforced Polymers (FRP) as Strengthening Materials of Concrete Structures. FRPRCS-7, SP-230-6.

Van der Pluijm R. 1997. Non-linear behaviour of masonry under tension. *Heron*, Vol. 42, pp. 25–54.

Venkatarama, R. B.V. and Vyas Uday. 2008. Influence of shear bond strength on the compressive strength and stress-strain characteristics of masonry. *Materials & Structures*– 41: 1697-1712.

Vicat, L.J. 1997. A practical and scientific treatise on calcareous mortars and cements. John Weale, London, 1837, reprinted by Donhead.

Willis, C.R., Yanga, Q., Seracino, R. and Griffith M.C. 2009. Bond behaviour of FRP-to-clay brick masonry joints. *Engineering Structures* 31 (2009), 2580-2587.

Witterhold, F. 1985. Demolition of Reinforced Concrete by Blasting Techniques. *Tiefbau Ingenieurbau Strassenbau*. Vol. 27 Issue 9 , 512, 515-516, 518-520.

Xue, Q. C. W. 2009. Post-earthquake loss assessment based on structural component damage inspection for residential RC buildings. *Engineering Structures*. Volume 31, Issue 12, 2947-2953.

Zhao, J. and Li, H. B. 2000. Experimental determination of dynamic tensile properties of a granite. *International Journal of Rock Mechanics and Mining Sciences*, Vol. 37, 861-866.

APPENDIX

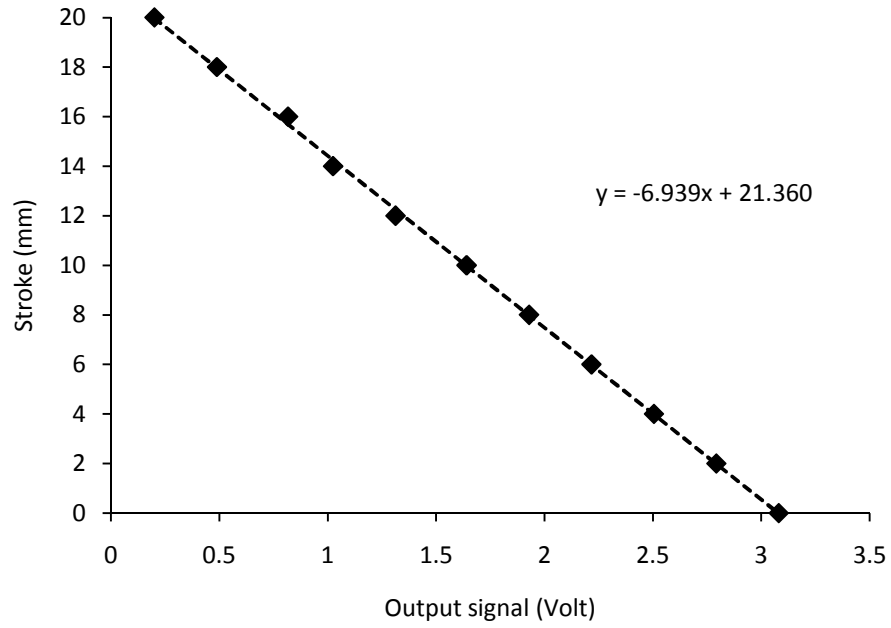


Figure A.1 Calibration chart for Lloyd test frame - Stroke

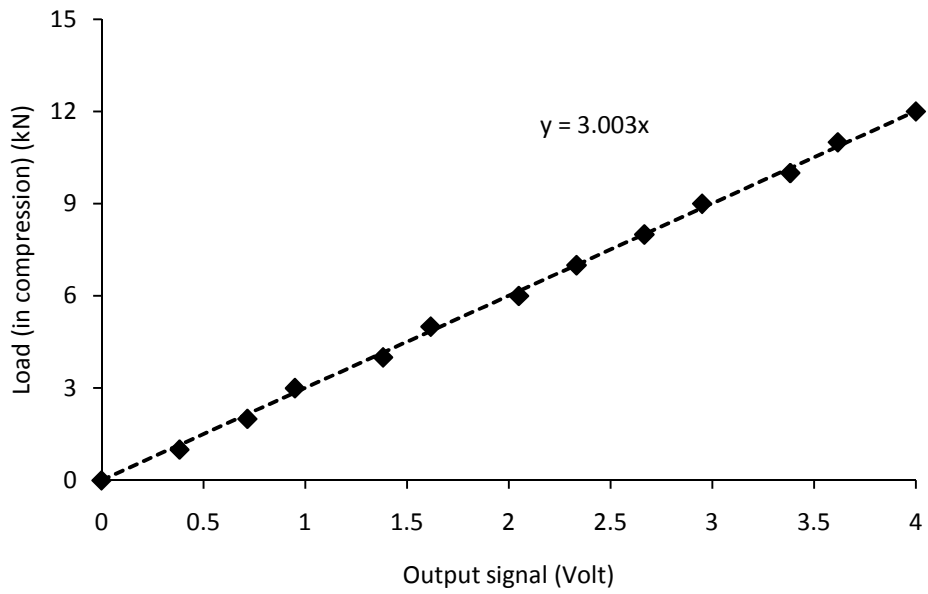


Figure A.2 Calibration chart for Lloyd test frame – Load Cell

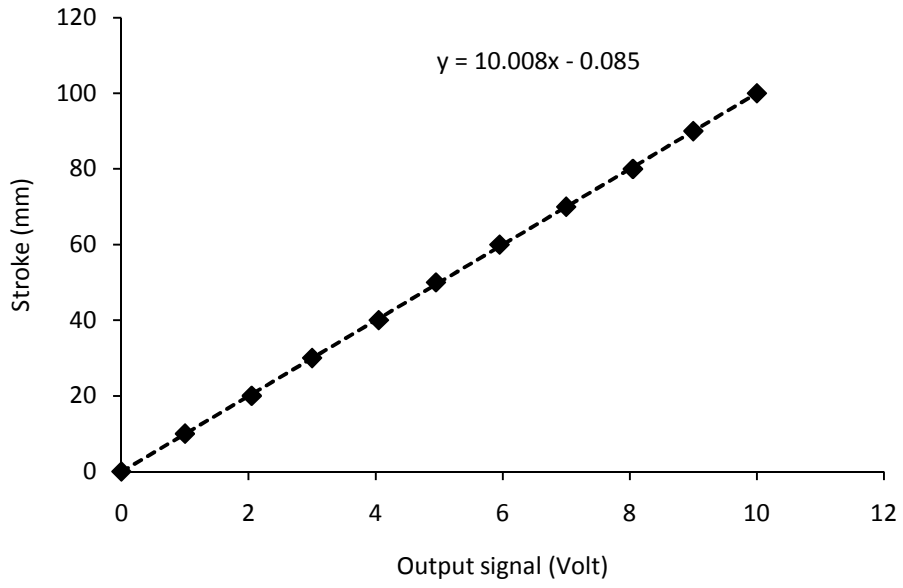


Figure A.3 Calibration chart for MTS 2600 – Stroke

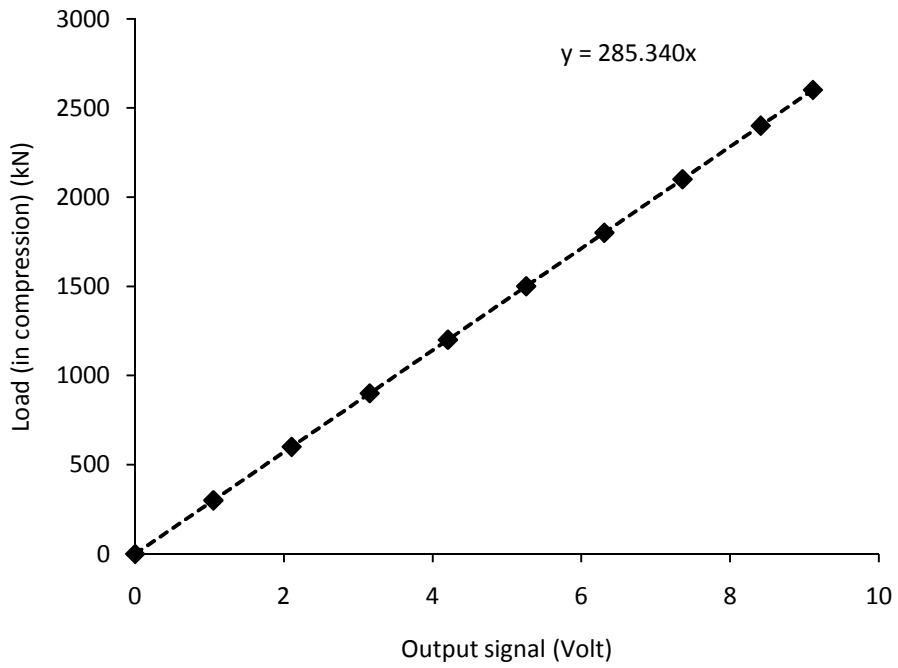


Figure A.4 Calibration chart for MTS 2600 – Load Cell

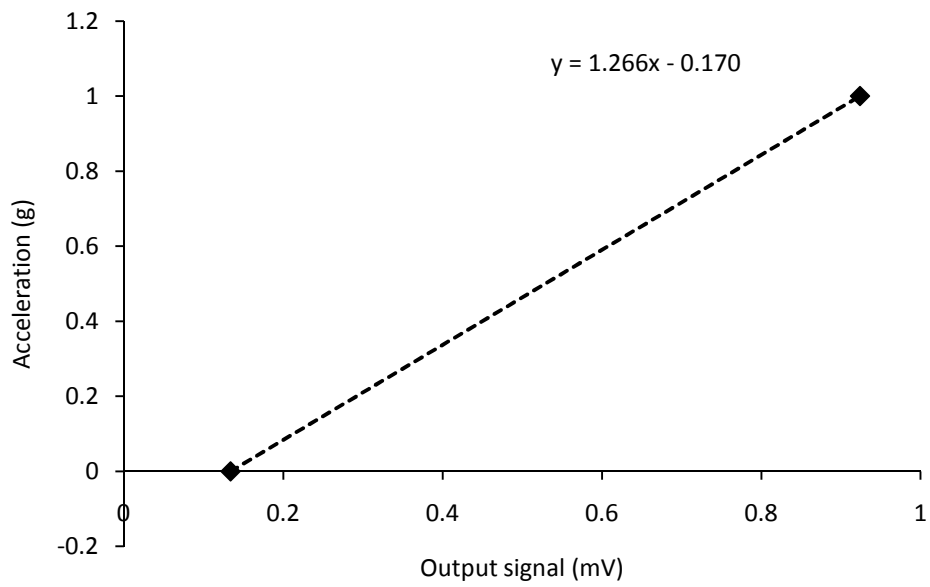


Figure A.5 Calibration chart for Drop-weight Impact Machine – Accelerometer

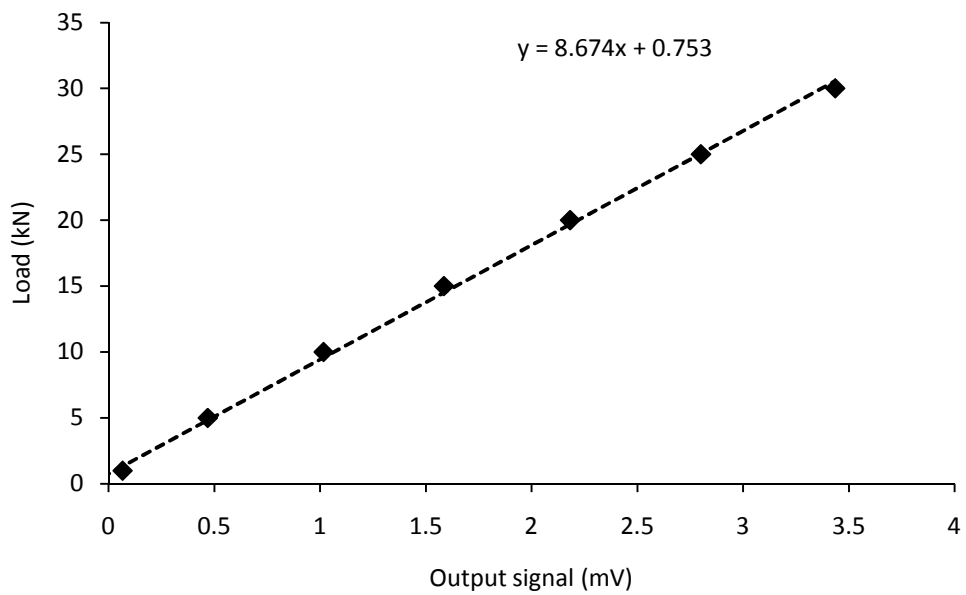


Figure A.6 Calibration chart for Drop-weight Impact Machine – Load Cell

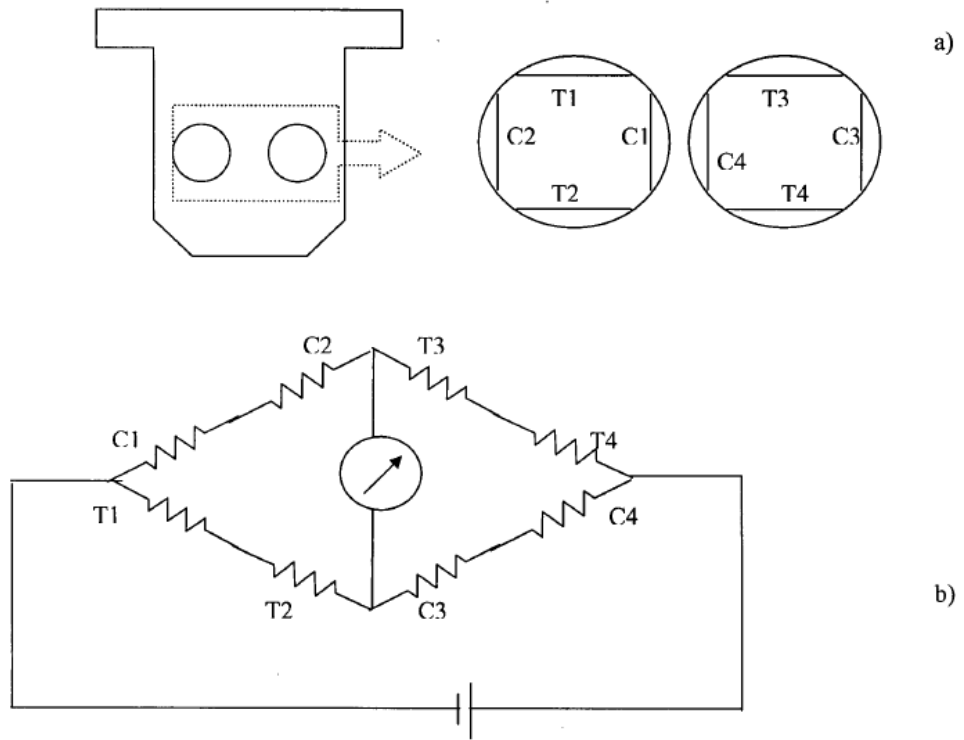


Figure A.7 Six inch Blade Load Cell used in Drop Weight Impact Machine a) Location of Strain Gauges in Tup b) Wheatstone Bridge Circuit